Investigating the diversity of extracellular vesicle microRNA in response to exercise-induced muscle micro-damage: comparison of targeted plasma microRNA to targeted and in-depth analysis of extracellular vesicle microRNA

by

Mr Jason Lovett

Dissertation presented for the degree of

Doctor of Philosophy in the Faculty of Science at

Stellenbosch University

Supervisor: **Professor Kathryn H. Myburgh**

December 2020

Declaration

"By submitting this thesis electronically, I declare that the entirety of the work contained therein is my own, original work, that I am the sole author thereof (save to the extent explicitly otherwise stated), that reproduction and publication thereof by Stellenbosch University will not infringe any third party rights and that I have not previously in its entirety or in part submitted it for obtaining any qualification."

June 2020

Verklaring

"Deur hierdie tesis elektronies in te lewer, verklaar ek dat die geheel van die werk hierin vervat, my eie, oorspronklike werk is, dat ek die alleen outeur daarvan is (behalwe in die mate uitdruklik anders aangedui), dat reproduksie en publikasie daarvan deur die Universiteit van Stellenbosch nie derdepartyregte sal skend nie en dat ek dit nie vantevore, in die geheel of gedeeltelik, ter verkryging van enige kwalifikasie aangebied het nie."

Junie 2020

Abstract

Background: Skeletal muscle (SkM) damage occurs routinely in sport and is present in acquired and inherited myopathies. Damage is confirmed by invasive muscle biopsy. Molecular events that occur during SkM injury and repair, including localized immune cell involvement, may be reflected in circulation. A detailed understanding is essential to the development of diagnosis and intervention strategies. Extracellular vesicles (EVs) are nanoscale (30 to 1000 nm) mediators of intercellular communication. EVs are released in abundance by all cell types, contain cargo including microRNA, and are stable in circulation. Circulating EV profiles adapt to differing physiological and pathological states. EVs may therefore serve as non-invasive biomarkers of SkM injury and regenerative processes.

Aims: To determine the biomarker potential of microRNAs in plasma, large EVs and small EVs in regard to skeletal muscle damage induced by unaccustomed eccentrically biased exercise.

Methods: Two consecutive bouts of muscle-damaging exercise (plyometric jumping and downhill running) were performed by 9 healthy male volunteers. Blood samples were taken at baseline, 2 and 24 hr post-exercise. Serum creatine kinase (CK) and perceived muscle pain (PMP) served as indirect markers of muscle damage. Canonical myomiRs, SkM-important miRs and immune-important miRs were analysed in 3 avenues of biomarker: plasma, large EVs and small EVs. Large EVs were isolated using a 10 000 G centrifugation step, whilst the subsequent supernatant was used for plasma analysis and qEV size exclusion isolation of small EVs. Small and large EV-enriched isolates were visualized using STEM, and size and numbers were quantified using NTA. Based on NTA results the highest particle fractions (7-10) from qEV columns were pooled for RNA analysis. qPCR analysis of plasma, large EV and small EV miRs was done with normalization to an exogenous control. Small RNA sequencing was done on 3 randomly selected participants' small EV samples from baseline and 24 hr.

Results: PMP and CK increased post-exercise. Small EVs were confirmed using gel electrophoresis, NTA and STEM. Large EVs were confirmed using NTA and STEM. Both small and large EVs were visualised using STEM. No change in small or large EVs size or number was seen post-exercise. Plasma miR-1, 133a and 206 increased in abundance at 2 hr, with miR-1 and 206 returning to BL levels at 24 hr. Conversely, plasma miR-208b & 499 also increased at 2 hr, but showed a trend toward a sustained increase at 24 hr. miR-31, a SkM-important miR, decreased in small EVs at 24 hr when compared to BL and 2 hr. No change in immune-important miRs was found in any biomarker source. Lastly, small RNA sequencing revealed an increase in 18 miRs in small EV at 24 hr post-exercise, with a concomitant decrease in 10 miRs.

Conclusion: Both small EV and plasma miRs changed in response to muscle-damaging exercise. Each exhibited distinct miR changes, and timing of changes as shown by qPCR. miR-31, for example, decreased only in small EVs post-exercise, whereas most myomiRs increased only in plasma. RNA sequencing revealed more small EV miR changes. However, these were not corroborated with qPCR.

Uittreksel

Agtergrond: Skeletale spier-(SkM)-beskadiging kom gereeld in sport voor en is teenwoordig in verworwe en oorerflike miopatie. Skade word bevestig deur indringende spierbiopsie. Molekulêre gebeure wat tydens SkM-besering en -herstel plaasvind, insluitend gelokaliseerde immuun sel betrokkenheid, mag in die sirkulasie weerspieël word. 'n Gedetailleerde begrip is noodsaaklik vir die ontwikkeling van diagnoserings- en intervensiestrategieë. Ekstrasellulêre vesikels (EVs) is nanoskaal-bemiddelaars (30 tot 1000 nm) van intersellulêre kommunikasie. EVs word in oorvloed vrygestel deur alle seltipes, bevat identifiseerbare vragte, insluitend mikroRNS, en is stabiel in sirkulasie. Sirkulerende EV-profiele pas by verskillende fisiologiese en patologiese toestande aan. EVs kan dus dien as nie-indringende biomerkers van SkM-beserings en regeneratiewe prosesse.

Doelstellings: Om die biomerkpotensiaal van mikroRNS'e in plasma, groot EVs en klein EVs te bepaal ten opsigte van skade aan skeletspiere, wat veroorsaak word deur ongewone eksentriek-bevooroordeelde oefening.

Metodes: Twee opeenvolgende instellings van spierbeskadigde oefening (pliometriese spring en afdraanddraf) is deur 9 gesonde manlike vrywilligers uitgevoer. Bloedmonsters was op basislyn, 2 en 24 uur na oefening geneem. Serum kreatien kinase (CK) en subjektief-waargenome spierpyn (PMP) het as indirekte merkers van spierskade gedien. Kanonieke “myomiRs”, SkM-belangrike “miRs” en immuunbelangrike “miRs” is geanaliseer in 3 weë van die biomerkerbron: plasma, groot EV's en klein EVs. Groot EVs is geïsoleer met behulp van 'n 10 000 G sentrifugeringsstap, terwyl die daaropvolgende supernatant gebruik was vir isolasie van klein EVs deur middel van qEV-grootte uitsluitende isolasie en plasma-analise. Klein en groot EV-verrykte isolate is gevisualiseer met behulp van STEM, en grootte en getalle is met behulp van NTA gekwantifiseer. Op grond van NTA-resultate is die hoogste deeltjiefraksies (7-10) uit qEV-kolomme saamgevoeg vir RNA-analise. kPKR-analise van plasma, groot EV en klein EV miRs is uitgevoer deur middel van normalisering tot 'n eksogene kontrole. Klein RNS volgorde ontleding is gedoen op 3 lukraak geselekteerde deelnemers se klein EV-monsters vanaf basislyn en 24 uur.

Resultate: PMP en serum CK het verhoog na oefening. Klein EVs is bevestig met behulp van gelelektroforese, NTA en STEM. Groot EVs is met behulp van NTA en STEM bevestig. Beide klein en groot EVs is gevisualiseer met behulp van STEM. Geen verandering in klein of groot EV-grootte of aantal is as gevolg van die oefening gesien nie. Plasma miR-1, 133a en 206 het op 2 uur in oorvloed toegeneem, met miR-1 en 206 wat op 24 uur na BL-vlakke teruggekeer het. Aan die ander kant het plasma miR-208b & 499 ook op 2 uur gestyg, maar het op 24 uur 'n neiging tot volgehoue toename getoon. miR-31, 'n SkM-belangrike miR, het in klein EVs op 24 uur afgeneem in vergelyking met BL en 2 uur vlakke. Geen verandering in immuunbelangrike miRs is in enige biomerkbron gevind nie. Laastens het klein RNS volgorde ontleding 'n toename getoon in 18 miRs in klein EV op 24 uur na oefening, met 'n gepaardgaande afname in 10 miRs.

Gevolgtrekking: Beide klein EV en plasma miRs het verander na afloop van spierbeskadigende oefeninge. Elkeen het unieke miR, asook tydstip veranderinge getoon, soos aangedui deur kPKR. Byvoorbeeld, miR-31 het slegs in klein EV afgeneem na oefening, terwyl meeste mio-miRs slegs in plasma vermeerder het. RNS volgorde ontleding het verdere veranderinge in klein EVs getoon. Hierdie veranderinge was egter nie met kPKR bevestig nie.

Acknowledgements

I would first and foremost like to acknowledge Dr Peter Durcan. I greatly appreciate your constant troubleshooting advice. I thank you for the intriguing discussions on new, cutting-edge techniques and methods. The microRNA analysis in this thesis would not have been possible without your knowledge of RNA.

I would like to thank my supervisor, Professor Kathy Myburgh. I thank you for your unconditional encouragement and support throughout a challenging and new area of research. Your insight into the scientific method, and ease at which you approach challenging information has helped me approach problems that I would not otherwise have considered. You always have an open door and a smile, allowing any urgent or stressful situations to be resolved quickly.

I would also like to thank Sister Erika, who was available to draw blood at a minute's notice. Your calm and professional demeanor helped streamline the many blood draws in this study.

I would like to thank the National Research Foundation for their financial support throughout my PhD.

A very big thank you to Christopher Reeves, Tersia Needham, Toni Goldswain, Kabous Visser, Megan Mitchell, Rhys McColl, Evan Knight and members of the Muscle Research Group for all you help, friendship and encouragement.

Lastly, I would like to thank my wonderful mother for her constant support throughout my education, and life in general. Thank you for convincing me that life is boundless, and that anything can be achieved. None of this would have been possible without your love and inspiration.

Table of contents

List of tables and figures

List of acronyms and abbreviations

AB	- Apoptotic body
ALIX	- ALG-2 interacting protein X
CD	- Cluster of differentiation
cDNA	- Complementary DNA
cel	- C. Elegans
CK	- Creatine kinase
Ct	- Cycle threshold
dH2O	- Distilled water
DHR	- Downhill running
DMD	- Duchenne muscular dystrophy
DOMS	- Delayed onset muscle soreness
EDTA	- Ethylenediaminetetraacetic acid
EIMD	- Exercise-induced muscle damage
ER	- Endoplasmic reticulum
ESCRT	- Endosomal sorting
EV	- Extracellular vesicle
Exo	- Exosome
FACS	- Fluorescence-activated cell sorting
HDL	- High-density lipoproteins
HGF	- Hepatocyte growth factor
HGS	- HGF-regulated tyrosine kinase substrate
HSP70	- Heat shock protein 70
IL-6	- Interleukin 6
ILV	- Intraluminal vesicles
ISEV	- International society for extracellular vesicles
LDL	- Low-density lipoprotein
miR	- microRNA
MRF	- Myogenic regulatory factors
MRF4	- Myogenic regulatory factor 4
mRNA	- Messenger RNA
MSC	- Mesenchymal stem cell
MV	- Microvesicle
MVB	- Multivesicular body
Myf5	- Myogenic factor 5
MyoD1	- Myogenic differentiation factor 1
Myog	- Myogenin
MyomiR	- Muscle microRNA
NTA	- Nanoparticle tracking analysis
PAGE	- Polyacrylamide gel electrophoresis
Pax 7 & 3	- Paired box transcription factor 7 & 3
PBS	- Phosphate-buffered saline
PCR	- Polymerase chain reaction
PHM	- Primary human myoblasts
PMJ	- Plyometric jumping
PMP	- Perceived muscle pain
qRT-PCR	- Quantitative Real-time PCR
RNA	- Ribonucleic acid
SEC	- Size exclusion column
VL	- Vastus lateralis

Chapter 1: Background and rationale

Skeletal muscle (SkM) is the largest internal organ in the human body, comprising approximately 40% of lean body mass [1]. At the center of force production required for movement, SkM is a common site for an extensive array of injuries. However, SkM tissue is equipped with great plasticity and exhibits an effective capacity for regeneration after incurring an injury. When minor injuries occur, SkM can generally repair itself successfully. It remains difficult, however, to quantify the extent of SkM injuries, as well as the efficacy to which it has healed, which is where this thesis aims to shed light.

SkM injuries emerge from numerous situations and usually present as either contraction-induced (e.g. a muscle strain) or contusion (e.g. from a blunt force) injury. Such injuries are abundant in both amateur and professional sports whilst also occurring in every-day settings of physical conflict, road accidents and falls [2]. Additionally, a multitude of SkM myopathies and dystrophies can be inherited or acquired (e.g. Duchenne's muscular dystrophy and sarcopenia) [3]. Furthermore, the loss of muscle in the presence of an underlying chronic condition, termed cachexia, can occur as a byproduct of diseases such as diabetes and cancer, implicating systemic signaling in muscle loss [4 5 6].

Currently, the most reliable method for measuring the magnitude of SkM damage is through direct visualisation of the damaged tissue, through scanning techniques like ultrasound and magnetic resonance imaging (MRI) [7]. Tissue sections taken from muscle biopsies can also be visualised using fluorescence or transmission electron microscopy [8 9]. These are currently the only direct methods for determining the extent of muscle damage. Although such techniques can be definitive, they are primarily qualitative or semi-quantitative strategies. Non-structural muscle injuries, which do not present with an easily identifiable anatomical lesion, account for 30 - 40 % of SkM injuries in mainstream sports such as soccer and can be missed by the above-mentioned scanning and imaging techniques [8 10]. In research and clinical settings, subjective rating of perceived muscle soreness and serum creatine kinase (CK) levels are conventionally used as

indirect markers of SkM damage [11]. However, analysis of these markers is complicated by diverse subjectivity and considerable variation between samples, respectively [8]. As a result, there is an inadequate amount of data on the reliability of injury quantification techniques as well as the diagnosis of more subtle injuries.

A detailed understanding of the molecular and cellular events that occur during muscle injury and repair is essential to the development of intervention strategies that can enhance the efficiency of regeneration and reduce the recovery time after injury. Furthermore, an improved understanding will aid in the development of strategies to delay muscle disease as well as injury progression. The following section presents an overview of SkM structure, providing context to the section on muscle damage that follows.

1.1 A brief overview of skeletal muscle structure

The muscle cell, a multi-nucleated fibre strand called a myofibre, is the unit responsible for force generation. At a molecular level, force is initially generated by cross-bridge cycling of myosin heads on actin filaments. This occurs within the sarcomere, the highly organised functional unit of SkM. A functional unit is the smallest unit responsible for the main role of a tissue, which, in the case of SkM, is force generation. Whole SkM is comprised of abundant myofibres surrounded by layers of connective tissue i.e. the perimysium and the epimysium (Figure 1.1). This network of connective tissue is not only necessary for transferring force to the bones, but also provides resilience and protection from stretch-induced damage. It is, in fact, SkMs role in tension development that makes it a common site for injury. Contraction of multiple myofibres is synchronised across the muscle to allow for sufficient tension during normal contractions. However, contraction at the sarcomere level is not always synchronised and, as a result, individual sarcomeres can become damaged. A theory of "popping sarcomeres" has been described in detail by *D. Morgan* in 1990 [12]. According to this theory, weaker sarcomeres "pop" when the muscle is stretched beyond the normal length-tension relationship. Apart from this contraction-induced SkM damage, there are some types of muscle contractions during which damage is more likely to occur [13]. These will be highlighted in the following section.

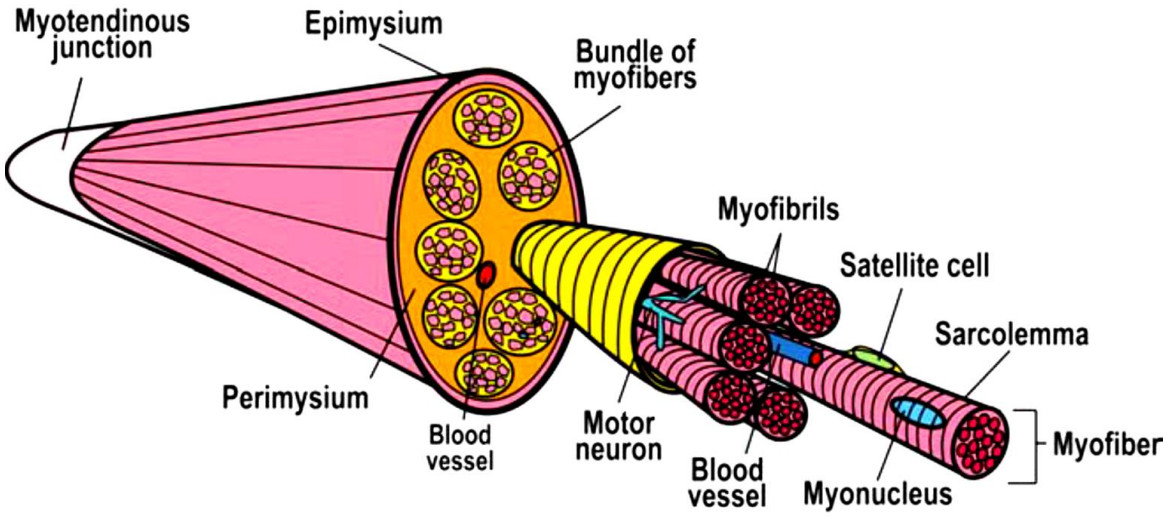

Figure 1.1. An overview of whole skeletal muscle structure. (Figure from *Scime et al.* with permission [14]).

1.2 Skeletal muscle and exercise-induced muscle damage

In trying to better understand SkM injury, many studies have been designed using animal models of injury, for example, crush injuries or cardiotoxin-induced muscle damage [15 16]. It is also possible to analyse regeneration in the context of naturally occurring injuries to the human muscle (e.g. sports or work-related injuries), but this method is unpredictable and a consistent, reproducible injury cannot be expected. Similarly, myopathies require regeneration, but the chronic nature of this affliction complicates research design aspects related to timing and clinical severity. One *in vivo* method that does allow for analysis of the full spectra of moderate muscle damage in healthy human subjects is exercise-induced muscle damage (EIMD). Through this model, voluntary recruitment of SkM for work can be manipulated through a defined exercise protocol and time-course, allowing for experimentation within the context of normal physiology.

EIMD is caused by unaccustomed, excessive, or eccentrically-biased exercise. Eccentric exercise primarily involves eccentric muscle contractions, which occur when the working muscle lengthens during contraction. Conversely, concentric contraction is when the muscle shortens

and lastly, isometric contraction is where no change in muscle length occurs. Eccentric contractions apply significantly more strain to muscles than the concentric ones because fewer motor units are recruited, which intensifies the force of contraction [17] [18] [19].

Muscle damage from eccentrically-biased exercise protocols manifests similarly to that of delayed onset muscle soreness (DOMS), a sensation often experienced 24 - 48 hours following an intense exercise session. These exercise protocols, including downhill running and plyometric jumping, have previously been shown to induce transient muscle damage in humans [11] [20] [21] [22]. It is important to note, however, that the aforementioned exercises do not exclusively produce eccentric contractions, but also include a concentric component.

There is ample evidence that eccentrically-biased protocols cause changes in circulating markers of mechanical damage and inflammatory damage - typical examples being creatine kinase (CK) and interleukin-6 (IL-6), respectively [23] [24]. However, changes in these markers are variable and do not reflect the extent and magnitude of damage, but rather indicate the fact that EIMD has occurred. The identification of alternative circulating biomarkers of EIMD has been previously pursued, with specific focus on the cytokine families such as Il-8 [25] and IL-10 [26]. However, these markers can originate from injured muscle cells, uninjured exercising muscle as well as from immune cells, thereby convoluting their interpretation[28]. Consequently, new options are continuously being sought after, in particular, circulating factors that are easily accessible through blood sampling.

1.3 Phases of muscle damage and the cells involved

The diversity of SkM injuries in humans ranges from minor damage of weaker sarcomeres to traumatic tears of the whole muscle. Although the magnitude may differ substantially, all injuries require a reparative response and indeed, as mentioned earlier, SkM exhibits a highly effective capacity for regeneration of the damaged area. The efficacy of this process is largely attributable to a resident pool of myoblast progenitor cells, known as satellite cells (SCs) [27]. Broadly, regeneration following damage of SkM can be grouped into the phases of inflammation,

proliferation and differentiation; each of which has distinct aspects of communication, which will be further discussed (Figure 1.2).

Following damage, a complex secretome of specific cytokines and chemokines, collectively termed myokines, is released into circulation by the SkM, activating a systemic communication response that attracts pro-inflammatory immune cells to the damaged area. Neutrophils are some of the first circulating cells to infiltrate the damaged area and they create a positive feedback loop through pro-inflammatory signalling, which recruits additional immune cells to the site of damage [11]. During this initial inflammatory stage, neutrophils release proteolytic enzymes, such as matrix metalloproteases (MMPs), myeloperoxidase (MPO), and reactive oxygen species (ROS) which function to degrade the damaged tissue in the area [28]. This is microscopically visualised as a loss of ultrastructural organisation, i.e. a lack of striated appearance in the damaged area, and Z-line streaming [20]. Pro-inflammatory, M1 macrophages are next to infiltrate the area in overlapping phases of degradation and phagocytosis of resulting cellular debris [29]. IL-6 is one of the most abundant pro-inflammatory cytokines in circulation following muscle injury and its sources can include infiltrating immune cells, damaged myofibres as well as resident macrophages [21]. Thus, the exact origin of damage-associated IL-6 release is difficult to delineate. However, the responsiveness of macrophages to IL-6 signalling is testament to a highly-orchestrated communication process that arises from muscle injury [23].

SC proliferation initiates the process of replacing lost muscle cells and restoring fibre integrity, provided the damage has not destroyed the entire fibre. SCs are uniquely positioned inside the basal lamina and outside the sarcolemma, allowing for sensitive communication from both local and systemic sources [27]. These progenitor cells exhibit enormous proliferative potential and are responsible for the potent regenerative plasticity of SkM [30].

The intricate control of proliferation and differentiation during myogenesis is achieved through a specific group of transcription factors, known as the myogenic regulatory factors (MRFs). Myogenic differentiation factor 1 (MyoD) is acknowledged as the "master regulator" of myogenesis, due to its influence on the cellular commitment to a myogenic profile [31]. MyoD levels increase after SC activation and remain integral to myogenesis until the completion of

differentiation. Other notable MRFs are Myf5, myogenin (Myog) and MRF4 (Figure 1.2) [32]. MRFs interact with a plethora of local and systemic signals, including growth factors, cytokines and microRNAs, and further details of the latter interaction will be provided in Chapter 3.

SkM's capacity for remodelling is principally responsible for its advanced regenerative plasticity. Effective differentiation and remodelling phases are critical for returning proper functional capacity to the tissue. *In vivo*, the remodelling phase is dominated by macrophages with a regenerative M2 phenotype [29]. Myog levels are also substantially elevated and for the new myoblasts derived from SC proliferation, Myog and MRF4 are essential during this phase [33]. Myog aids the transcription of factors such as cyclin-inhibiting proteins, which inhibit proliferation and allow for myoblast differentiation to proceed.

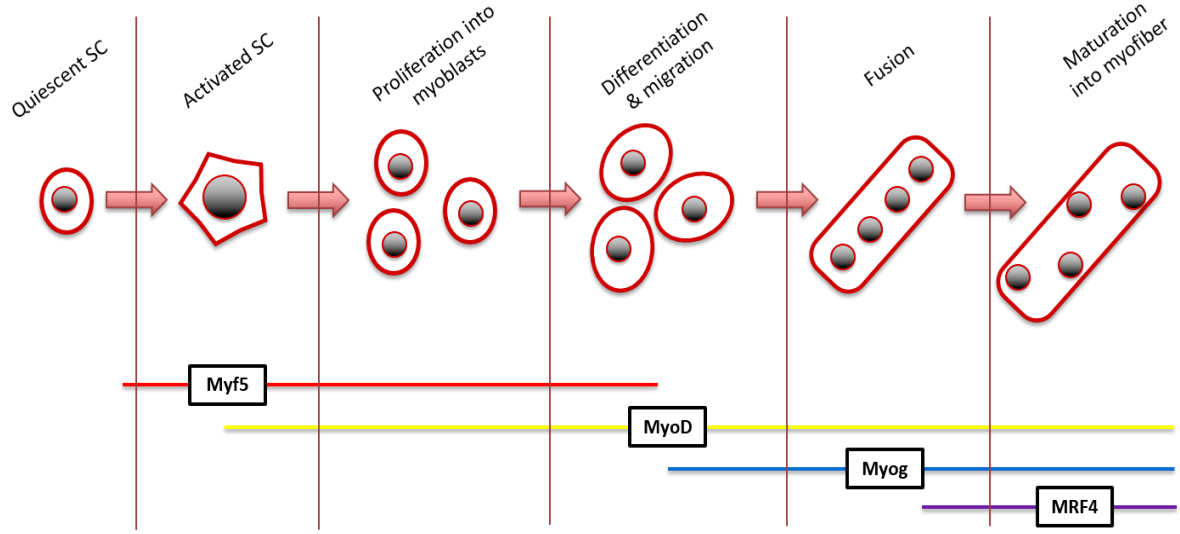

Figure 1.2. Schematic of satellite cell activation, proliferation and differentiation, with the corresponding myogenic regulatory factors involved, and timelines of involvement (SC: Satellite cell).

1.4 The ideal marker for SkM damage

The lack of reliable biomarkers for the diagnosis and quantification of SkM damage has directed much research toward the search for a suitable candidate. The ideal biomarker of SkM damage must: (1) be present in an easily attainable sample; (2) be constitutively present at low levels in

non-damaged muscle; (3) consistently increase in response to damage, and hence have specificity; (4) increase proportionally to the extent of the injury; and (5) have a temporary change in response to acute damage and its subsequent resolution, thus requiring sensitivity following treatment or natural healing [34].

Blood samples are relatively easy to attain, consequently fulfilling the first criterion of an ideal biomarker. In this context, a blood sample is referred to as a "liquid biopsy" and is recognised as a less invasive method for determining the state of hard-to-reach internal tissues. Although it most commonly refers to blood samples, the term liquid biopsy, in recent biomarker research, includes the analyses of almost all bodily fluids [35] [36].

The most commonly utilised circulating marker of SkM damage is CK and, for a long time, it was the only indirect marker. However, the specificity of CK has continuously come into question due to its overlapping use as a clinical marker of myocardial damage [34]. With similar disadvantages, proteins such as myoglobin and lactate dehydrogenase, which leak from injured muscle tissue, may also be used in the indirect assessment of SkM damage [34].

SkM, like most internal organs, is under continuous demand to maintain homeostasis through the coordination of local and systemic communication signals. A vast network of capillaries is closely associated with the myofibre bundles and their surrounding interstitial fluid so that myofibres can be readily nourished with oxygen, nutrients and other biological molecules such as hormones, cytokines and growth factors. Recently, SkM was recognised as an important endocrine organ, with the ability to release several types of biomolecules into circulation; a previously under-appreciated property [37] [38]. In 2012, *Pedersen and Febbraio* described the concept of myokines ("myo" = muscle & "kinesis" = movement), where circulating cytokines and other soluble factors contribute to the homeostasis of both muscle and other tissues [39] [40]. It has subsequently been proposed that the subset of myokines released in response to exercise be termed "exerkines" [41] [42].

IL-6 has also been explored as a marker of SkM damage. Muscle is well-known to release IL-6 that can act in an autocrine manner within the tissue. IL-6 and several other myokines have been implicated in cell division in *in vitro* studies [43] and it is therefore plausible that they may influence

the progenitor cells involved in the regeneration of damaged muscle *in vivo*. Muscle-released IL-6, for example, acts in an autocrine and paracrine manner to affect muscle and other organs such as the liver, pancreas and adipose tissue [44] [43] [45]. In the context of muscle damage, plasma IL-6 has been used as an indirect assessment of the severity of the inflammatory response [48]. However, IL-6 may lack specificity as a biomarker for EIMD, given its exerkine status and that it's major source could be from the immune cell response.

1.5 Novel circulating communicators: microRNA and extracellular vesicles

Myokines and exerkines are biomolecules that passively traverse the muscle membrane, differing from the transporter-associated release of lactate, for example [46]. Another category of biological communicators is extracellular vesicles (EVs), which contain and transport biomolecules, including myokines [41], though little is known about the use of EVs, and their contents, as biomarkers of SkM damage. Recently, the myokine family has expanded to include microRNA - the small, non-coding RNA. However, the use of microRNA as a biomarker of damage is complicated, as they may be released passively or within vesicles. However, increasing evidence provides an impetus for the potential of SkM tissue to contribute significantly to the circulating milieu of EVs in either magnitude, microRNA profile, or both [47] [48] [49] [50] [51].

The following literature review will provide a detailed overview of EVs (Chapter 2) and microRNA (Chapter 3), and their use as potential biomarkers in the context of exercise-induced SkM damage.

Chapter 2: Extracellular vesicles

2.1 An introduction to extracellular vesicles

Extracellular vesicles (EVs) have emerged as a novel and important mode of intercellular/inter-organ communication [52]. Three subgroups of EVs are delineated by their diameter as follows, small exosomes (Exo: 30-150 nm), medium microvesicles (MV: 100-1000 nm), and large apoptotic bodies (AB: >1 um); each of which exhibits unique modes of biogenesis and exocytosis [52] (Table 2.1). Apoptotic bodies are important mediators of cell death, however, only Exo and MV have been shown to carry selectively packaged cargo [53]. Therefore, in this dissertation, EVs will henceforth refer to Exo and MV only. Comprised of a spherical, cell-like lipid bilayer, EVs are nano-sized carriers that afford bioactive molecules with protection and are present in a diverse range of biofluids (e.g. blood, urine and saliva [35]). The lipid bilayer of EVs is particularly enriched with cholesterol and glycosphingolipids (i.e. lipid rafts) when compared to the parent cell from which they originated, and this composition contributes to the rigidity and stability of EVs in circulation [54]. EVs encapsulate a diverse range of biomolecules (e.g. proteins, lipids and RNA) that retain functionality in the recipient cell to which they are delivered [55]. Notably, the structural components of EVs may also serve as important signalling molecules i.e. transmembrane proteins and prostaglandins [56]. Correlations have been reported between EV cargo and both pathological and physiological states (e.g. cancer [57], exercise [50] and diabetes [58]), suggesting the use of EVs as diagnostic and prognostic tools [59] [38].

Table 2.1. Summary of key extracellular vesicle characteristics (adapted from Witwer *et al.* [60]). Size, sedimentation and density are important factors to consider when choosing a method for EV isolation.

	Exosomes	**Microvesicles**	**Apoptotic Bodies**
Biogenesis	Endosomal pathway	Plasma membrane	Cell disintegration
Size	30-150 nm	100-1000 nm	>1000 nm
Sedimentation	100 000 G	10 000 G	2 000 G
Density	1.11 – 1.19 g/ml	1.11 – 1.19 g/ml	1.16 – 1.28 g/ml

2.2 Extracellular vesicle biology

The presence of EVs was first established in blood research by *Chargaff and West* in 1946 [61]. With the aim of better understanding the mechanisms of clotting in human blood, these researchers noted a protein pellet with particulate matter following high-speed centrifugation of the plasma, at 31,000 g [61]. Derived from the blood of a healthy donor, the aforementioned pellet was supplemented into the plasma from a patient with hemophilia (i.e., blood that was devoid of clotting factors) and blood coagulation was observed. Therefore, this pellet appeared to have functional content. In 1967, *Wolf* visualised similar protein pellets using transmission electron microscopy (TEM) and was able to visualise intact particles [62]. He termed these spherical particles, "platelet dust", and hypothesised that they could confer the previously noted thrombogenic activity. These spherical particles were later noted to be EVs. Almost two decades later, a study on reticulocyte maturation in sheep, a process characterised by a loss of the transferrin receptor from the reticulocyte membrane, helped to provide empirical evidence for the role of EVs in important cellular processes [63]. By labelling the transferrin receptors with immuno-gold conjugated antibodies and using TEM, Pan and colleagues observed transferrin receptors on the surface of secreted EVs [63]. This result raised the possibility that EVs may undergo a process whereby specific proteins are incorporated into the EV membranes. Questions remained on the actual function of EVs or whether their exclusive role was to provide a mechanism of removing unwanted cellular debris in the form of cargo.

In a pioneering study by *Raposo et al.,* EVs were revealed to confer antigen-presenting information between leukocytes *in vitro* [64]. These researchers added EVs derived from antigen-exposed B-cells onto unexposed T-cells and, thereafter, recorded the transfer of antigen information through major histocompatibility complex (MHC) class-2 integration into EV membranes. This study established a role for EVs in the context of transferring immune competency between cell types, thereby helping to validate EVs as functional mediators of intercellular communication. A decade later, *Ratajczak et al.* noted the presence of messenger RNA (mRNA) transcripts associated with EVs and found that some transcripts were enriched in EVs when compared to their abundance

within the parent cells [65]. However, it was not until an important study by *Valadi et al.* a year later, that truly notable findings in EV biology began to emerge [66]. Using radio-labelled nucleotides, Valadi and colleagues showed that EVs not only encapsulate RNA but deliver these RNA species to other cells [67]. The transferred RNA was shown to remain functional and could be translated into protein within the recipient cell. These findings have greatly propagated further research into EV biology, and into its RNA cargo, in particular.

2.2 Extracellular vesicle biogenesis, release and uptake

Both MVs and Exo originate from the plasma membrane. The larger of the two, MVs, bud directly from the cell membrane in a "blebbing-like" process (Figure 2.1. A). Multiple smaller Exos, however, form through endocytosis of the cell membrane into an early endosome. Maturation of this early endosome occurs in the cytoplasm in a process similar to pinocytosis. It involves repeated steps of inward budding of the original early endosome's membrane. The result is a multivesicular body (MVB) - a type of mature endosome - containing numerous intraluminal-vesicles (ILVs - Figure 2.1. B) [68]. Some of these MVBs fuse with and enter the lysosomal pathway via mechanisms that are still poorly understood. Other MVBs, upon receiving the necessary signal, fuse with the plasma membrane of the parent cell causing the release of ILVs into the extracellular space by exocytosis. Once exocytosed, ILVs are termed exosomes.

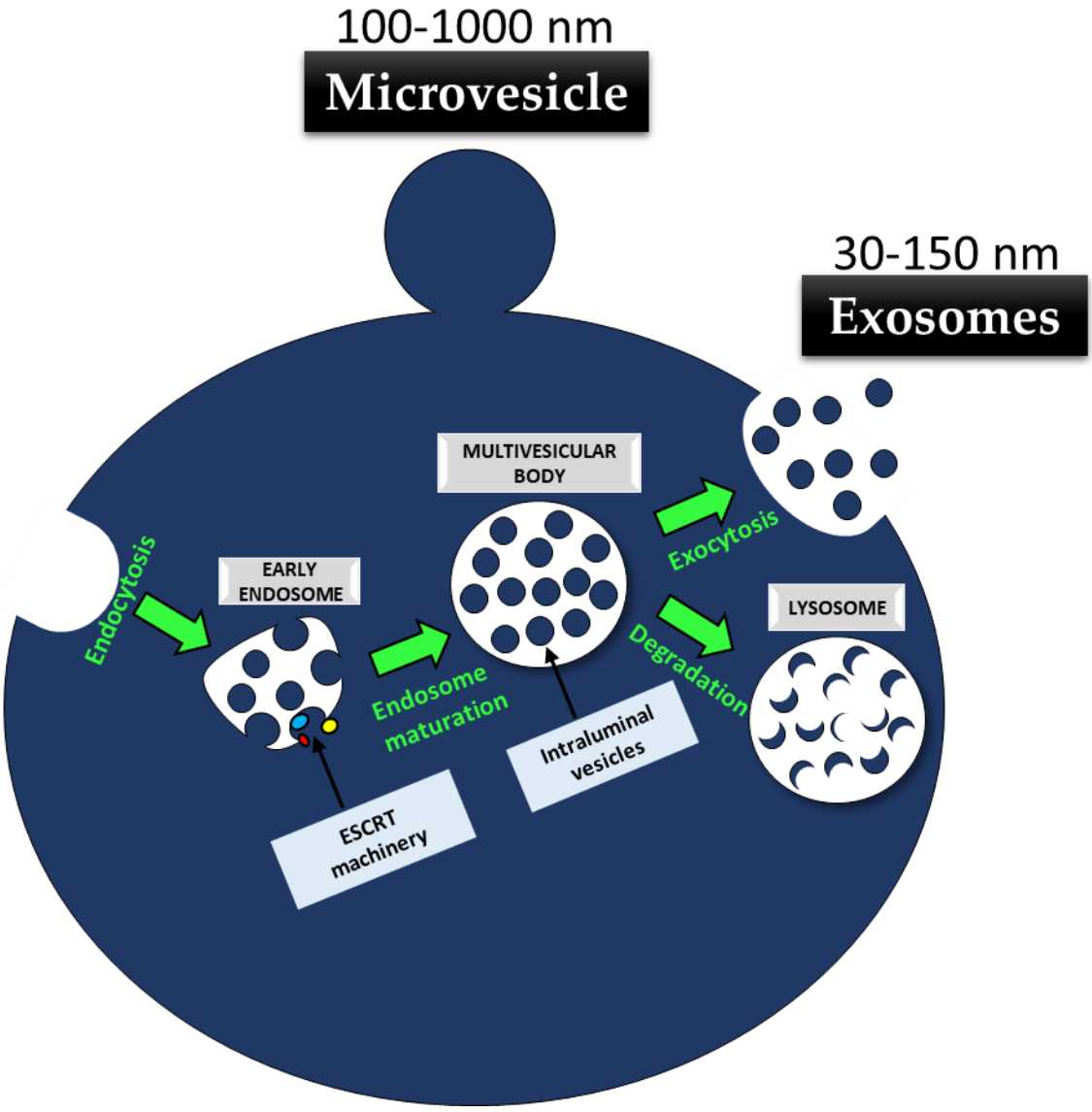

Figure 2.1. Diagram of extracellular vesicle (exosome and microvesicle) biogenesis and release (adapted from Colombo *et al.* [69]). **A** depicts the early endosome maturation process to eventually produce extracellular exosomes. **B** depicts membrane blebbing for microvesicle release of vesicles not formed using ESCRT machinery. **C** depicts the alternative path of MVB fusion to lysosomes.

Although Exos are also released by exocytosis, they exhibit a different mode of biogenesis. Hence, Exos display different sizes and cargos when compared to MVs. The most comprehensively described pathway for Exo biogenesis, and/or MVB composition, involves a family of ± 20

proteins, collectively termed the Endosomal Sorting Complex Required for Transport (ESCRT) [70]. The ESCRT family forms four complexes (ESCRT-0, -1, -2 and -3) that, along with their associated proteins, are the key coordinators of ILV packaging and MVB formation [69]. In the first step, ESCRT-0 proteins incorporate ubiquitin-tagged membrane proteins into ILVs through the actions of the proteins HRS (hepatocyte growth factor-regulated tyrosine kinase substrate) and STAM (signal transducing adaptor molecule) [71]. ESCRT-1 & 2 are responsible for intracellular bud formation and cargo packaging of ILVs, which occurs during maturation of an early endosome into an MVB. This process is aided by the accessory proteins TSG101 (tumour suppressor gene 101) and ALIX (Alg-2 interacting protein X), both of which are commonly identified at elevated levels in EVs. [20]. Although the exact reason for their enrichment in EVs is not fully elucidated, studies have suggested a role in cytoskeleton rearrangement for these proteins [70] [72]. Finally, ESCRT-3 proteins are responsible for the excision of the bud, allowing for isolation of ILVs from the cytosol of the parent cell [69].

It is important to note that the exact mechanisms of cargo selection and recruitment to the ILVs are yet to be established. Given this, the ESCRT family cannot assume sole responsibility for Exo formation. For example, MVBs have been shown to form in the absence of some ESCRT proteins [73]. Non-ubiquitinated proteins were shown to be packaged into ILVs, suggesting that the packaging process is not reserved exclusively for proteins tagged for degradation and thus confirming that non-ESCRT-0 related mechanisms are also present [74]. A candidate for directing cargo to ILVs is heat shock protein 70 (HSP70), an established protein chaperone in physiological processes (e.g., in cancer-associated muscle cachexia) [75] [76]. Whereas removal of ubiquitinated proteins into ILVs may be seen as non-specific, the alternate mechanism suggests more control is exerted for some of the cargo.

Taken together, these studies suggest that Exo biogenesis is both complex and highly specific. It is this specificity that makes EVs interesting as potential biomarkers in health and disease. Although key players in EV formation remain to be precisely elucidated, advances in EV analyses are piecing together the fragmented picture at a rapid rate.

Compared to EV biogenesis, less is known about the uptake and fate of EVs after entering circulation, since the elucidation of EV uptake has, thus far, been largely reliant on *in vitro* techniques. Generally, EV uptake occurs through one of three mechanisms following a ligand-receptor type interaction with the plasma membrane. An EV can either fuse with the cell membrane to release its cargo into the recipient cell [77]; be engulfed (intact) and directed to intracellular compartments [78 79]; or behave more like a ligand, not releasing its cargo and resulting in a classic receptor-ligand intracellular signalling cascade [80]. Endocytosis of EVs may be clathrin-dependent or caveolin-mediated [77].

The internalisation of intact EVs has been described through the mechanisms of polymerisation-dependent phagocytosis by macrophages, receptor-mediated endocytosis and lipid-raft dependent fusion, to name but a few [78 81 82 83]. The modes of EV internalisation may also be dependent on cell type. An example of EVs, or their cargo, not being internalised by the recipient cell was shown in a study by Denzer *et al.* [84]. Isolating EVs from antigen-presenting cells, the authors noted that internalisation was not necessary for the transference of immune competency. To better understand EV uptake and whether or not it is specific, Alvarez-Erviti *et al.* engineered EVs to present a surface receptor containing an amino acid sequence that would be recognised by muscle cells [85]. This muscle-specific peptide was discovered by phage display. The engineered EVs preferentially bound to cells of the muscle cell line, to which their surface receptor sequence had been targeted. Although the exact actions of the muscle-specific peptide are not known, this study implies that EV uptake is most likely highly specific.

2.4 Extracellular vesicle isolation techniques

The substantial diversity in EV isolation techniques apparent in the published literature makes the comparison of data between labs and studies challenging. A consensus on the best or most suitable isolation method is not yet agreed upon. An absolute method may not be possible, as many research teams have shown that various downstream applications can vary considerably depending on the means of EV isolation [86 87 88 89]. A brief overview of the advantages and

disadvantages of the different EV isolation methods is shown in Table 2.1. Isolation methods that most often appear in the literature can broadly be grouped into; differential centrifugation, density gradients, chemical precipitation, immune-affinity and size exclusion [90].

2.4.1 Differential centrifugation

High-speed centrifugation was used in the initial EV discoveries [91]. Differential centrifugation is a term describing the combined use of normal and ultracentrifugation. The technique is employed to systematically rid the sample of cells, debris and unwanted particles, based on sedimentation factors. After multiple supernatant clarification steps, the sample is ultracentrifuged at high speeds (i.e., ≥ 100,000 g) to "pellet" the EVs. This is currently the most widely used method for small EV isolation and is considered to be the gold standard. It is now commonplace for researchers to combine differential centrifugation with sequential steps of filtration (i.e., 0.22 - 0.45 μm pore size filters) to differentiate between microvesicles and exosomes.

2.4.2 Density gradients

More recently, differential centrifugation has been supplemented with sucrose or Iodixanol (OptiPrep) gradients and sucrose cushions to achieve a more resolved isolate of greater purity. This method makes use of the known EV density range of 1.1 - 1.9 g/ ml, resulting in the fractionation of the sample per density, rather than size.

Table 2.1. Comparison of commonly used extracellular vesicle isolation techniques.

	Advantages	**Disadvantages**
Differential centrifugation	Widely used and therefore translatable. Inexpensive.	Requires large equipment. Time-consuming. Aggregation of EVs.
Density gradients	High specificity. Low contamination. Inexpensive.	Isolation of an undefined EV subpopulation. Difficult to perform. Time-consuming.
Chemical precipitation	Easy to use. Inexpensive.	Non-specific. Potential high contamination

Immune-affinity	High specificity.	Isolation of an undefined EV subpopulation. Dependent on antibody quality. Costly.
Size exclusion	Short isolation time. Easy to use.	Costly. Dilutes sample.

2.4.3 Chemical precipitation

EV isolation using precipitating polymers (e.g. Polyethylene glycol, ExoQuick, Total Exosome Isolation Reagent) has gained popularity of late. Many researchers favour this technique due to its low cost and ease of use [86]. The use of precipitating polymers is a well-established technique in the isolation of viral particles. These polymers readily neutralise the charge of biomolecules, thereby decreasing their solubility and causing them to precipitate. However, others have highlighted the potential of this precipitation method to co-isolate a significant amount of contaminating protein due to its non-specific nature [43]. More recent use of chemical precipitation of EVs has added further isolation steps (such as size exclusion) for sample clean up.

2.4.4 Size exclusion

The use of size exclusion columns (SEC) for the isolation of EVs is a technique that is rapidly increasing in popularity, largely due to its passive isolation of EVs. Most size exclusion techniques make use of Sepharose (GE Healthcare Life Sciences), a bead-based form of the common cross-linking polymer, Agarose. Size exclusion columns (SEC) can be used to resolve EV fractions derived from other methods. Alternatively, SEC can be used as a standalone technique. Due to the passive nature of SEC EV isolation, the potential for this method to yield intact and functional vesicles is high. The small size of the SEC renders them suitable for use in any lab, eliminating the need for access to an expensive ultracentrifuge.

2.4.5 Immune-affinity

Immune-capture, or immune-affinity, using conjugated antibodies, is a multidisciplinary technique. This isolation technique includes the use of flow cytometry, magnetic beads or precipitant-conjugated antibodies to capture specific subgroups of EVs in an isolate. Additionally, immune-affinity can be used to remove known contaminants from a sample.

2.5 Extracellular vesicle cargo

Whether carried as a structural component of an EV membrane or transported intra-EV, much interest has been directed toward the study of EV cargo. The following categories of EV cargo predominate; proteins, lipids and RNAs (Figure 2.2). However, due to varying EV isolation strategies, characterisation techniques and downstream analyses, it is challenging to formulate the exact profile of many of these EV constituents with good repeatability [90]. Therefore, the International Society for Extracellular Vesicles (ISEV) has put much effort into creating position papers to standardise EV techniques where possible [92 93]. The standardisation process has adopted proteomic, sequencing and lipidomic big data approaches to uncover information on EV cargo. New online databases, such as EVpedia (evpedia.info), ExoCarta (ExoCarta.org) and Vesiclepedia (microvesicles.org), have been established to sort and, with more time, to standardise the large amount of data currently being generated on EV proteins.

2.5.1 Protein

Most EV studies make use of some form of protein analysis for the identification of the endosomal nature of Exo, or the identification of an EV-enriched protein [90]. The most commonly used protein markers are the tetraspanins: CD9, CD63 and CD81 [93]. However, these tetraspanins can also be detected on cell membranes and are, therefore, often used in combination with proteins of known endocytotic origin, such as TSG101, ALIX, and HSP70 [93]. It is then recommended to add a negative control such as calnexin, for example, an endoplasmic reticulum protein [93]. There is currently no single marker for EVs, and it is through a combination of proteins that the presence of EVs is

established. Not surprisingly, the ESCRT family proteins are also enriched in EVs. It is important to note that the abundance of EV-enriched proteins is altered between different physiological conditions and cell/organism types [11], and a consistent profile has not been established. This may be why no definitive protein has been identified as an exclusive EV marker. Nonetheless, attempts have been made to promote ESCRT-associated proteins, i.e., TSG101 and ALIX, as appropriate identifiers [60].

Analysis of EV proteins is not only important for the identification of EVs, but also for determining the protein cargo that they transport. Advances in mass spectrometry have aided the identification of a vast number of proteins in EVs and a wide variety of proteins have been found, e.g., transcription factors, cytokines, receptors and growth factors [94] [95] [96]. Furthermore, diversity of the EV proteome is also apparent between cell types and physiological states, as well as between EV subtypes [97].

2.5.2 Lipid

To date, lipids have received the least attention with regard to EV analysis (Figure 2.2) [90] [98]. Despite the important role of lipids in EV membranes, it is only with mass spectrometry-based lipidomic techniques that this field has really started to take off [98].

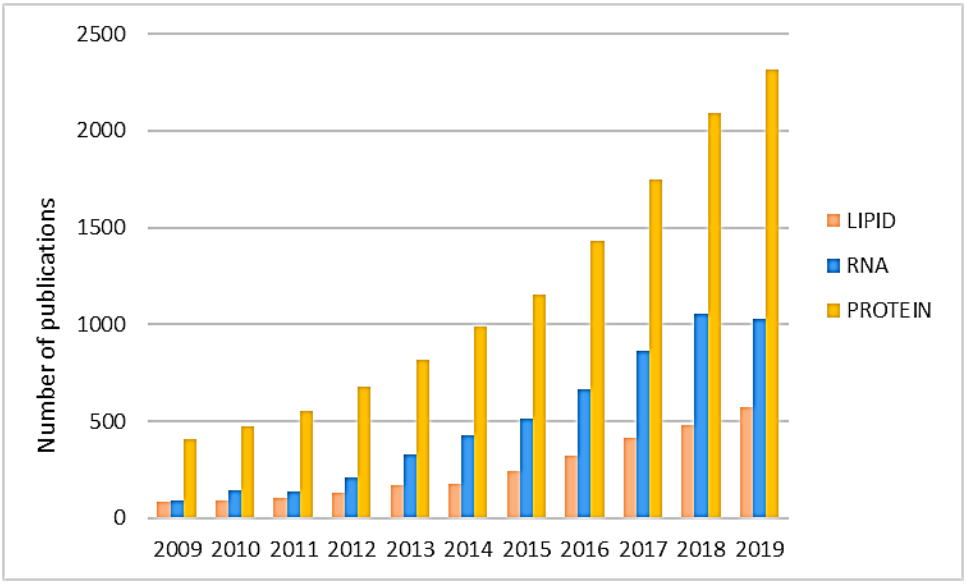

Figure 2.2. The number of published EV papers focusing on lipids, RNA or protein as structural elements or cargo published from 2009-2019. Data was taken from PubMed, using an advanced search for "extracellular vesicles" OR "exosomes" OR "microvesicles" AND "protein" or "RNA" or "lipid".

Cholesterol, phosphatidylserine and sphingomyelin are particularly abundant in EV membranes when compared to the cell membranes from which they were derived [5]. Collectively, these lipids accumulate in the tightly-packed, organised and lipid-dense regions of the EV membrane, known as lipid rafts [99]. The existence of lipid rafts on EV membranes is substantiated by the presence of the lipid raft-associated protein, flotillin-1, which is also characterised as one of the EV-enriched proteins [54]. Lipid rafts are widely considered to be essential to the stability of EVs within biofluids, as their constituent lipids are known to provide rigidity [54]. However, whether these lipid rafts are formed at the early endosome, or are endocytosed from the parent cell membrane, is yet to be established. Nonetheless, the use of EV membrane profiles as biomarkers may emerge as important.

A difference in lipid profile between urine-derived EVs (from healthy individuals) and cancer cell media-derived EVs has been observed, with higher cholesterol levels in the former [57]. This further supports the hypothesis that circulating EVs display a lipid profile that allows for their stability within biofluids. The lipid profile of EVs has received significant attention from cancer

researchers [57] [59]. Cancer cells likely exhibit a different lipid profile to aid their survival in hypoxic, acidic and ROS-filled environments.

Lipids are not only responsible for the structure of EVs but can also play a role in communication between cells. Subra *et al.* have shown the capacity for EVs to transfer a physiologically relevant concentration of prostaglandins into the cytosol of recipient cells *in vitro* [100]. The lipid nature of both the EV membranes and their cargo further highlights the role of EVs as a key role-player in intercellular communication.

2.5.3 RNA

The presence of RNAs in EV was first seen in 2006 [65]. In 2007, Valadi *et al.* identified the presence of over 1300 different mRNAs and 120 different microRNAs (miRs) in EVs using microarray profiling of RNAs that were isolated from a mast cell line (MC/9) [55]. The authors reported the mRNA and miR content in EVs in comparison to that of the parent cells and revealed an enrichment of particular RNAs in EVs. Furthermore, the same study reported the capacity of EVs to transfer RNA to recipient cells. This study raised a torrent of intriguing questions and has subsequently been instrumental in the propagation of the EV research field (see Figure 2.2).

Messenger RNA is an important intermediary in the central understanding of molecular biology since DNA is transcribed into RNA, which is subsequently translated into protein. The transport of mRNA via EVs provides a unique opportunity for its translation to protein in a separate cell/tissue from that in which it was initially transcribed. However, the RNAs found in EVs are predominantly smaller than mRNA transcripts. Indeed, EVs are known to be enriched with miR as well as the 3' untranslated region (UTR) of mRNA fragments. Other small RNAs such as piwi-interacting RNA, tRNA, rRNA, yRNA and non-coding RNA have also been detected. Of these, the most studied are miRs, which are small (± 22 nucleotides), non-coding RNAs, involved in the transient repression of mRNA translation into protein. Greater focus will be placed on these small RNAs in chapter 3.

2.6 An EVolution of myo-communication to and from skeletal muscle

The substantial proportion of SkM in human body mass has led researchers to postulate that SkM-derived EVs likely constitute a large percentage of total circulating EVs *in vivo* [50]. Subsequent research has elucidated that SkM EVs are powerful mediators of intercellular communication through their ability to alter the state of recipient cells, primarily shown by *in vitro* experimentation [101]. The analysis of circulating EVs *in vivo*, however, remains a complicated issue, as the experimental disruption of SkM usually implicates additional cell types/organs, for example, aerobic exercise may perturb both SkM and endothelial cells. Consequently, challenges remain for the determination of a pure population of SkM-derived EVs *in vivo.* The next sections will initially cover *in vitro* studies on SkM-derived EVs, after which SkM-associated changes in EVs will be investigated *in vivo*.

2.6.1 EVidence for intercellular EV communication arising from skeletal muscle

The first identification of SkM cells secreting EVs occurred in a study that used the immortalised murine C2C12 myoblast cell-line (Figure 6.1. A) [102]. Subsequently, EVs were shown to be secreted by primary human myoblasts (PHMs), too (Figure 6.1. B) [103]. Both studies considered the EV cargo in detail, using proteomics. In the first study mentioned, C2C12 myoblast-secreted EVs, released during proliferation, were shown to carry proteins predominantly involved in signal transduction. These proteins included, for example, 14-3-3 family proteins and insulin-like growth factor binding protein. When analysing differentiating PHM-derived EVs, Le Bihan *et al.* found a more diverse protein profile than hypothesised. The presence of proteins not previously considered in the process of myogenesis led them to hypothesise that myoblast-derived EVs may be important in both inter-myoblast communication as well as intercellular communication between myoblasts and other cell types. Taken together, these two studies suggest that the communication arising from SkM cells may be different depending on the degree of immaturity (proliferating) or maturity (differentiating or fully differentiated).

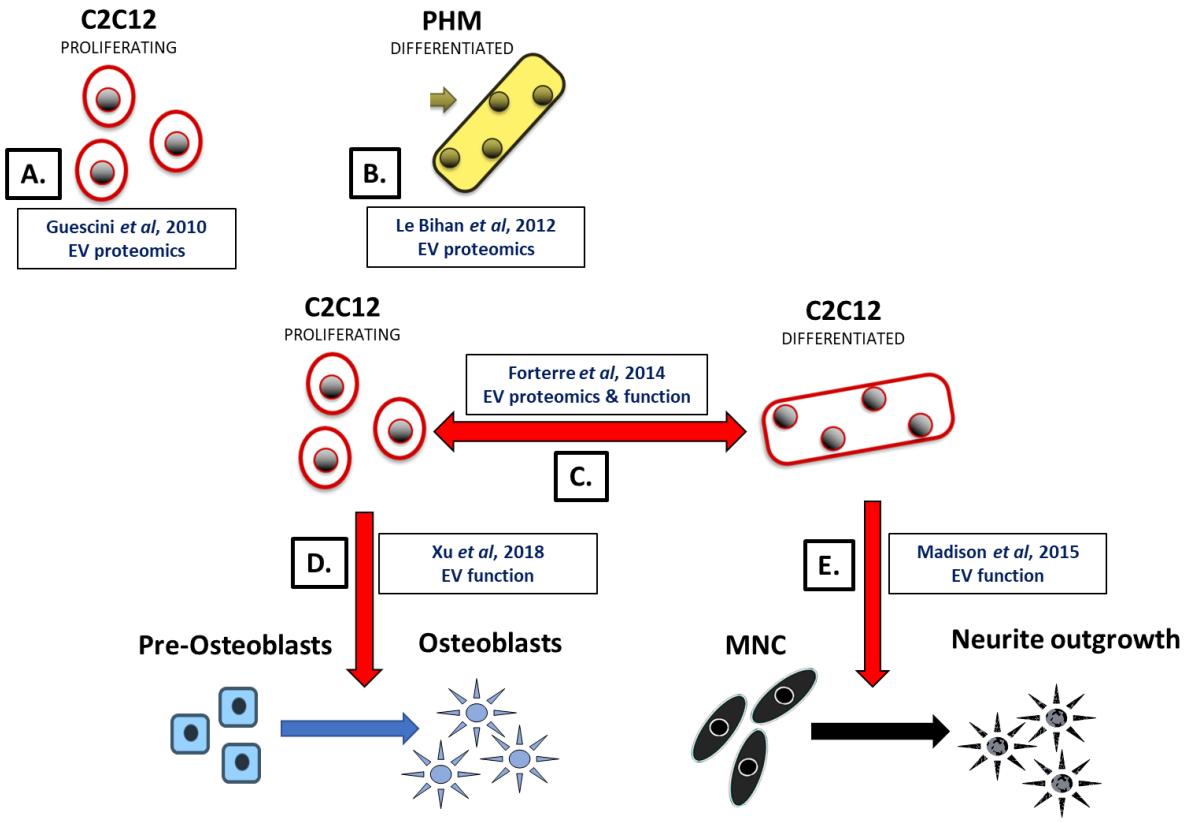

Figure 2.3. Diagramme illustrating some of the first studies to investigate EVs explicitly from skeletal muscle *in vitro*. MNC: motor neuron cell. PHM: primary human myotubes.

The differentiation of SkM relies on multiple signalling pathways to ensure the efficient alignment and fusion of myoblasts. Myogenesis, and the differentiation of myoblasts into myotubes, in particular, has proven to be a powerful catalyst for alterations of secreted paracrine factors *in vitro* [101] [104]. The first study on EV function comparing EVs derived from myoblasts and differentiated myotubes was done by Forterre and colleagues in 2014 [104] (Figure 6.1. C). Using proteomics and bioinformatics, it was confirmed that myoblasts and myotubes secreted EVs with distinct protein profiles. Thereafter, myotube-derived EVs were supplemented onto proliferating myoblasts and it was found that myoblast commitment into differentiation was accelerated. This was, at least in part, due to the downregulation of cyclin D1 mRNA and the up-regulation of Myog mRNA in the myotube-derived, EV-treated myoblasts. In an *in vitro* model of muscle damage, differentiating C2C12s were oxidatively damaged through the addition of hydrogen peroxide (H_2O_2 - an oxidative stressor when administered at 0.3 mM), and EVs were collected [105].

Isolated EVs contained increased levels of DNA and were used to treat myoblasts that had been primed for differentiation through serum removal. The EVs were derived from damaged C2C12s and as a result, the treatment effects differed from those previously described in experiments on normal myoblasts. Effects included a decrease in myotube diameter and MHC levels, and increased myoblast proliferation. In addition, these functional changes were associated with decreases in Myogenin mRNA and increases in proliferating cell nuclear antigen (PCNA).

Much work has gone into establishing the mechanisms of EV-mediated crosstalk between SkM and other tissues by examining different cell types *in vitro*. This is most often done by collecting the conditioned, EV-enriched media from one cell type and supplementing these EVs onto another cell type. It is hypothesised that myoblast differentiation is a strong stimulus for significant alterations in recipient cell phenotype that are mediated by EVs. In support of this, Madison *et al.* added myotube-derived EVs onto motor neuron cells *in vitro* and found a significant increase in cell survival and neurite outgrowth (Figure 6.1. E) [101]. This study provides insight into the possibility of EV-mediated, inter-organ communication, into the potential workings of the neuromuscular junction and its actions in regeneration, as well as a better comprehension of the transfer of muscle-derived factors to tissues other than muscle, but within their vicinity.

Considering the crosstalk between SkM and bone, Qin *et al.* showed that myostatin (MSTN), - a pivotal inhibitory growth factor in myoblast differentiation and a well-established myokine, - can alter osteogenic signalling [106]. Treatment of osteocytes with MSTN decreased the presence of cellular and EV miR-218. Furthermore, when EVs were harvested from the media of MSTN treated osteocytes and then supplemented onto osteoblasts, they caused a decrease in differentiation. This result was reversed when the osteocytes were loaded with exogenous miR-218 using a lentiviral construct. Instead of using a specific muscle-derived factor (such as the study on MSTN), Xu *et al.* used EVs released from C2C12 myoblasts and showed that differentiation of pre-osteoblasts into osteoblasts was accelerated [107] (Figure 6.1. D). Using a sequencing approach, these researchers found that an osteo-important miR, miR-27a-3p, was

enriched in myoblast-derived EVs. miR-27a-3p targets allow for the activation of the b-catenin pathway which promotes osteogenesis.

2.6.2 EVidence for EV communication to skeletal muscle

The effects of EVs in the context of SkM are not unidirectional. EVs from many other cell types exhibit the potential to alter SkM. Here, two examples will be given in the context of cancer and muscle regeneration.

In order to investigate possible crosstalk between soft-tissue cancer and SkM, Mu *et al.* designed a co-culture experiment using a sarcoma cell (K7M2) and muscle-derived stem cell (MDSC) co-cultured in a trans-well system with 400 nm pores, allowing for the transfer of media and small-sized EVs [5]. The K7M2 cells' EVs carried increased Notch mRNA when compared to the MDSC EVs, though Notch mRNA and protein expression were increased in the MDSCs. On further analysis, it was determined that EVs from the K7M2 cell line exhibited increased Notch packaging, which inhibited SkM cell (MDSC) differentiation. The addition of DAPT (a gamma-secretase inhibitor that decreases EV secretion), however, rescued myogenic potential. The researchers postulated that EVs may mediate, at least in part, cancer-associated SkM cachexia and that the mechanism may involve HSP70 & 90. Both of these heat shock proteins (HSPs) are increased in a variety of tumour cells and are known to target TLR4 receptors on muscle, resulting in SkM catabolism. The addition of HSP neutralising antibodies attenuates signs of muscle wasting both *in vitro* and *in vivo*. Conversely, the addition of recombinant HSP results in exacerbated cachexia. Since HSP70 & 90 were seen to be enriched within the blood-derived EVs from tumour-bearing mice, this mechanism of delivery and functional response in the target tissue seems feasible [75].

Mesenchymal stem cells (MSCs) are multipotent cells with key roles in the regeneration of multiple tissue types. A comprehensive study on MSC-derived EVs and SkM regeneration was published by Nakamura *et al.* [108]. These researchers elaborated on the paracrine effects of MSCs by showing that their EVs could promote myogenesis and angiogenesis in C2C12 cells and

human umbilical vein endothelial cells (HUVEC), respectively. These same effects were confirmed on SkM *in vivo*, where MSC-derived EVs were injected into the site of cardiotoxin-induced muscle injury in a mouse model.

Evidence from *in vitro* studies, therefore, suggests that skeletal muscle is not only the source of mediatory EVs but can also be modified by EVs that were generated in neighbouring tissues. It is worth considering a method of replicating these findings in a setting where both the donor and the recipient cell types, one of which would be SkM, are *in vivo*.

2.7 Extracellular vesicles and skeletal muscle *in vivo*

In various studies, EVs derived from blood samples collected from rodents or human volunteers in different states/treatments have been assessed *in vivo*. Additionally, EVs derived from conditioned media have been applied in an *in vivo* setting. Much of the current research regarding SkM-generated EVs *in vivo* focuses on muscular disease, regeneration and exercise, and therefore this pattern of review will be taken in the following sections.

2.7.1 Extracellular vesicles and their cargo in the context of skeletal muscle disease

EVs may serve as biomarkers and mediators of disease. SkM is the site for various inherited (e.g., Duchenne's muscular dystrophy) and acquired (e.g., sarcopenia and cachexia) myopathies. Both SkM injuries and myopathies currently lack efficient diagnostic, monitoring and treatment strategies, and have a high economic cost to society. Therefore, a better understanding of SkM regeneration is a necessity for the easy diagnosis and rapid initiation of treatment for these afflictions.

SkM-derived EVs have been studied in muscular dystrophy patients, investigating the potential for circulating EVs as non-invasive diagnostic tools in patient blood samples. Canonical myomiRs (as mentioned before: miR-1, 133a, 133b & 206) within EVs are elevated in Myotonic Dystrophy patients when compared to healthy controls [38]. In this study, EV myomiRs were more elevated in patients with progressive muscle wasting when compared to disease-stable individuals,

suggesting a possible use for EV myomiRs as a prognostic tool to determine and track the stage of the disease. This may aid in the more precise interpretation of systemic changes and, indirectly, the state of muscle tissue, where the number of EVs in circulation could be reflective of the disease state. Indeed, Matsuzaka *et al.* showed that *in vivo* injection of the EV secretion inhibitor, GW4869, resulted in a decrease in circulating myomiRs in whole sera of *mdx* mice (a murine model of Duchenne's muscular dystrophy) [109]. Collectively, therefore, circulating myomiR changes are present when the muscle is chronically afflicted, and these changes are reflected in circulating EVs.

Given that EVs are both released and taken up, either locally or distantly, by similar or different cell types, an understanding of the effect of serum-derived EVs is highly relevant. Two studies in the context of the mouse *mdx* model are informative in this regard. In one study, fibroblasts originating from muscle tissue were immune-magnetically isolated from biopsies derived from Duchenne's muscular dystrophy (DMD) patients [16]. The fibroblasts were cultured and the EVs isolated from that media displayed an increased miR-199a-5p content. When these EVs were supplemented onto control fibroblasts from healthy individuals a myofibroblastic phenotype was noted (i.e., increased α-smooth muscle actin, collagen and fibronectin). Myofibroblasts are an important cell type in the development of fibrosis in the musculature. Indeed, when DMD fibroblast-derived EVs were injected into mice following a cardiotoxin-induced injury, a subsequent increase in fibrosis was seen [16]. In contrast, when EVs harvested from *mdx* mouse serum were added to C2C12 cells, cell survival was improved over 24 hours, suggesting that EVs may contain factors that mitigate muscle degeneration [109]. The exact mechanisms of this action remain to be determined, however.

SkM and EV research has not been limited to the analysis of myomiR cargo. Frattini *et al.* established an *in vivo* model of alpha-dystroglycanopathy by generating Fukitin-related protein (FKRP) knockout mice [110]. The FKRP gene mutation results in defective alpha-dystroglycan glycosylation, which leads to a loss in sarcolemma integrity. CD133 positive cells (hematopoietic stem cells) were isolated from FKRP knockout mice after which the wild type FKRP gene was transfected into these cells *in vitro*. They subsequently re-injected these transduced cells into the

tibialis anterior muscle of knockout mice, noting a proportion of plasma-derived EVs that were positive for the wildtype FKRP gene two weeks post-injection. The successful addition of the wild type gene was able to increase alpha-dystroglycan expression in the TA.

2.7.2 Extracellular vesicles and their cargo in the context of skeletal muscle regeneration

Synchronised cell-to-cell communication and tissue crosstalk are critical during the orchestrated signalling processes of SkM regeneration. With its high force output as well as its anatomical proximity to bone, which is far less pliable, SkM has a high likelihood of injury during sports, exercise and some everyday activities. However, despite significant research on the involvement of SkM in systemic communication via myokine signalling to nearby cell types during regeneration, a paucity of information is available regarding the additional role of EVs in such communication.

Choi *et al.* [111] demonstrated that EVs, derived from differentiating primary human myoblasts, can decrease the fibrotic area and enhance regeneration at the injury site of experimentally-lacerated mouse muscle *in vivo*. Important for understanding the conserved nature of EVs, this study demonstrated that EV-encapsulated signals for myogenesis may be conserved across species (i.e., human to mouse).

Further illuminating the role of EVs in the context of SkM regeneration, Fry *et al.* [112] have shown that EV myomiR-206, secreted by myogenic precursor cells, can control the collagen and fibronectin synthesis as well as deposition of fibroblasts. This conclusion was founded on their evidence for the EV-mediated transfer of myomiR-206 *in vitro* and *in vivo* and its subsequent repression of the ribosomal binding protein 1 (a master regulator of collagen synthesis) mRNA transcript. This study provided detailed insight into how satellite cells may regulate their microenvironment, as the depletion of satellite cells in Pax7 knockout mice has been shown to cause greater extra-cellular matrix (ECM) deposition *in vivo*. This pivotal study described a

paracrine action for EVs, whereby communication occurred between different cell types with independent functions and within a specific microenvironment.

2.7.3 Extracellular vesicles and skeletal muscle in the context of exercise

The relatively new research involving EVs and exercise science has combined prior knowledge from the fields of microRNAs (miRs) and exercise science. miRs have been extensively investigated in SkM tissue samples as well as in circulation. Initially, the analysis of miRs in blood samples relied on the extraction of total RNA. Only a few studies have investigated whether or not it was encapsulated/complexed into EVs. Different modes of exercise have been shown to release a different profile of miRs into the blood, yet less is known about the EV-miR profile in response to exercise, specifically [113]. In addition, EVs carry forms of cargo other than miRs. The physiological function of these specific changes is unknown and could represent a preferential release or a method of clearance.

Within the context of human aerobic fitness, Guescini *et al.* examined both miR and protein cargo of EVs [50]. Their study demonstrated that the baseline expression of most myomiRs within plasma EVs is positively correlated with VO_2max. Furthermore, they showed that the SkM-specific myomiR-206 was enriched in alpha-sarcoglycan-positive EVs when compared to either all plasma EVs or non-immuno captured supernatant. Alpha-sarcoglycan (SGCA) is an important muscle membrane protein. These forms of separation provide greater certainty for the SkM origin of some circulating EVs. The researchers established that 1-5% of circulating EVs were SGCA-positive. The number of EVs identified as SGCA-positive may change after exercise, but this remains to be properly elucidated. In the same year, Kramers *et al.* shed light on the transient release of EVs into circulation following aerobic exercise, showing elevated EV numbers immediately after exhaustive cycling [114]. The levels returned to baseline 90 min post-exercise. This study provided evidence for the immediate rise and rapid fall in circulating EVs following non-weight-bearing exercise. Following exhaustive treadmill running, however, the authors point out that a more sustained increase in EVs was seen, with elevations remaining significant at the sampling timepoints of baseline, immediately post and 90 min post-exercise. It remains to be

determined, however, to what proportion the muscle tissue may have contributed to this change, as many other cell types are also involved in the physical response to exercise [42].

Limited data is available regarding EV cargo changes following various types of exercise. However, previous research focusing on general circulating miRs, without EV analysis, has shown that myomiRs in plasma exhibit larger changes in response to muscle-damaging, eccentrically-biased exercise than seen with resistance or aerobic exercise [113]. In lieu of this, our group has previously reported a decrease in EV miR-31-5p (a miR with importance in myogenesis) following two consecutive bouts of muscle-damaging exercise [51]. Notably, the most pronounced change in circulating myomiRs was seen at 6 hours post-exercise in the Banzet *et al.* study, yet the largest change in circulating EV miRs occurred at 24 hours post-exercise in our study. Interestingly, both changes occurred at the peak circulating creatine kinase time-point. In delineating differences such as these, D'Souza *et al.* (2018) measured the abundance of 29 selected circulating miRs previously associated with a response to exercise, in muscle tissue, whole plasma and EVs. They found that, following aerobic exercise, there was no notable consistency in miR alterations between the different types of samples. Furthermore, the changes were not relatable in either timing or magnitude. They also found that EVs exhibited the most discernible changes in miR abundance and suggested that the vesicles may hold value as a distinct and relevant form of intercellular communication. However, this study investigated miR responses to aerobic exercise, and the temporary changes in these tissues following damage and regeneration remain to be determined.

Both EV biology and the physiological responses to exercise are uniquely complex. In the search for exercise and/or SkM biomarkers, the presence of circulating cell-free DNA in blood has been investigated. Circulating DNA is present despite an abundance of circulating nucleases, which led Helmig *et al.* to investigate the possible relationship of EVs with this phenomenon [115]. In their experimental model of exhaustive exercise, they showed that most cell-free DNA was found in the plasma supernatant, rather than within EV fractions, concluding that results would not be contaminated provided that EVs are appropriately isolated before cargo analysis.

Brahmer *et al.* showed that a large proportion of EVs released into circulation originates from platelets, leukocytes and endothelial cells; determined by a multiplexed, immune-coupled, magnetic bead sandwich capture [42]. Blood was taken at baseline, at a respiratory exchange ratio of 0.9, and immediately after an exhaustive, incremental cycling protocol. The exercise intervention was not found to elicit any changes in particle number, although, modifications of EV-related proteins, such as Alix and LAMP-1, suggested a post-exercise increase in EV numbers. In support of this, an increase in EV-associated proteins following exercise has previously been shown by Whitham *et al.* [116]. These researchers also provided evidence that chylomicrons and/or some low-density lipoprotein species provide a substantial quantity of particles picked up by nanoparticle tracking analysis. This was determined by comparing participants after a high-fat meal and after fasting, which indicates that fasting status is important for more accurate assessment of circulating EVs.

In a study investigating the cardio-protective benefits of exercise, Hou *et al.* looked at EVs at baseline and 24 hours after 4 weeks of swim-training in rats [117]. Similar to our previous study, they found no significant change in EV number 24 hours post-exercise [51]. EVs from trained rats showed cardio-protection following experimental I/R injury. Through miR sequencing, these researchers found that EV miR-342-5p was a key cargo component for this protection; where miR-342-5p inhibition significantly blunted the cardio-protective effects of EVs. They found that this cardio-protection was achieved through the targeting of Caspase-9 and Jnk2 mRNA. They also showed that exercise training or laminar shear stress significantly increased the abundance of miR-342-5p in endothelial cells.

Yin *et al.* [118] made use of both downhill (DHR) and uphill running (UHR) in rats to determine EV myomiR changes in plasma. Although no change in EV myomiRs was seen after UHR, all EV myomiRs were shown to increase immediately post-exercise. Interestingly, these all returned to baseline levels at 24 hours post-exercise.

Chapter 3: microRNA

3.1 An introduction to microRNAs

MicroRNAs (miRs) are a group of small, non-coding RNAs that are approximately 22 nucleotides in length and are involved in gene regulation [119]. The first description of miRs occurred nearly three decades ago (1993) by Lee *et al.*, who, in researching the developmental stages of C. elegans discovered that the gene, Lin-4, encoded a small, 22 nucleotide RNA fragment rather than a protein [120]. They found that this fragment was complimentary to the 3′ untranslated region (UTR) of Lin-14 mRNA, a gene of known importance in embryogenesis, and suggested that some form of RNA to RNA interaction/regulation may contribute in the maturation from embryogenesis to adult cell development [120] [121]. Around the same time Wightman *et al.* showed that there was a significant decrease in Lin-14 protein with no concomitant decrease in Lin-14 mRNA during C.Elegans development [122]. Together, these two groups were credited with the discovery of microRNA and showing that microRNA was involved in repressing mRNA translation. It was later established that another gene in C.Elegans, Let-7, also encoded a small RNA fragment [123]. These small RNAs were then termed "small, temporal RNAs" due to their timely involvement in C. elegans development [119]. Soon after, the first use of the term "microRNA" was published by Lagos-Quintana *et al.,* where a host of new miRs were also discovered [119]. They found that many of these miRs were present in an array of other species, including humans [124]. Novel miRs are still being discovered, as well as their specific roles in gene regulation [125].

In humans, miRs are now known to exert their effects through the transient repression of mRNA translation [120] [121] [122]. This repression is achieved through the incomplete binding, that is only partially complimentary, of a miR to an mRNA transcript. It is the miR seed sequence of approximately 6-8 nucleotides (nts) at the 5′ end of an miR that is of most importance in recognizing mRNAs with specificity [126]. It has also been found that miRs predominantly bind the 3′ untranslated region (UTR) of mRNA transcripts to prevent expression [123]. It has also been reported that miRs can activate gene expression under specific conditions [127]. In plants most miRs

bind with complete complementarity, and seemingly always result in mRNA degradation [128]. However, due to the incomplete binding of human miRs, these miRs possess the unique ability to target multiple mRNA transcripts [129]. Consequently, predictive tools regularly establish approximately 300 proposed targets per miR. It is thought that miRs have the ability to target approximately 60% of the human genome [130]. It is now well known that one mRNA transcript can be targeted by more than one miR, and it is possible for one miR to bind one mRNA transcript at multiple sites [131]. This convolution of information makes the establishment of definitive miR roles challenging.

3.2 microRNA biogenesis

miRs are either encoded within their own loci in intergenic regions, or from within the introns or exons of other genes, termed "host genes" [132]. RNA polymerase 2 is an important enzyme that transcribes these loci into RNA transcripts, which immediately fold back on each other to form a partly double stranded hairpin-like structure, termed a primary miRs (Figure 3.1). Cleavage of this semi-looped strand of RNA by the enzymes Drosha and DiGeorge syndrome critical unit 8 (DGCR8) within the nucleus results in a 60-70 base pair stem-loop structure, termed a precursor miR (Figure 3.1.A). This configuration is necessary for the precursor miR to be recognized and exported out of the nucleus by Exportin 5. However, knockout (KO) experiments have shown that there exists both a canonical and non-canonical miR biogenesis pathway e.g. Drosha KO results in a complete abolition of canonical miR pathways [133]. Nevertheless, once in the cytosol, the precursor miR can be cleaved into two ± 22 nucleotide mature miR transcripts (from here on referred to as miRs) by the enzyme dicer [134] (Figure 3.1.B). Due to poorly understood mechanisms one mature miR (i.e. a leading strand) is then selectively incorporated into a conglomeration of proteins known as the RNA-induced silencing complex (RISC), whilst the other (i.e. a passenger strand), which is often not 100% complimentary, is thought to be ubiquitin-tagged for degradation (denoted by a "*" suffix) [135]. RISC proteins facilitate miRs in their transient repression of messenger RNA (mRNA), a process that is largely thought as predominately intracellular. However, RISC-family proteins have been detected in blood [136]. miRs can be complexed with

high-density lipoproteins or protein aggregates, the latter of which is poorly understood [137]. miRs can also be transported by extracellular vesicles. Whether or not these miRs are sorted into EVs with the aid of RISC family proteins is not yet known.

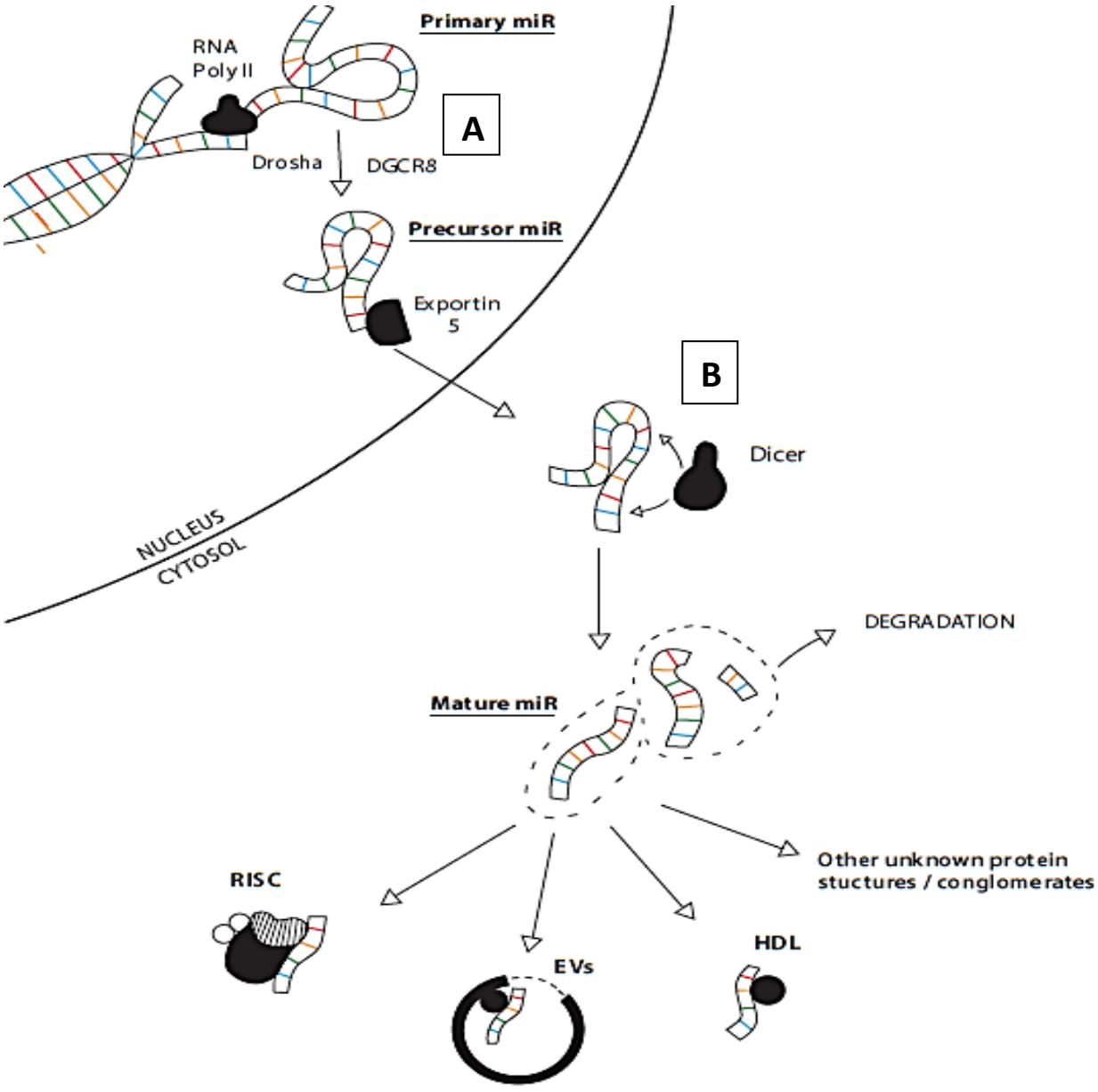

Figure 3.1. Diagram showing the key steps in microRNA biogenesis. **A** depicts intra-nuclear splicing of a primary miR by Drosha and DGCR8 to form a precursor miR. **B** shows the extra-nuclear action of Dicer, forming a mature miR, which is then sorted into complexes/vesicles.

3.3 microRNA nomenclature

miRs are named according to their position on their stem loop precursor, either at the 5p or 3p end (i.e. miR-133a-3p & miR-133a-5p), both with unique functions. As mentioned before, one of these transcripts is often expressed at a lower level or is degraded, and it is even possible that one of the transcripts may not be present at any level whatsoever [138]. However, it is important to note that an undetectable mature miR could be present yet not detected due to different rates of synthesis and degradation, and it is therefore important to consider the temporal expression of miRs [139]. Furthermore, it is conceivable that these miRs bind quickly to a target mRNA strand, or are only present in certain species [128]. Two miRs from completely different chromosomes can result in sequences that differ by just one nucleotide. These near-identical miRs are denoted with the suffix a or b (i.e. miR-133a vs miR-133b). Similarly, two identical transcripts can be processed from different chromosomes. These identical miRs are labelled with the suffix 1 or 2 (i.e. miR-1-1 & miR-1-2) and can be derived from different stem loop precursors.

3.4 A miRacle of skeletal muscle: myomiRs

miRs have been found in most, if not all, cell types and tissues [124]. SkM exhibits a unique profile of tissue specific or enriched miRs that have been termed "myomiRs" ("myo" = muscle and "miR" = microRNA) [140] [141]. A tissue specific miR is defined as being present in greater than 20-fold abundance in that tissue when compared to its average in other tissues, whereas a tissue enriched miR is detected in greater abundance in that tissue but in less than 20-fold greater abundance [142]. Originally, the term myomiRs encompassed just four archetypal SkM miRs; myomiR-1-3p, 133a-3p, 133b and 206 [143]. The definition of myomiRs later expanded to include myomiR-486-5p, 208a-3p, 208b-3p, and 499a-5p, of which myomiR-208a-3p, 208b-3p and 499a-5p are transcribed from within the host genes of muscle-enriched protein (i.e. myosin heavy chain). A total of eight myomiRs have thus been identified to date; six are present in both cardiac and SkM, whereas each muscle type has one that is specific to that tissue. miR-208a-3p is cardiac-specific, whereas miR-206 is the SkM-specific miR [142]. The eight myomiRs are therefore: miR-1-3p, miR-133a-3p, miR-133b, miR-206, miR-208a-3p, miR-208b-3p miR-486-5p and miR-499a-5p (Figure 3.2).

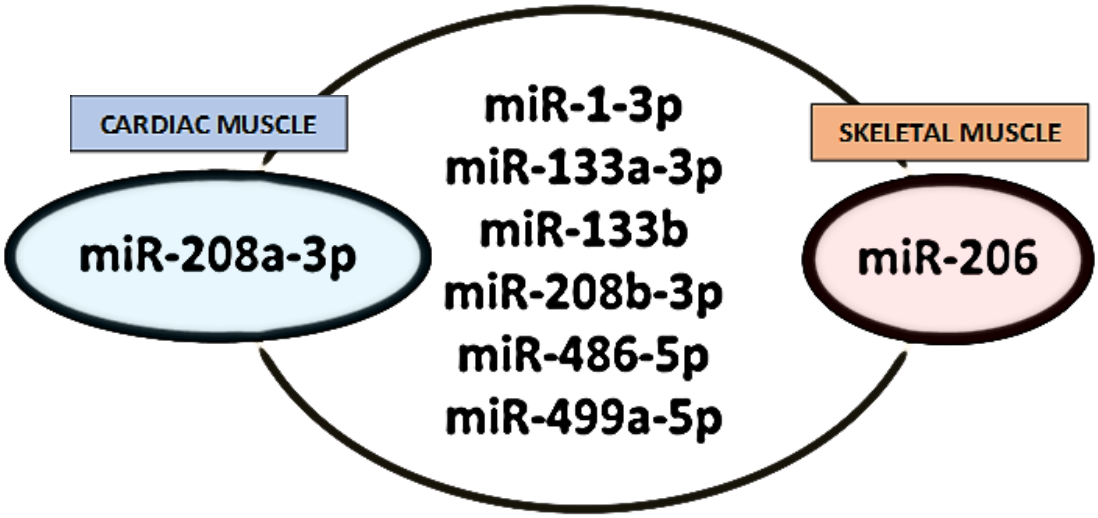

Figure. 3.2. A summary of the eight myomiRs named to date, including the skeletal muscle specific and cardiac specific myomiRs.

Principles that hold true for all miRs need to be considered when looking at myomiRs too. For example, myomiRs exist in gene clustering. The four original myomiRs exist in bicistronic gene clusters (Figure 5.1 A & B). With two genes in close proximity (within ± 10 kbp) in each myomiR gene cluster, the three resulting gene clusters are:

- myomiR-1-3p-1 and myomiR-133a-3p-2
- myomiR-1-3p-2 and myomiR-133a-3p-1
- myomiR-133b and myomiR-206

What can be seen is that the first two clusters listed here each have different "versions" of miR-1-3p and miR-133a-3p, whereas the third cluster does not overlap with the other two. It is not known whether these duplicate gene clusters (miR-1-3p-1 and miR-1-3p-2) imply redundancy. Clustered genes are known to produce transcripts or proteins with similar functions and are designated as a gene family. The case of the myomiR-1-1 and 1-2 gene clusters provides insight into miR complexities. Although these two separate gene clusters arise from different chromosomes they result in primary transcripts with the same -3p sequence. These -3p transcripts arise from two different precursor miRs that are transcribed from these genes, yet only miR-1-1 exhibits a detectable -3p and -5p mature miR. myomiR-1-1 and 1-2's clustered genes, miR-133a-1

and 133a-2 respectively, both produce mature -3p and -5p transcripts. miR-133a-2 spans both an intron and exon, highlighting the unique mode in which miRs can be transcribed (Figure 3.3. A).

As mentioned earlier, miRs are often located within the introns or exons of host genes. Interestingly, some myomiR gene loci are within host genes encoding muscle enriched proteins. Considering the two types of striated muscle, cardiac and skeletal, it was mentioned above that miR-208a is a cardiac-specific myomiR. It exists as a miR-208a / MYH6 / -208b / MYH7 miR-gene/host-gene cluster. miR-208a is within an intron of MYH6 (cardiac-enriched myosin isoform) host gene, whilst miR-208b is within an intron of MYH7 (skeletal muscle-enriched myosin isoform) host gene (Figure 3.3. C). The miR-499a gene is found within the myosin heavy chain isoform 7B (MYH7B) host gene, the protein of which is enriched in cardiac and skeletal muscle. These genes form the miR-gene/host-gene cluster: miR-499a / -499b and MYH7B (Figure 3.3. D). However, only miR-499a and not miR-499b is within the MYH7B gene.

miRs are often aligned in the same direction as their host gene, suggesting that they are transcribed together. However, this is not always the case. The incomplete understanding of miR gene transcription is highlighted when looking at the miR-486-1 / -486-2 / Ankyrin 1 (ANK1) gene cluster (Figure 3.3 E). miR-486-1 exists within the ANK1 host gene, yet miR-486-2 (seemingly uniquely) is transcribed in the opposite direction, rather than along, the coding strand, of this host gene. These two myomiR-486 genes are transcribed into different precursor miRs with different lengths and different hairpin structures, yet both result in the exact same mature -3p and -5p transcripts. These genes do not show complementarity to each other, but rather the mature -3p of one miR is derived from a region complimentary to the mature -5p miR of the other gene, and vice versa. This uncomplimentary, palindromic, mirror transcription is allowed by both the -5p transcripts being 22 nts, and both -3p transcripts being 21 nts. An accumulating body of evidence points toward miR-486-1-5p being the most enriched miR found in baseline human blood samples [144]. However, little is known regarding this gene's function [144].

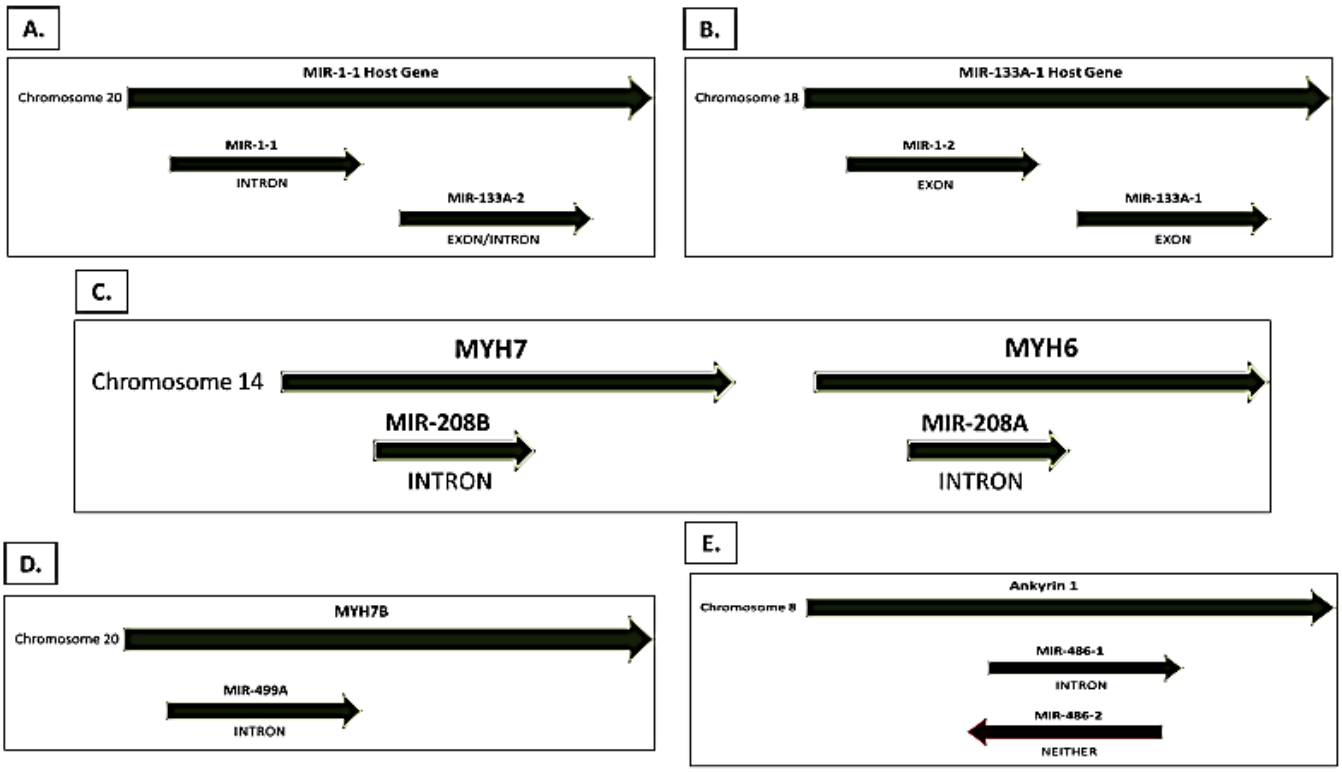

Figure 3.3. Schematic showing the clustering of myomiRs, as well as their position within host genes.

3.5 Circulating microRNAs

Human blood contains an abundance of RNases, and it is therefore easy to consider that RNA is somehow protected within circulation (i.e. within protein conglomerates or EVs). Indeed, it has been shown that miRs are present in a diverse range of extracellular fluids, including serum, plasma, saliva, and urine [35] [145]. This knowledge is attractive to many researchers, such as those looking at biomarkers for a variety of diseases, inter-organ communication, regeneration, normal physiology, and therapeutics. Importantly, miRs can be delivered to targeted cells or organs and influence several cellular processes [66]. The ability to detect actively secreted genetic material in circulation could potentially provide a novel level of interpretation in physiology. The emerging field of this type of cellular communication has been termed "horizontal genetic information transfer", and its capture has formed part of liquid biopsy.

EVs initially offered an easy explanation for the presence of intact miRs in circulation, however, new carriers have come to light [146]. Lasser *et al.* have shown that extracellular RNAs can be carried by lipoproteins, EVs, ribonucleo-proteins and currently unidentified carriers [147]. Each avenue likely representing a distinct avenue of biomarker research [148].

It is important to consider that circulating miR abundances are the sum of release, clearance and uptake rates. These miR dynamics have been highlighted in a study by Coenen-Stass *et al.*, showing that different miRs had different half-lives, and that this was seemingly sequence dependent; with a greater half-life being proportional to a higher GC content [139]. This GC-dependent stability in circulation complicates the interpretation of circulating miR results following an intervention, as these miRs display their own temporal pattern in response to a perturbation [51].

3.6 myomiRs and exercise

Since the first paper relating to myomiRs and exercise in mice was published in 2007 [149], a significant body of work has gone into identifying myomiR changes in response to exercise. This is perhaps owing to the promise of biomarker discovery for differing exercise parameters related to e.g. cardiovascular fitness or the state of hypertrophy or injury.

3.6.1 myomiR changes following a single bout of exercise

The following is a detailed chronology of studies involving exercise and myomiRs. Much of the earlier studies involve the analysis of canonical myomiRs; miR-1, 133a, 133b and 206, with later studies including the analysis of additional myomiRs; miR-208b, 486 and 499. Many of the early studies also determined myomiR abundances in SkM tissue lysates only. Later studies have incorporated the analysis of circulating myomiRs in blood, or both SkM tissue lysates and blood [148]. Following this chronological overview, a summary is presented in Table 3.1.

To begin with, McCarthy *et al.* were the first to show a change in myomiR abundances in SkM lysates following an acute bout of resistance exercise in mice [149]. These researchers showed that 1

week of overload of the *plantaris* muscle (with bilateral synergist ablation of the *gastrocnemius* and *soleus* muscles) caused a decrease in both myomiR-1 and 133a abundances within *plantaris* lysates. With the purpose of comparing the responses of young versus older men, Drummond *et al.* investigated the response of volunteers subjected to a combination of an acute bout of resistance exercise, along with the ingestion of essential amino acids [150]. This intervention, which is essentially less severe than synergist ablation, or at least of a briefer time course, was enough to induce a decreased abundance of myomiR-1 in *vastus lateralis* lysates in young male participants at 3 and 6 hr post-exercise, with no change in older male participants. Together these two studies showed that there was a decrease in tissue abundance of some myomiRs post-resistance exercise.

Considering aerobic exercise interventions, Safdar *et al.* were the first to determine myomiR responses to 90 min of running [151]. Again, this first study concerning prolonged exercise was done in mice rather than in human volunteers. In the *quadriceps femoris*, myomiR-1 increased 3 hr post-exercise, with no change noted in myomiR-133a. The increase in myomiR-1 transcripts following an aerobic bout contrasted the decrease seen after resistance exercise.

In 2008, using qPCR, Mitchell *et al.* showed for the first time that selected miRs were stable in circulation, and could be used to delineate between prostate cancer patients and healthy controls [152]. Mizuno *et al.* were the first to explicitly investigate myomiRs in serum of mice following exercise, however, did not find any change in miR-1, 133a and 206 in a mouse model of Duchenne's muscular dystrophy (mdx) following an acute bout of aerobic exercise (i.e. incremental running) [153]. In contrast, the serum abundance of myomiRs was higher in mdx mice when compared to wildtype mice at baseline. Additionally, myomiR abundances were not found to change in mdx mice following the exercise intervention. Interestingly, it is now well established that circulating myomiRs are increased in mdx and muscular dystrophy serum in both mouse models and human patients [146 154 155].

Baggish *et al.* determined that plasma myomiR-133a was not changed pre or post an acute bout of aerobic exercise in competitive athletes, a finding that was repeated after 90 days of training [156]. Conversely, in comparing miR responses to three different types of exercise, it has been shown that plasma myomiR-133a abundances increased after a marathon as well as after eccentric

resistance exercise, but not after an acute exhaustive bout of 4 hr cycling [157]. Substantiating the potential of eccentric exercise to be a strong impetus for circulating myomiR changes it has been shown that myomiR-1, 133a, 133b and 208b were increased 6 hr post an acute bout of eccentrically-biased exercise (downhill walking), but not after concentrically-biased exercise (uphill walking) in humans [113]. These researchers thus went on to suggest that circulating myomiRs may serve as potential biomarkers for muscle damage. This would hold particularly for an acute bout, at this stage of the published literature. Aoi *et al.* showed that serum myomiR-486 decreased after both an acute bout of exercise (steady state cycling for 1 hr) and after a 4 wk aerobic training programme [158].

In SkM it is possible to measure changes in the proteins responsible for exosome biogenesis (or their transcripts) as well as the miRs that may become the cargo. Russell *et al.* analysed *vastus lateralis* biopsies and showed that an acute bout of aerobic exercise was sufficient to increase Drosha and Exportin 5 transcripts 3 hr post-exercise, with a concomitant increase in myomiR-1, 133a and 133b. This effect may have been less due to the aerobic nature of the exercise and more because the intervention was exercise.

Rivas *et al.* showed that myomiR-133a and 133b increased in muscle lysates from human biopsies 6 hr post an acute bout of resistance exercise [159]. This finding, however, was not repeated in old individuals. Suggesting a role for myomiRs in anabolism, Camera *et al.* [160] used a combined resistance and aerobic exercise bout, along with supplementation of either whey protein or a placebo. Here they chose a combination exercise in aiming to elucidate "anabolic interference", whereby concurrent aerobic exercise (with resistance exercise) attenuates muscle hypertrophy. They found that myomiR-133b increased in human *vastus lateralis* lysates at 4 hr post-exercise in the whey protein supplemented group only.

A series of three studies allowing for conclusions regarding high intensity exercise was published by Cui *et al.* between 2015 and 2017. The first study showed that there was a decrease in circulating myomiR-1, 133a and 133b post an acute bout of high-intensity aerobic exercise in humans, with no change in myomiR-206 and 499 [161]. A study with a longitudinal-comparative design determined myomiRs in plasma pre and post either high-intensity interval exercise (HIIE:

intensity determined by heart rate), or vigorous intensity continuous exercise (VICE) over the same distance performed by the same participants 3 weeks later. The results indicated that plasma myomiR-1, 133a, 133b and 206 abundances increased after both, with miR-1 increasing significantly more after VICE when compared to HIIE [162]. This indicates that the first 4 respond to both the intensity and the volume of exercise whereas miR-1 appears to be related to volume. Cui *et al.* compared plasma miRs pre, immediately post, 1 and 24 hr post of participants randomly assigned to an acute exercise bout aimed at either strength endurance (16-20 reps at 40% of 1 rep max), hypertrophy (12 reps at 70% of 1 rep max) or maximum strength (6 reps at 90% of 1 rep max) [163]. MyomiR-208b decreased immediately post strength endurance exercise and remained decreased at 24 hr post. In response to the bout of hypertrophy, myomiR-133a decreased post, whereas myomiR-133b increased at 24 compared to post, and myomiR-206 increased at 24 hr when compared to immediately post exercise. For max strength, myomiR-133a decreased post, and myomiR-133b increased at 1 hr vs post. This study showed that circulating myomiRs show unique time-course changes in response to differing strength training loads and/or intensities

Responses, or the extent of response, to any type or intensity of exercise may differ depending on the training status of the volunteers. Most of the above studies were done in healthy human volunteers; here, a brief overview of studies on trained athletes will be presented. Wardle *et al.* found no difference in myomiR-1, 206 or 499 at 12 hr post-exercise resting plasma between endurance-trained and resistance-trained athletes, and untrained individuals [164]. Denham *et al.* [165] showed that endurance athletes exhibited significantly higher myomiR-1 and 486 plasma abundances when compared to healthy controls. In healthy subjects, myomiR-1, 133a and 486 increased immediately after an acute bout of max aerobic exercise. D'Souza *et al.* looked at both VL lysates and plasma of trained athletes at BL, 2 and 4 hr post an acute bout of high-intensity interval training in humans. myomiR-133a was the only miR to change in plasma, showing an increase at 4 hr post. In VL, myomiR-133a and 206 increased at 2 hr, and myomiR-486 increased at 4 hr.

	Year	Type of exercise	Sample	Timepoint	Notes	miRs measured	miR changes
McCarthy *et al.*	2007	Resistance	Mouse *P*	BL & Post	Overload-induced hypertrophy	miR-1, 133a & 206	Decrease miR-1 & 133a (Post)
Drummond *et al.*	2008	Resistance	Human *VL*	BL, 3 & 6 hr	Amino acid supplementation	miR-1, 133a & 206	Decrease miR-1 (3 & 6 hr)
Safdar *et al.*	2009	Aerobic	Mouse *QF*	BL & 3 hr		miR-1 & 133a	Increase miR-1 (3 hr)
Mizuno *et al.*	2011	Aerobic	Mouse serum	BL, 0.5, 6 & 48 hr	mdx mouse	miR-1, 133a & 206	No change
Baggish *et al.*	2011	Aerobic	Human plasma	BL & Post	Exhaustive cycling	miR-133a	No change
Banzet *et al.*	2013	Aerobic	Human plasma	BL, Post, 2, 6, 24, 48 & 72	Uphill vs Downhill walking	miR-1, 133a, 133b & 208b	Increase miR-1, 133a, 133b & 208b (6hr. Downhill only)
Aoi *et al.*	2013	Aerobic	Human serum	BL & Post	Other miR abundance too low to compare	miR-1, 133a, 133b, 206, 208b, 486 & 499	Decrease miR-486 (Post)
Russell *et al.*	2013	Aerobic	Human *VL*	BL, 3 hr & 48 hr	Drosha, Dicer & Exportin-5 increased 3 hr post	miR-1, 133a, 133b & 206	Increase miR-1, 133a & 133b (3 hr)
Uhlemann *et al.*	2014	Resistance	Human plasma	BL, Post & 1 hr	Eccentric	miR-133a	Increase miR-133a (Post)
Rivas *et al.*	2014	Resistance	Human *VL*	BL & 6 hr	No change in older participants	miR-1, 133a, 133b, 208b, 486 & 499	Decrease miR-133a & 133b (6 hr)
Cui *et al.*	2015	Aerobic	Human plasma	BL & Post	Intensive sprint cycling	miR-1, 133a, 133b, 206 & 499	Decrease miR-1, 133a & 133b (Post)
Wardle *et al.*	2015	Resistance & aerobic	Human plasma	BL & 12 hr		miR-1, 133a, 206 & 499	No change
Camera *et al.*	2016	Resistance & aerobic	Human *VL*	BL & 4 hr	With protein ingestion	miR-1, 133a, 133b & 486	Increase miR-133b (Protein group only)
Cui *et al.*	2016	Aerobic	Human plasma	BL, Post HIIT & Post VICE	VICE 3 days after HIIT	miR-1, 133a, 133b & 206	Increased miR-1, 133a, 133b & 206 (Post HIIT & VICE)
Cui *et al.*	2017	Resistance	Human plasma	BL, Post, 1 hr & 24 hr	Strength endurance (SE), hypertrophy (H) & max strength (MS)	miR-1, 133a, 133b, 206 & 208b	SE: decrease miR-208b (Post & 24) H: decrease miR-133a (Post), 133b (24 hr) & increase miR-206 (24 hr) MS: decrease miR-1 (Post) & increase miR-133b (1 hr)
Denham *et al.*	2018	Aerobic	Human whole blood	BL & 0.5hr	Sprint interval training	miR-1, 133a, 133b & 486	No change
D'Souza *et al.*	2018	Resistance	Human plasma & *VL*	BL, 2 & 4hr		miR-1, 133a, 133b, 206, 208b, 486 & 499	VL: Increased miR-133a (2 hr), 206 (2 hr) & 486 (4 hr) Plasma: Increase miR-133a (4 hr)

Table 3.1. Chronological detailing of some of the first studies involving exercise and myomiRs. BL = baseline, *VL = vastus lateralis, QF = quadriceps femoris* and *P = plantaris.*

3.6.2 Exercise training

Compared to myomiR changes following an acute bout of exercise, fewer studies have investigated their alterations in response to exercise training. In 2011, Davidsen *et al.* determined the changes in myomiR abundances in *VL* lysates of healthy young individuals before and after a 12 wk resistance training programme, and found no myomiR change in muscle lysates [166]. Even when considering responders who increased strength to non-responders despite the training, neither sub-group changed. Conversely, 5 months of resistance training has been shown to cause a decrease in *VL* lysate myomiR-133b in older sedentary individuals (65 - 80 years) [167]. These differing results may be explained by differing training loads, and/or the different muscles recruited (i.e. the latter study particularly focused on knee extensor exercises). Importantly, the changes were only seen in sedentary subjects, perhaps adapting the most to the exercise regimen. A shorter duration of training intervention, just 8 days of resistance training, has been shown to be enough to decrease *gastrocnemius* myomiR-133b abundance in sedentary rats [168]. However, this particular myomiR showed no change in obese rats after resistance training. Two other miRs that showed no change in lean rats with training were myomiR-1 and 133a. Both these myomiRs increased in trained obese rats when compared to obese sedentary. This study highlights that although myomiR-133a and 133b differ by just one nucleotide, they seemingly act in different pathway (Note: myomiR-1 and 133a, and myomiR-206 and 133b are gene clusters).

An aerobic exercise training programme (12 weeks of endurance training in trained subjects) has been shown to result in a decrease in the four canonical myomiRs in *VL* lysates after 60 min of cycling, which reverted back to pretraining levels after 2 wk of training cessation [169] These researchers also showed that myomiR-1 and 133a increased in *VL* lysates 1 hr post an acute bout of aerobic exercise. Denham *et al.* found that plasma miRs following 6 wk of sprint interval training in untrained males [170]. Blood was sampled at baseline and between 2 and 4 days after their final session. Training decreased circulating myomiR-1, 133a, 133b and 486, a result which was not found after an acute bout of sprint interval training.

Nie *et al.* showed an increase in *tibialis anterior* myomiR-133a after 6 wk of aerobic exercise training in mice [171]. A different approach to investigating the effect of daily muscle loading, is to remove the load. Egawa *et al.* showed that unloading of mouse hindlimbs decreased myomiR-1 in *soleus* lysates following 2 wk of unloading [172].

3.6.3 A marathon

The response to a marathon event combines an acute response and training, since only trained individuals can complete a marathon. The duration of this acute bout of exercise is long and study volunteers run at the best speed possible considering the distance. Circulating myomiR-1, 133a and 206 have been found to increase following a half marathon [173]. Indeed, these same myomiRs have also been shown to increase immediately after a full marathon, and remain elevated for the subsequent 24 hr thereafter [174]. Clauss *et al.* showed an effect of a marathon on plasma myomiRs, and found that myomiR-1 and 133a were increased in plasma immediately post a marathon in both elite and non-elite athletes [175]. This suggests that the distance is important rather than the speed or extent of training, although the relative intensity might have been similar, because both groups ran as fast as they could. Another study showed the same pattern of increase for these myomiRs following a marathon, however, also showed that myomiR-208b and 499 returned back to baseline levels 24 hr after, a finding that was not repeated with other myomiRs (i.e. canonical myomiRs remained elevated) [174]. In support of this return to baseline abundances 24 hr post-marathon, Min *et al.* found that myomiRs-1, 133a and 206 increased immediately after a marathon, but returned back to baseline abundances 24 hr after [176]. The results from the study by Baggish *et al.*, confirmed the other studies increased plasma myomiR-1, 133a and 499 post-marathon, with the addition of an increase in myomiR-208a (cardiac-specific miR). In this study, all the myomiRs just mentioned returned to baseline levels at 24 hr post-marathon [177]. Uniquely, Calvo *et al.* found no change in myomiRs in serum taken immediately or 24 hr post a 10 km run, a half marathon, or a full marathon [178].

In summary, almost all myomiRs have been shown to increase in plasma levels immediately following a marathon. This is despite the opposing physiological function of some myomiRs.

Conflicting results remain to be elucidated, particularly whether or not circulating myomiRs return to baseline levels 24 hr post-marathon, the understanding of which will aid our knowledge of myomiR dynamics.

3.6.4 Prediction of aerobic capacity

Correlation analyses have begun to reveal the relationship between circulating myomiR abundance and aerobic capacity in humans; aiding the premise of their release into circulation with physical activity. Denham *et al.* have found that both myomiR-1 and 486 abundances in healthy, untrained individuals at baseline were directly correlated to VO_2max. Additionally, myomiR-486 was found to be inversely correlated to resting heart rate. This ultimately suggests a role for these myomiRs as biomarkers of fitness [165]. Conversely, Aoi *et al.* have found that the VO_2max of untrained individuals was inversely correlated to the change ratio of myomiR-486 between pre and post an acute bout of exercise [179], suggesting that myomiR responses to exercise may also serve as a marker of fitness. Similarly, it has been shown that circulating myomiR-1, 133a and 206 changes following a marathon were positively correlated to VO_2max, as well as running speed at participants' lactate threshold [174].

The studies discussed in the previous paragraph, however, did not segment miR analysis based on the constituent circulating miR carriers. As mentioned in section 3.4 of this chapter, circulating miRs can be transported by proteins and extracellular vesicles. It is likely that the general lysis techniques used during the RNA isolation process in the aforementioned studies result in myomiR abundances that are the sum of myomiRs associated with all carriers. In light of this, Guescini *et al.* showed that abundances of myomiR-1, 133b, 206 and 499 in EVs at baseline was positively correlated to VO_2max, suggesting that myomiRs are specifically packaged in EVs [50]. Taken together, these results suggest that myomiRs within circulation are indicative of aerobic capacity in humans.

Correlations are not limited to circulating myomiRs and aerobic capacity. Zhang *et al.* showed that myomiRs have the potential to be used as biomarkers of strength by showing that knee

extensor strength increases after 5 months of resistance training was correlated to myomiR-133a, 133b and 206 SkM lysate abundances [167].

Chapter 4: Aims and objectives

Following review of the literature, the hypothesis formulated for this thesis was that:

"Two consecutive bouts of muscle-damaging exercise cause changes in circulating small and large extracellular vesicles, as well as plasma microRNA"

To address this hypothesis this thesis aimed:

"To determine whether two consecutive bouts of muscle-damaging exercise can alter systemic communication, particularly with regard to extracellular vesicles and their microRNA cargo "

Specific Objectives:

1. To isolate and characterize small and large extracellular vesicles from human participants pre and post exercise.
2. To compare miR abundances in small EVs, large EVs and plasma from human participants pre and post exercise.
3. To perform RNA sequencing on small EVs isolated from human participants pre and post exercise and examine differences between subjects and timepoints.

Chapter 5: Materials and methods

5.1 Ethical considerations

This study was approved by Stellenbosch University's Health Research Ethics Committee (Study reference: S17/03/061) and was carried out in accordance with the guidelines of the South African Medical Research Council and the Declaration of Helsinki.

5.2 Participants

Nine healthy, untrained males between the age of 18 and 30 volunteered for this study. Exclusion criteria for participants included; regular exercise exceeding 2 bouts per week, participation in professional sport, smoking, or the use of anti-inflammatory medication within 3 months preceding the study. Furthermore, participants were required to be in good health (i.e. with no chronic illnesses) and were not to have participated in any strenuous exercise in the week preceding the study, or throughout the duration of study.

5.3 Eccentric exercise regimen

Each participant performed two consecutive bouts of eccentrically-biased, muscle-damaging exercise. This consisted of a combined regimen of both plyometric jumping (PMJ) and downhill running (DHR). Both exercise modes result in diffuse muscle damage, and antagonise the large quadriceps muscles, maximizing the potential for SkM-associated changes in circulating. The protocol was modified from similar protocols previously used in our lab [21] [51].

Briefly, fasted participants arrived at the exercise lab at 8am in the morning and were guided through a 5 min warm-up focused to the quadricep muscles. Following this, all participants completed 10 sets of 10 plyometric jumps at 90 % of their maximum achievable jump height, with a 1 min standing interval between sets. Upon completion of the PMJ regimen, a 5 min rest period was given before commencement with DHR. Participants were then required to perform between 2 and 5 bouts of 3 mins sets of DHR at 10 km/ hr, at a 10 % decline (Figure 4.1), and were given a

2 min standing interval between sets. The exercise intervention was stopped if a rating of perceived exertion value of 20 was reached.

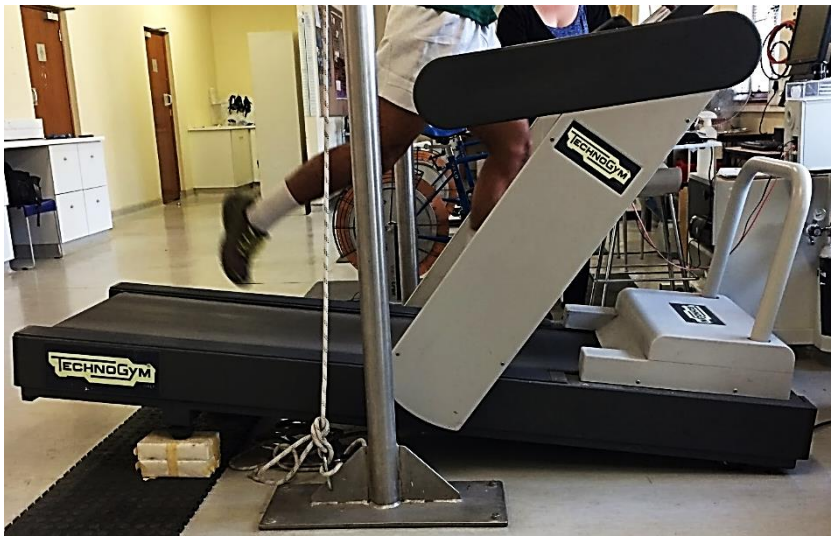

Figure 5.1. Image of a participant performing the downhill running regimen. The rear end of the treadmill was elevated to achieve a 10 % angle of decline.

5.4 Perceived muscle soreness

Perceived muscle soreness (PMP) was assessed using a Delayed onset muscle soreness (DOMS) scale of 1 to 10. A score of 1 signifying no pain, and a score of 10 signified extreme, or unbearable pain. Scores were recorded at baseline and at 2hr, 6hr, 24hr, 48hr and 72hr post-exercise.

5.5 Blood sampling

Approximately 25ml of whole blood was drawn from the antecubital vein by a qualified phlebotomist at baseline, and at 2hr and 24hr post-exercise. Blood was collected into either EDTA-coated (plasma) or heparin-containing tubes (serum). All blood draws were taken in the fasted state. Blood plasma was isolated from whole blood for subsequent analysis by centrifugation at 2 000 g for 10 mins at 4° C. Plasma was then aliquoted and immediately frozen at - 80° C. Blood serum was collected for serum creatine kinase analysis (analysis done by PathCare, South Africa).

5.6 Extracellular vesicle isolation

Extracellular vesicles were isolated from clarified plasma using qEV size exclusion columns (Izon Science), according to the manufacturer's protocol (Figure 4.2). Briefly, plasma was thawed on ice and centrifuged at 10 000 g for 10 mins to remove cellular debris. The resultant pellet, henceforth termed large EVs, as well as the clarified plasma making up the supernatant were kept for subsequent analysis. 1 ml of clarified plasma was added to the top of the qEV column (Figure 4.2 blue arrow), and 15 x 500 µl fractions of the eluent was collected. qEV columns were continuously topped added with PBS, as to not allow the frit to run dry. Samples were aliquoted and frozen at -80° C.

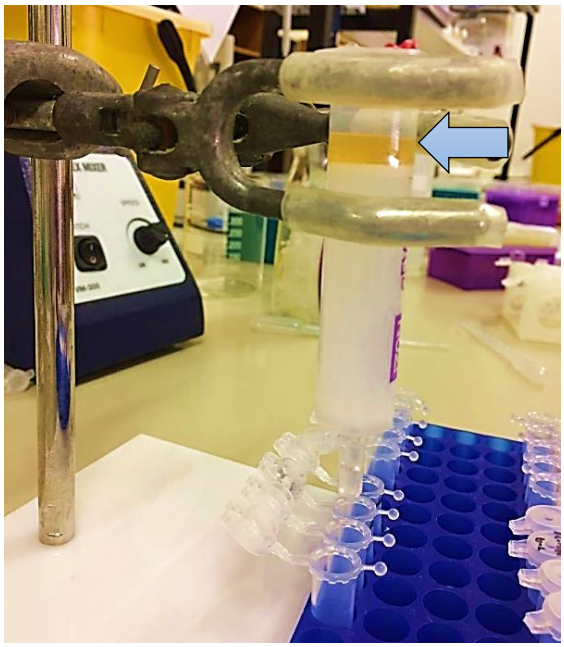

Figure 5.2. Image of small EV isolation process using a qEV size exclusion column (Izon Science). Clarified plasma is loaded above the stationary phase (see blue arrow), following which constituents are separated according to size through a Sepharose media. 15 x 500 µl fractions were collected into 2 ml Eppendorf tubes, and fractions 7-10 were pooled for downstream analysis.

5.7 Scanning transmission Electron Microscopy

Two hundred mesh carbon-coated copper TEM grids were incubated on 10 µl droplets of small EV or large EV aliquots for 10 mins (Figure 4.3). Grids were then washed with dH_2O and carefully

dabbed onto Whatman paper. Following this, grids were incubated on 10 µl of freshly filtered 2 % Uranyl acetate Zero (a negative stain) for contrast (Agar Scientific). Small EV loaded grids were viewed using a Zeiss Merlin field emission scanning electron microscope (Zeiss) at 20 kV. Large EV grids were viewed at 22 kV on an Apreo Volumescope (ThermoFisher).

Figure 5.3. 200-mesh, carbon-coated copper TEM grids were incubated on 10 µl of sample for maximum proximity of grids to sample. After each step, grids were passed over distilled water, and carefully dabbed onto absorbent Whatman paper before being contrast stained with Uranyl acetate.

5.8 Nanoparticle tracking analysis

Vesicle size and number were assessed using nanoparticle tracking analysis (NTA), with the NanoSight LM10 (Malvern Instruments). EV isolates were diluted in PBS (25X – 200X) for a suitable number of particles per frame (± 35), and three 30 second videos were used to determine mean particle numbers per ml and mean particle diameters. The detection threshold was kept constant for all samples, at 6. (See Appendix 5 for more information on NTA theory).

5.9 Gel electrophoresis

Samples were run on 1.5 mm SDS-PAGE gels with a 12 % resolving gel. A 10-well comb was used to enable a maximum loading volume of 66 µl. Gels were electrophoresed at 70 V for 2-3 hours. Gels were washed with dH_2O and incubated with Coomassie brilliant blue dye (Sigma-Aldrich) for 30 mins. Following this, sequential steps of de-staining (30 % Methanol, 10 % Acetic

acid and 60 % dH_2O) was done for 5, 30 and 120 mins. Gels were detected using the Bio-Rad ChemiDoc imaging system.

5.10 RNA isolation

Small EV (400 ul), large EV (50 ul) and clarified plasma (50 ul) samples were used to isolate Total RNA using the Norgen Plasma/Serum RNA Purification Mini Kit (Norgen Biotek; 55000). During RNA isolation, C. Elegans-miR-39 (cel-miR-39. Sequence: UCACCGGGUGUAAAUCAGCUUG) was added as an exogenous/spike-in control to a final concentration of 10pM. This sequence does not exist in humans and was used as an exogenous/ spike-in control. All qPCR reactions were normalised to the cel-miR-39 Ct values.

5.11 microRNA reverse transcription

Reverse transcription and pre-amplification of microRNA was achieved with the TaqMan Advanced miRNA cDNA synthesis kit (ThermoFisher Scientific; A28007). In an initial poly-A tailing reaction, 2 µl of total RNA was added to a poly(A) polymerase mix. Next, the product underwent ligation with an adaptor sequence. The adaptor ligase activity is dependent upon a 5' phosphate, only present on mature microRNAs. In the reverse transcription reaction, the poly(A) tail is recognised by an oligo-dt primer that aids the action of a universal reverse transcriptase in transcribing the ligated microRNA. Given the low copy numbers of miRs found in biofluids, an extra miR amplification step is added with the use of universal forward and reverse primers that recognise the adaptor sequence.

5.12 microRNA qPCR

10 µl of the amplified reverse transcription product was diluted in a 1:10 ratio for subsequent qPCR analysis with TaqMan Advanced miRNA assays; miR-1-3p (477820_mir), miR-21-5p (477975_mir), miR-31-5p (478015_mir), miR-133a-3p (478511_mir), miR-133b (480871_mir), miR-

146a-5p (478399_mir), miR-155-5p (483064_mir), miR-206 (477968_mir), miR-208b-3p (477806_mir), miR-486-5p (478128_mir) and miR-499a-5p (478139_mir) (all obtained from ThermoFisher Scientific). 5 µl of this diluted cDNA was loaded into fast optical 96-well plates, and the plates were sealed with optical adhesive film. qPCR analysis was performed in duplicates on a StepOne qPCR thermocycler (Applied Biosystems).

5.13 Small RNA sequencing

Total RNA was isolated from pooled small EV fractions (F7-10) using the Norgen Plasma/Serum RNA Purification Mini Kit (Norgen Biotek: 55000). Prior to sequencing the quantity of RNA was determined with the use of a small RNA chip (Bioanalyzer 2100, Agilent technologies). Next generation small RNA sequencing was done on 3 baseline and 3 matched 24 hr post-exercise samples using an Illumina NextSeq500 (Norgen Biotek), specifying between 15 – 50 nucleotides in length.

5.14 Statistical analysis

All data are represented as mean ± standard error of the mean (SEM). Data were analysed by means of a one-way ANOVA, with a Fisher LSD post-hoc test. miR Ct values were normalised to an exogenous control by dividing the sample by the control value. For sequencing, read counts per million normalized by the trimmed means of M-values (TMM) method was used. Here, data were compared by means of a paired t-test. Graphs were made using version 5 of GraphPad Prism (GraphPad Software inc, USA), and statistical significance was set at a 5 % confidence interval i.e. $p < 0.05$.

Chapter 6: Results

6.1 Participants and indirect markers of muscle damage

Nine healthy, untrained male participants between the ages of 18 and 27 volunteered to take part in this study. Participant age, height and weight are displayed in Table 6.1.

Table 6.1. Participant age, height and weight at baseline (Mean ± SEM).

Age	Height (cm)	Weight (kg)
20.6 ± 0.9	178.2 ± 1.6	72.1 ± 2.1

6.1.1 Physical performance characteristics of participants

All nine participants were able to complete the full PMJ regimen. For the DHR regimen, 7 of the 9 participants were able to complete the five bouts. The other 2 participants in the cohort performed 2 bouts of DHR before becoming too fatigued to carry on and opted to stop. (Table 6.2). The mean maximal jump height of the participants was 265 ± 6.3 cm while the mean relative jump height (calculated by max jump height – participant height) was 86 ± 5.2 cm (Table 6.2).

Table 6.2. Number of completed plyometric jumping and downhill running bouts, as well as maximum jump height and relative jump height (both measured in centimeters). NA = missing data point.

Participant	Completed PMJ bouts (n = 9)	Completed DHR bouts (n = 9)	Max jump height (cm)	Relative jump height (cm)
1	10	5	NA	NA
2	10	5	267	84
3	10	5	270	86
4	10	5	258	83.5
5	10	5	305	121.7
6	10	2	246	75.1
7	10	5	260	83.3
8	10	5	253	79.7
9	10	2	258	77

6.1.2 Perceived muscle pain (PMP) of participants post-exercise

Perceived muscle pain was assessed at baseline, and at 2, 6, 24, 48 and 72 hr post-exercise for n ≥ 7 participants. It was found that PMP scores within the first 24 hr post exercise increased gradually as time progressed (see Figure 6.1). Significant differences were observed between BL (baseline score taken to be 1 = no pain) and 2 hr (4.2 ± 0.68, p = 0.0018), 6 hr (5 ± 0.74, p = 0.0003), 24 hr (5.78 ± 0.84, p = 0.0000), 48 hr (5.2 ± 0.87, p = 0.0000) and 72 hr (3.6 ± 0.75, p = 0.0174). At the later timepoints post-exercise a gradual decrease in PMP scores was observed (Figure 6.1). Significant differences between 24 hr and 72 hr (p = 0.0396) post exercise were observed.

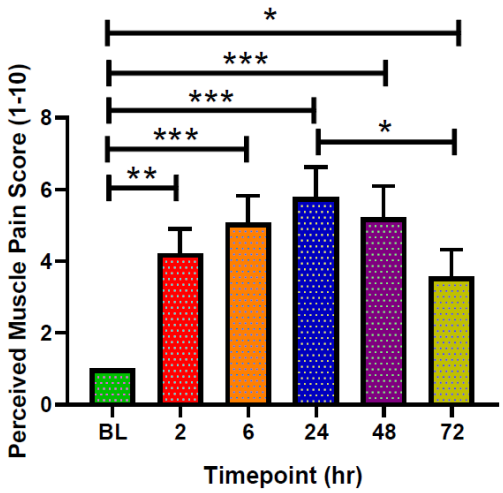

Figure 6.1. Perceived muscle pain of the *anterior quadriceps* muscles upon walking, expressed on a scale of 1 - 10. (One-way ANOVA with an LSD posthoc test Mean ± SEM. * p < 0.05, **p < 0.01 and ***p < 0.001. n ≥ 7).

6.1.3 Serum creatine kinase (CK) levels

Serum CK levels, measured in international units/liter (IU/L), are a clinically used indicator of cardiac muscle damage and can be indicative of general muscle damage [20]. Therefore, to support the findings that suggested participants had skeletal muscle damage, as shown by PMP scores, serum CK levels were determined at baseline (BL), and at 2 hr (2) and 24 hr (24) post exercise for n ≥ 8 participants. As seen in Figure 6.2, an increase in CK levels over time was observed post-exercise. Significant differences in CK levels occurred between BL and 24 hr, with an almost

threefold increase (BL = 243 ± 58 vs 24 = 896 ± 278, p = 0.0168). No significant differences were found between 2 and 24 hr (Figure 6.2).

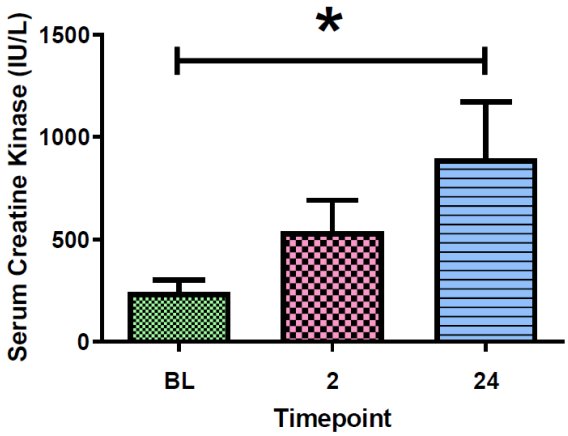

Figure 6.2. Serum creatine kinase levels before and after muscle-damaging exercise. Values are presented in international units per litre (IU/L) and timepoints are represented in hours. A large increase in CK levels is seen at 24 hr post-exercise (One-way ANOVA with an LSD posthoc test, Mean ± SEM. * $p < 0.05$. $n \geq 8$). BL = baseline.

6.2 EV analysis

EVs were isolated from 1 ml of plasma using qEV size exclusion columns (SEC) and by following previously validated protocols and as described in 5.6 of the methods section [51 180 181 148].

6.2.1 Qualitative assessment of protein abundance and diversity present in qEV SEC isolated fractions

The first few fractions (i.e. fractions 1 - 6) derived from qEV columns are known to contain very low amounts of proteins or to be devoid of proteins altogether (see qEV brochure), hence the samples loaded on an SDS PAGE gel started at the upper end of these fractions, at fraction 4 . Fractions 4 - 15 were initially assessed using Coomassie-stain to obtain qualitative information on protein size diversity and abundance in the isolated fractions obtained from the qEV column. Three void fractions (i.e. fractions 4, 5 and 6) were included to confirm the lack of protein present. An equal volume of sample (40 ul) from each fraction was loaded per lane. Sparse

protein was detectable in fractions 4 -9 (Figure 6.3). In contrast, fractions 10 - 15 exhibited abundant protein, with fractions 13 - 15 showing visibly more protein (Figure 6.3). Some diversity in the abundance of different protein bands between fractions was observed. Major protein bands were present at approximately 65, 80 and 150 kDa in fractions 10-15, with particular abundance of these bands in fractions F13 - F15 (Figure 6.3 **blue arrows**). These bands are likely to represent abundant plasma proteins like Albumin (± 65 kDa) and IgG (± 150 kDa). Smaller proteins bands 30 and 50 kDa were more evident in fractions F10 to F12 (Figure 6.3 **yellow arrows**) and these are unknown proteins.

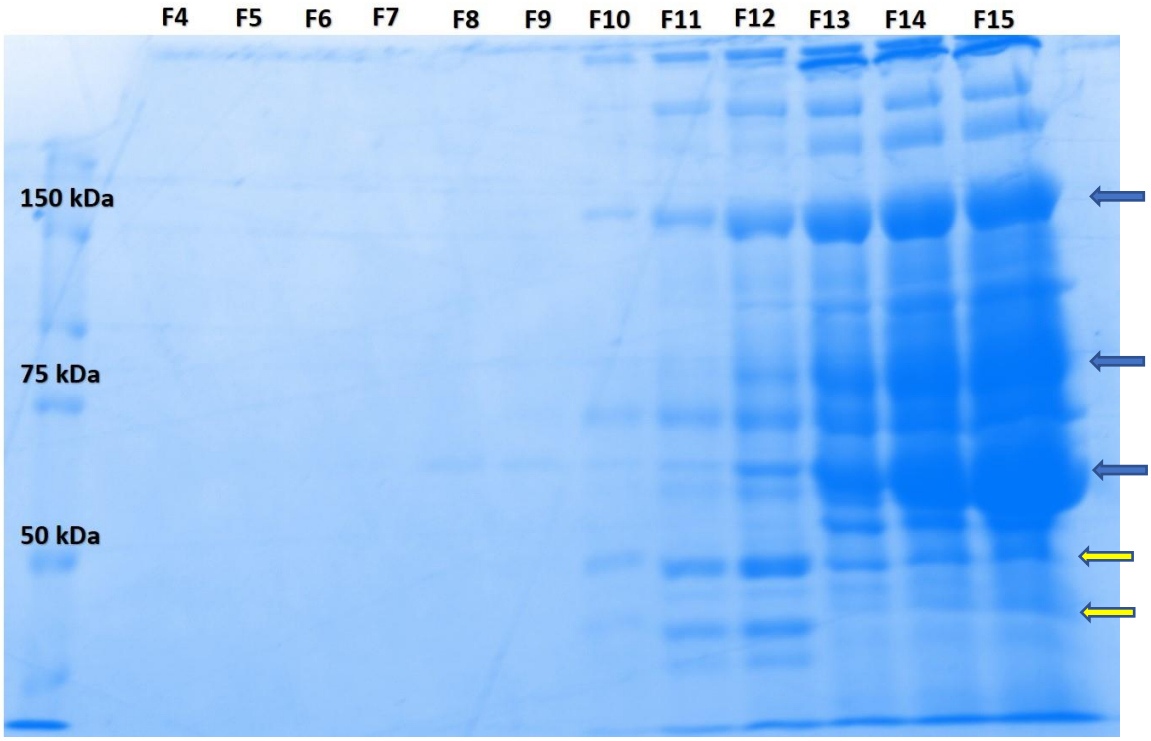

Figure 6.3. Representative image of a Coomassie stained SDS PAGE gel of size exclusion fractionated human plasma from one study participant. Protein molecular weight ladder in left lane with molecular weights indicated. F4-F15 (Fractions 4-15) obtained from qEV column fractionation of a baseline plasma sample.

6.2.2 Quantitative Protein concentrations of qEV SEC isolated fractions

An initial exploratory assessment of protein concentrations present within the qEV SEC isolated fractions was performed on 3 participants' baseline samples (fractions 1 -15) using the BCA assay. Quantifiable protein was only detectable from fractions 11 - 15 (Figure 6.4). There was an increased protein concentration in higher fractions.

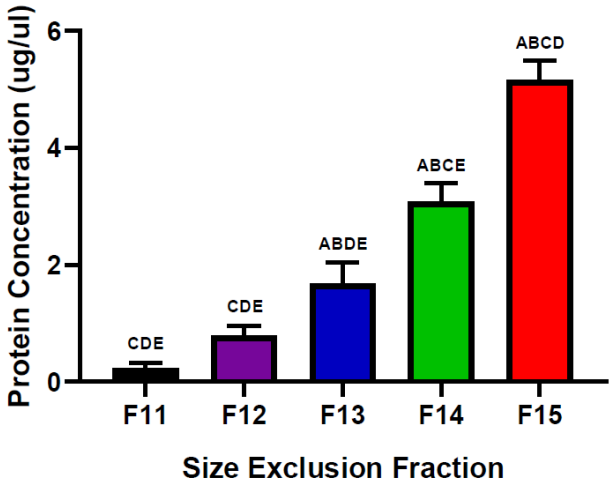

Figure 6.4. Protein concentration readings measured using a BCA assay (in ug/ul). Protein was measured in all SEC fractions from 3 participants' samples; fractions below F11 had undetectable levels.

6.2.3 Scanning transmission electron microscopy (STEM) of specific qEV fractions

Previously published reports using qEV SEC show that fractions 7 – 9 generally contain the most abundant small EV-sized particles [180] [51] [110] [182]. To qualitatively confirm this, fraction 8 from a baseline timepoint of an individual was visualised using STEM (Figure 6.6). Particles corresponding to the small EV size range (30 – 150 nm) were observed (Figure 6.6.B). Furthermore, these particles exhibited the classic cup-shaped morphology that is associated with EVs (Figure 6.6) [181].

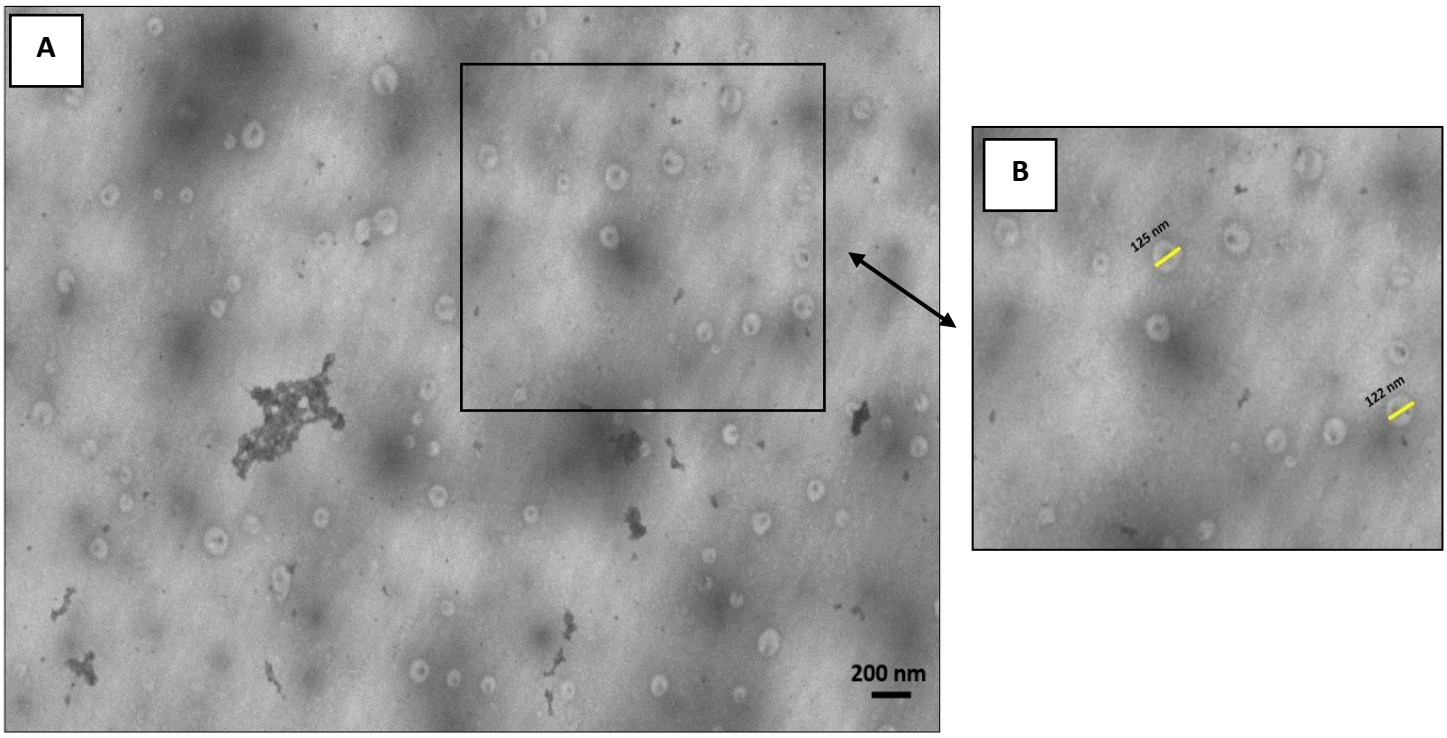

Figure 6.5. Small EVs, derived from qEV size exclusion columns, were visualized in widefield using scanning transmission electron microscopy (A). This representative image is of eluted fraction 8. ImageJ was used to represent the approximate EV size (B: yellow lines).

6.2.4 NTA analysis of qEV SEC isolated fractions

To determine quantitatively which fractions had the most particles that corresponded to the diameter size of small EVs (30 – 150 nm), NTA was utilized. Initially, a subset of baseline samples (n = 5) was analysed. No detectable particles were found to elute earlier than fraction 7 or later than fraction 12. The vast majority of EV-sized particles (approximately 85 %) were found to be present in Fractions 7 – 10. Due to the high abundance of small EV-sized particles in these fractions it was decided to pool these samples for subsequent analysis, as has been done in previous studies [148] [181]. These pooled fractions will hereafter be referred to as small EVs.

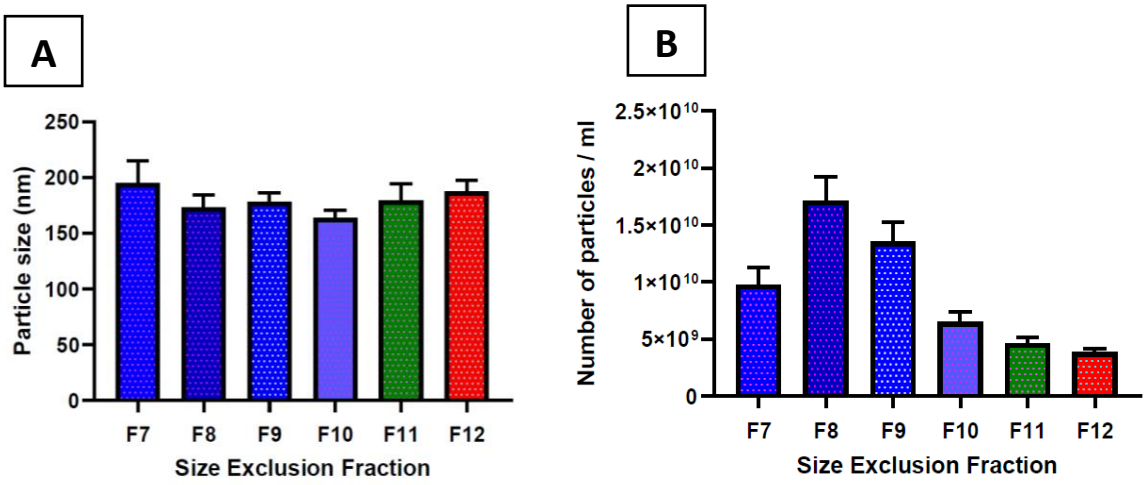

Figure 6.6. Nanoparticle tracking analysis was done on 15 fractions, for n = 5 baseline samples; results for 6 of these fractions are displayed (i.e. Fractions 7 - 12), as other fractions had no detectable particles. Particle size is expressed in nm (A) and number of particles is expressed in particles/ml (B). (Mean ± SEM. n = 5).

6.2.5 The effect of muscle-damaging exercise on small EV number and diameter

To determine whether the two consecutive bouts of muscle-damaging exercise had any effect on small EV (i.e. pooled fractions) number or diameter, samples from n = 5 participants at BL, 2 hr and 24 hr post exercise were analysed using NTA. No significant change in vesicle number (BL = $1.4 \times 10^{10} \pm 2.8 \times 10^{9}$, 2 = $1.2 \times 10^{10} \pm 2.9 \times 10^{9}$ and 24 = $1.3 \times 10^{10} \pm 2.6 \times 10^{9}$. Figure 6.7 A) or diameter (BL = 196.6 ± 8, 2 = 204.2 ± 3.5 and 24 = 210.8 ± 6.4. Figure 6.7 B) was found between timepoints.

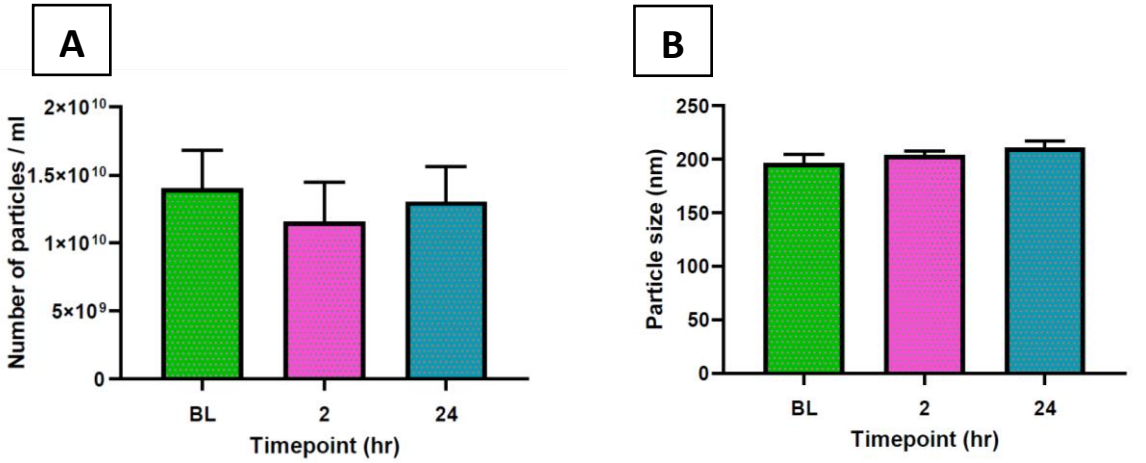

Figure 6.7. Small EV number (A) and size (B) were determined with NTA for pooled samples (F7 - 10). No change in either particle number or size was seen as a result of the exercise intervention. (One-way ANOVA with LSD posthoc test. Mean ± SEM).

6.2.6 The effect of muscle-damaging exercise on small EV-associated myomiRs

The abundance of four canonical myomiRs, miR-1-3p, 133a-3p, 133b and 206, was assessed in the pooled small EV fraction (i.e. fractions 7-10) using qPCR. Samples from BL, and 2 hr and 24 hr post-exercise were analysed. No significant difference for any canonical myomiR was found between timepoints (Figure 6.8). Although there was no difference in temporal abundance of the four myomiRs at all three timepoints, these myomiRs were found to be at a lower abundance than the exogenous control. Given the equal isolation, reverse transcription and amplification of miRs during qPCR, this shows that the abundance of myomiRs in the pooled fractions analysed here is less than 10 pM, the amount of spike in control added during RNA isolation.

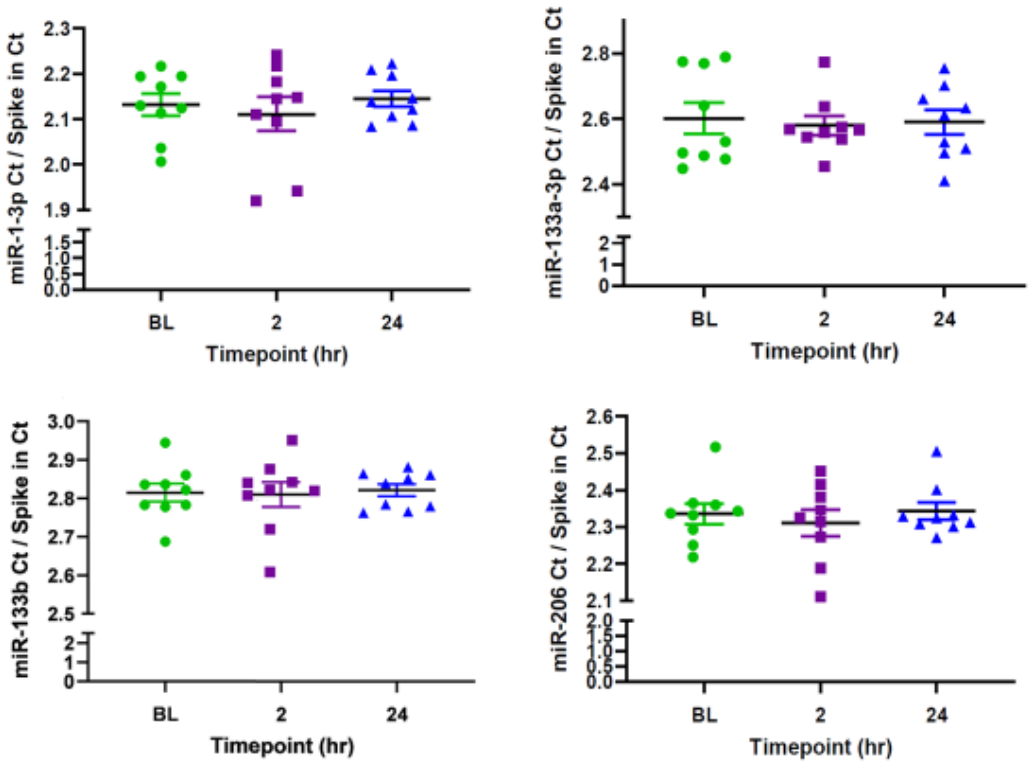

Figure 6.8. Abundance of four canonical myomiRs in 400 ul of the pooled small EV fractions, normalised to the exogenous control, cel-miR-39. No change was seen as a result of the exercise intervention (One-way ANOVA with LSD posthoc test. Mean ± SEM).

6.2.7 The effect of muscle-damaging exercise on small EV-associated SkM-important miRs

In addition to the four canonical myomiRs examined above, four non-canonical, but still "SkM-important", miRs were analysed: miR-31-5p, 208b-5p, 486-5p and 499-5p. These miRs have been previously reported regarding their importance in SkM processes [32] [183] [184] [185]. Of the non-canonical myomiRs investigated here, miR-208b-5p, 486-5p and 499-5p showed no significant difference in abundance between BL and post-exercise timepoints (Figure 6.9). miR-31-5p, however, exhibited a decreased abundance in small EVs at 24 hr when compared to BL (BL: 2.41 ± 0.048 vs 24: 2.51 ± 0.05, p = 0.022). This decrease was also apparent at 24 hr post-exercise compared to 2 hr post-exercise (2: 2.38 ± 0.023, p = 0.005).

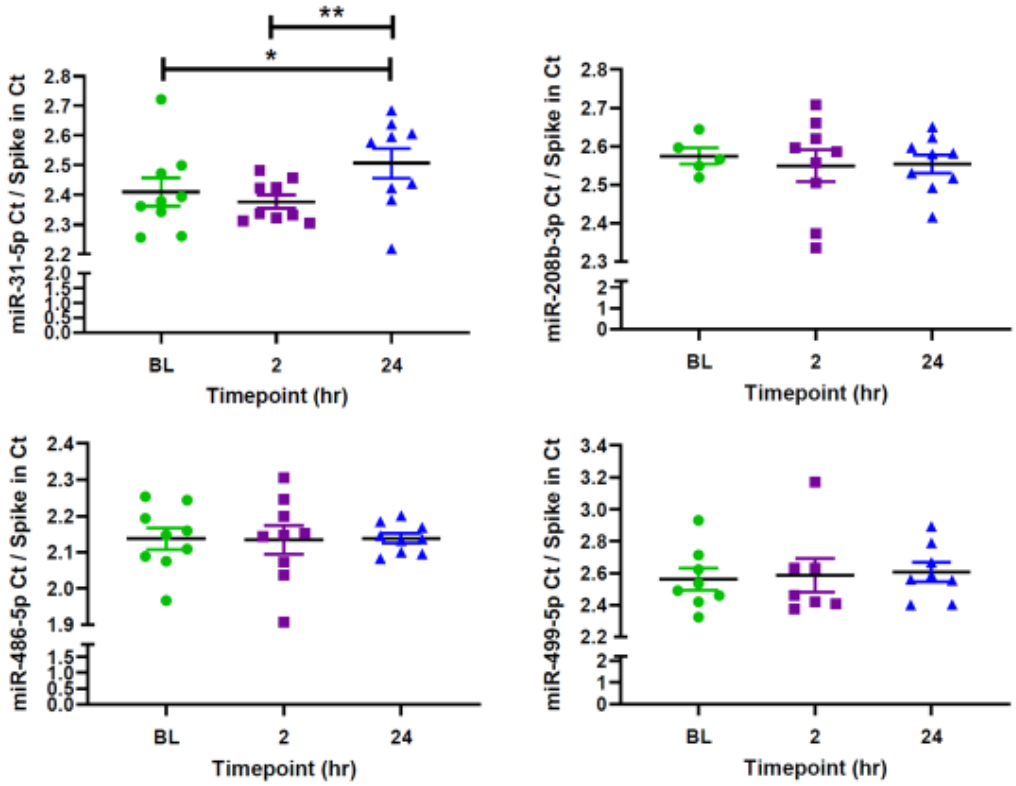

Footnote: *Figure data is represented as miR relative abundance, achieved by dividing the sample cycle threshold (Ct) by that of the control. The cycle threshold is the point at which the miR abundance begins to exponentially increase. All spiked-in/exogenous control Ct values were lower than that of sample, meaning that they exhibit a greater miR abundance as this control miR levels are detected exponentially earlier on in cycling. Therefore a larger re;ative abundance in the figures represents a lower miR abundance in the volunteers' samples.*

Figure 6.9. Abundance of four SkM-important miRs (including 3 non-canonical myomiRs) in 400 ul of pooled small EV fractions, normalised to the exogenous control cel-miR-39. miR-31-5p significantly decreased at 24 hr when compared to both BL and 2 hr (One-way ANOVA with LSD posthoc test. Mean ± SEM. * $p < 0.05$ and ** $p < 0.01$).

6.2.8 The effect of muscle-damaging exercise on small EV-associated immune miRs

Since the immune system plays an important role in SkM regeneration following injury [26] [25] [21], three immune miRs, miR-21-5p, 146a-5p and 155-5p, were also investigated for possible changes in response to the two consecutive bouts of muscle-damaging exercise. The aforementioned immune miRs are associated with the inhibition of monocyte differentiation [186] and polarisation [177] [187], as well as general inflammation [177]. Therefore, it was hypothesized that these immune miRs could be related to the resolution of the SkM damage induced by the protocol. No significant change in small EV immune miR abundance was observed between BL, 2 hr and 24 hr post-exercise (Figure 6.10). miR-21-5p exhibited the highest abundance of all small EV-associated miRs (mean Ct = 21 compared to 24 to 26).

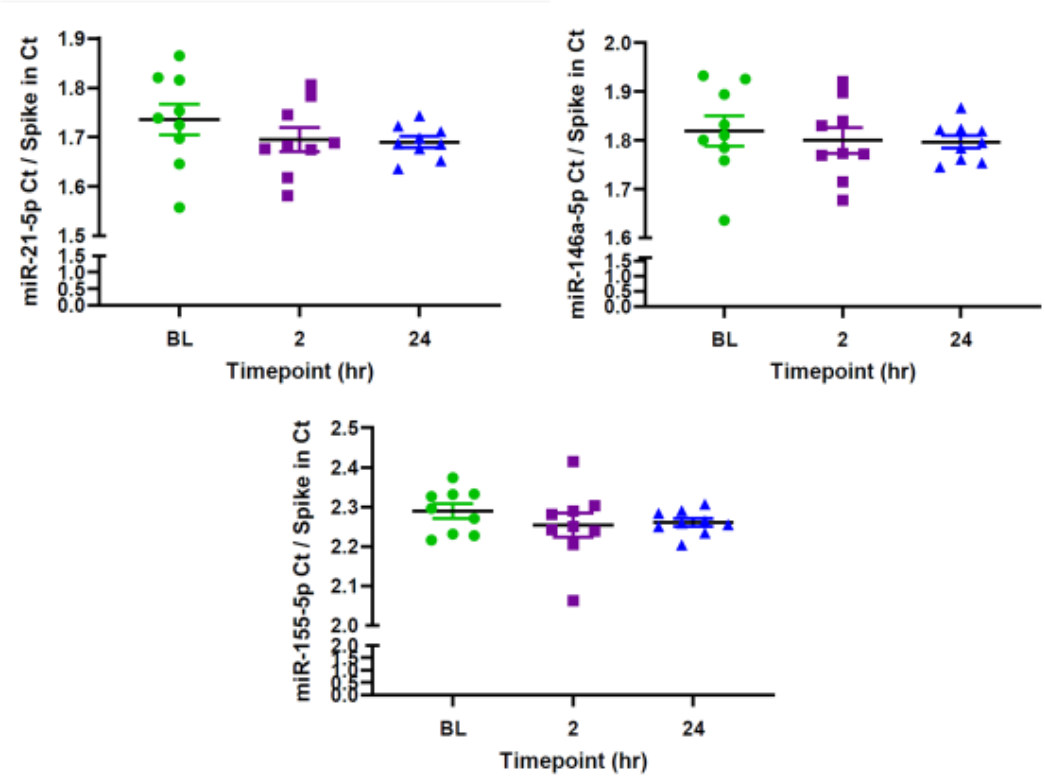

Figure 6.10. Abundance of three immune miRs in 400 ul of pooled small EV fractions, normalised to the exogenous control cel-miR-39. No change was seen as a result of the exercise intervention (One-way ANOVA with LSD posthoc test. Mean ± SEM).

6.3 Large EV analysis

As discussed in Chapter 2 of this thesis, larger EVs of the size range 100 - 1000 nm are also known to be present in plasma. These EVs, termed microvesicles/ microparticles/ ectosomes were isolated using a 10 000 G plasma centrifugation step (as described in 5.6 of the methods section). This large EV pellet was resuspended in PBS and analysed using NTA and STEM. Thereafter, the miR content of large EVs was assessed using qPCR.

6.3.1 Scanning transmission electron microscopy (STEM) of large EVs

Successful isolation of large EVs was confirmed qualitatively, by STEM. An abundance of large EV-sized particles (100 – 1000 nm) with a classic cup-shaped morphology was observed (Figure 6.11).

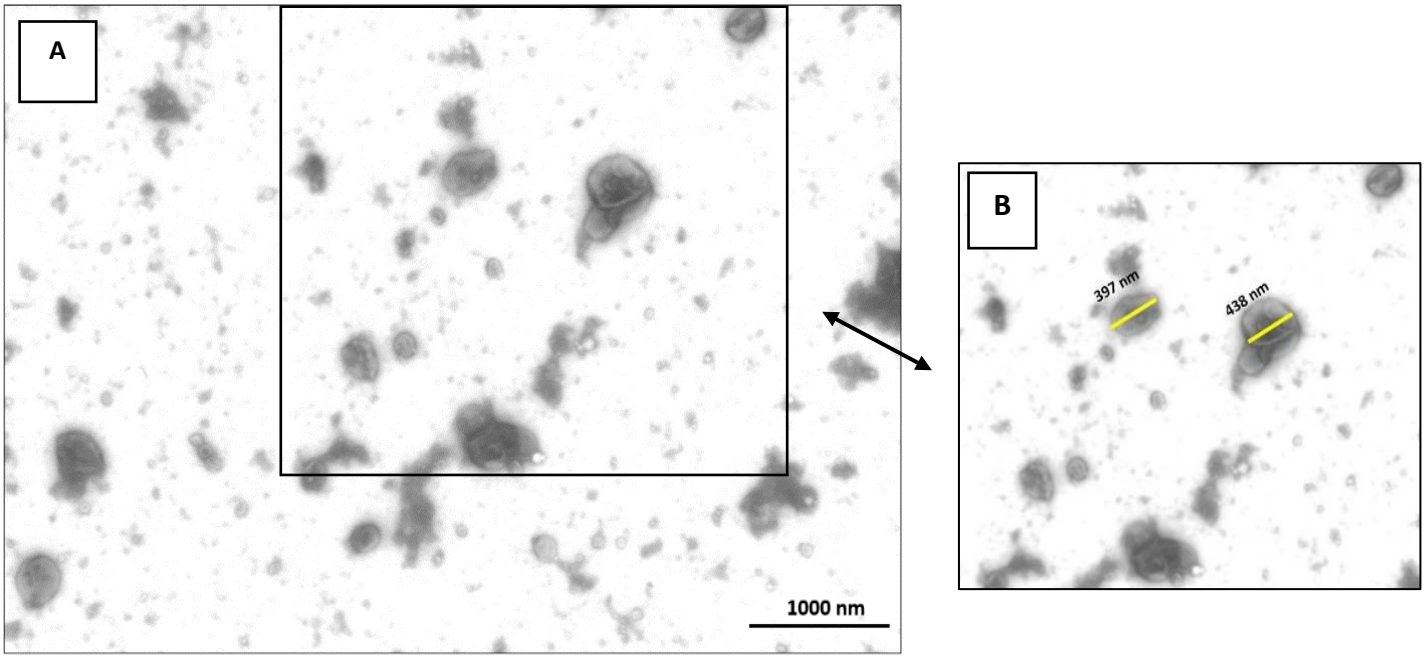

Figure 6.11. Large EVs, derived from a 10 000 G plasma centrifugation step, were visualized in widefield using scanning transmission electron microscopy (**A**). ImageJ was then used to represent the approximate EV diameter (**B**: yellow lines).

6.3.2 The effect of muscle-damaging exercise on large EV number and diameter

To determine whether the two consecutive bouts of muscle-damaging exercise had any effect on large EV number or diameter, NTA was performed on samples obtained from BL, 2 hr and 24 hr post exercise. No significant difference in vesicle number between BL ($2.52 \times 10^{11} \pm 7.2 \times 10^{10}$), 2hr ($2.57 \times 10^{11} \pm 6.1 \times 10^{10}$) or 24 hr ($2 \times 10^{11} \pm 1.1 \times 10^{10}$) was observed (Figure 6.12.A). Similarly, no difference in vesicle diameter between BL (167.4 ± 24.8), 2hr (185.6 ± 17.3) or 24 hr (197.9 ± 6.2) was observed (Figure 6.12.B). The combined result of TEM and NTA demonstrate that successful isolation of large EVs from human plasma had been achieved, with the exercise intervention having no effect on either EV number or size. Due to the large size of particles as shown by NTA and STEM, these resuspended pellets were henceforth referred to as large EVs.

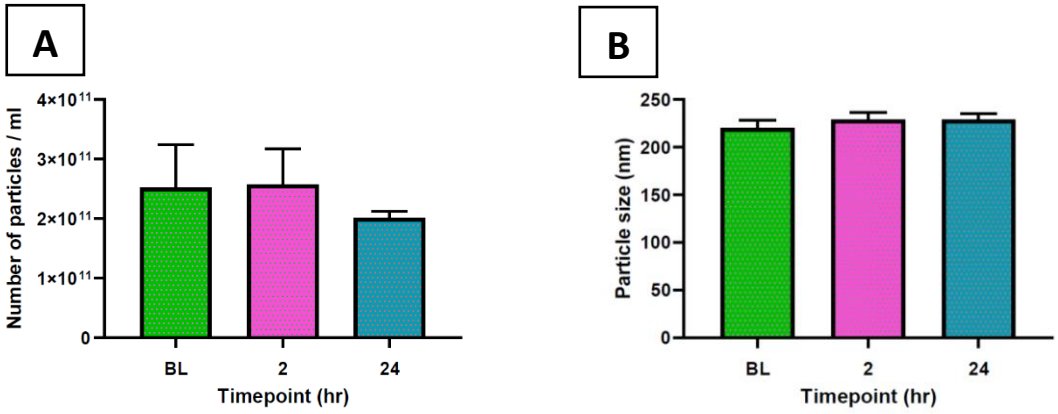

Figure 6.12. Large EV number (A) and size (B) were determined with NTA. No change in either was observed as a result of the exercise intervention. (One-way ANOVA with LSD posthoc test. Mean ± SEM).

6.3.3 The effect of muscle-damaging exercise on large EV-associated myomiRs

The abundance of the four canonical myomiRs in the resuspended large EV pellets was assessed at BL, and at 2 hr and 24 hr post-exercise (Figure 6.13). No change in large EV-associated myomiRs

was seen as a result of the exercise intervention. Figure 6.13 illustrates that myomiR-1-3p exhibited the highest abundance, with a mean Ct value of 24 (as shown by a lower ratio of sample miR to spike in value). Conversely, myomiR-133b displayed the lowest Ct of the canonical myomiRs (mean Ct = 32).

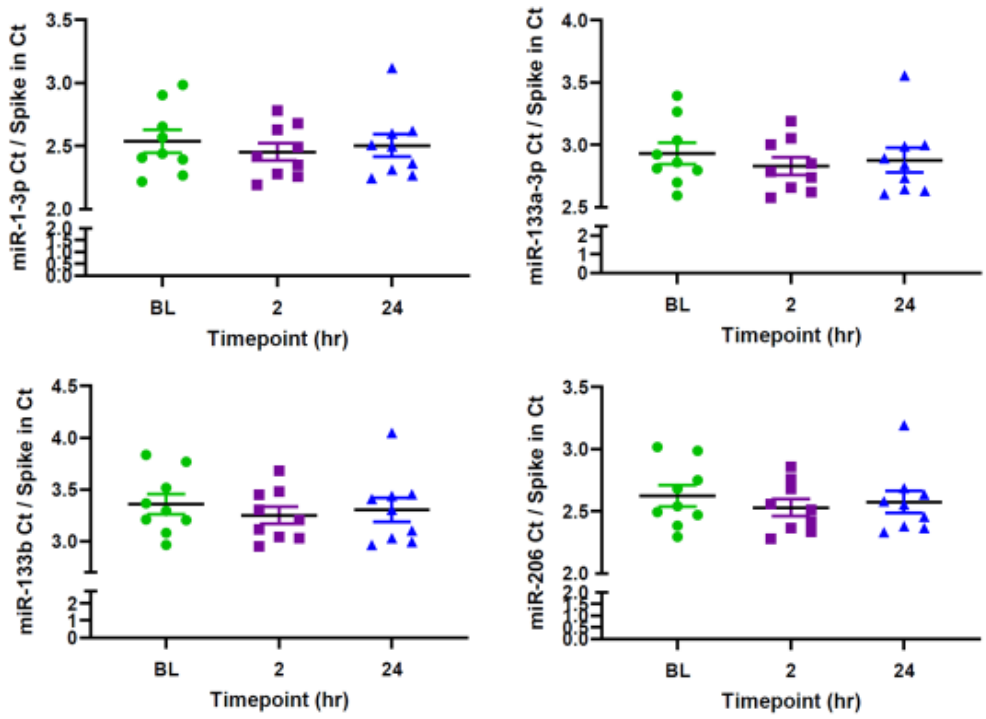

Figure 6.13. Abundance of four canonical myomiRs in 50 ul of large EVs, normalised to the exogenous control, cel-miR-39. No change was seen as a result of the exercise intervention (One-way ANOVA with LSD posthoc test. Mean ± SEM).

6.3.4 The effect of muscle-damaging exercise on large EV-associated SkM-important miRs

As with the qPCR of small EV-associated miRs, four SkM-important miRs were analysed in large EVs. All showed no significant difference in abundances between baseline and post-exercise timepoints (Figure 6.14). myomiR-486-5p, however, was found in much higher abundances than the other three miRs (mean Ct = 23).

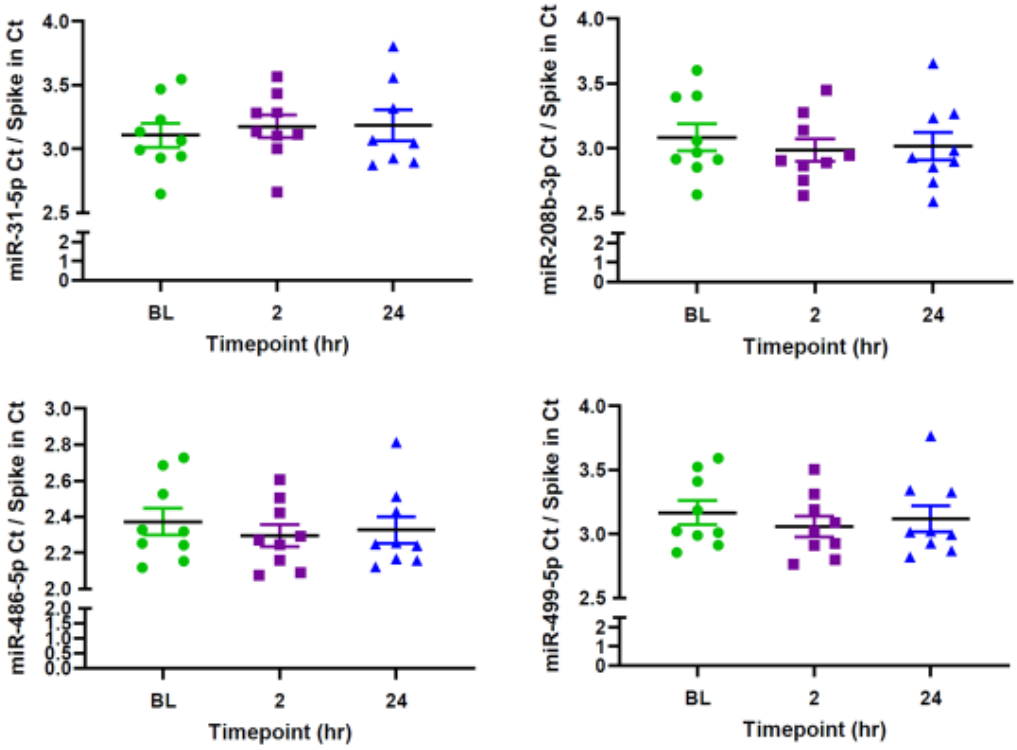

Figure 6.14. Abundance of four SkM-important (including 3 non-canonical myomiRs) miRs in 50ul of large EVs, normalised to the exogenous control, cel-miR-39. No change was seen as a result of the exercise intervention (One-way ANOVA with LSD posthoc test. Mean ± SEM).

6.3.5 The effect of muscle-damaging exercise on large EV-associated immune miRs

Three large EV-associated immune miRs were also investigated for possible changes in response to muscle-damaging exercise. Although no significant change in abundance was observed between BL, 2 hr and 24 hr post-exercise for any of the immune miRs, miR-21-5p exhibited the highest abundance (mean Ct = 18) of all miRs analysed in large EVs (Figure 6.15).

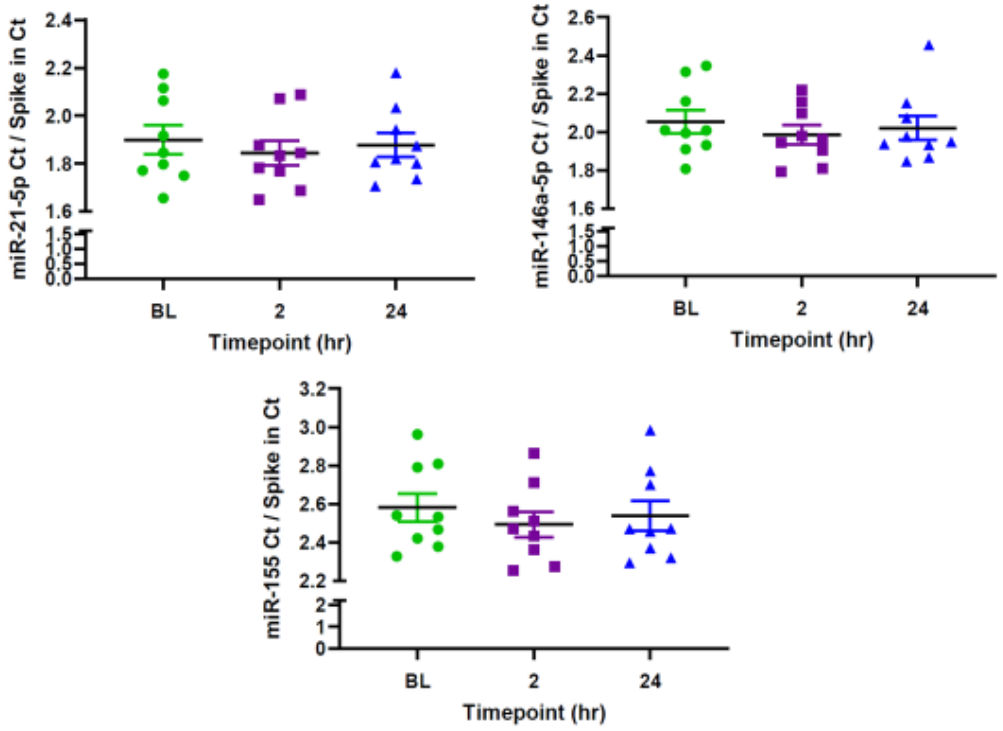

Figure 6.15. Abundance of three immune miRs in 50 ul of large EVs, normalised to the exogenous control, cel-miR-39. No change was seen as a result of the exercise intervention (One-way ANOVA with LSD posthoc test. Mean ± SEM).

6.4 Plasma analysis

The third avenue of miR investigation in response to muscle-damaging exercise was via the analysis of clarified plasma (i.e. plasma centrifuged at 10 000 G).

6.4.1 The effect of muscle-damaging exercise on plasma myomiRs

A significant effect of the muscle-damaging exercise was seen for three canonical myomiRs (Figure 6.16). myomiR-1-3p exhibited a significant increase at 2 hr post-exercise when compared to BL (1.74 ± 0.02 vs 1.61 ± 0.03, p = 0.002995), returning to BL levels at 24 hr (1.71 ± 0.03, p = 0.032577). Similarly, myomiR-133a-3p increased at 2 hr post-exercise (2.08 ± 0.02 vs 1.97 ± 0.03, p = 0.016670). Additionally, following the pattern of myomiR-1-3p, myomiR-206 also exhibited a significant increase at 2 hr post-exercise when compared to BL (1.84 ± 0.02 vs 1.67 ± 0.04, p =

0.002957), returning to BL levels at 24 hr (1.67 ± 0.04 vs 1.80 ± 0.04, p = 0.033083). No change in myomiR-133b was found.

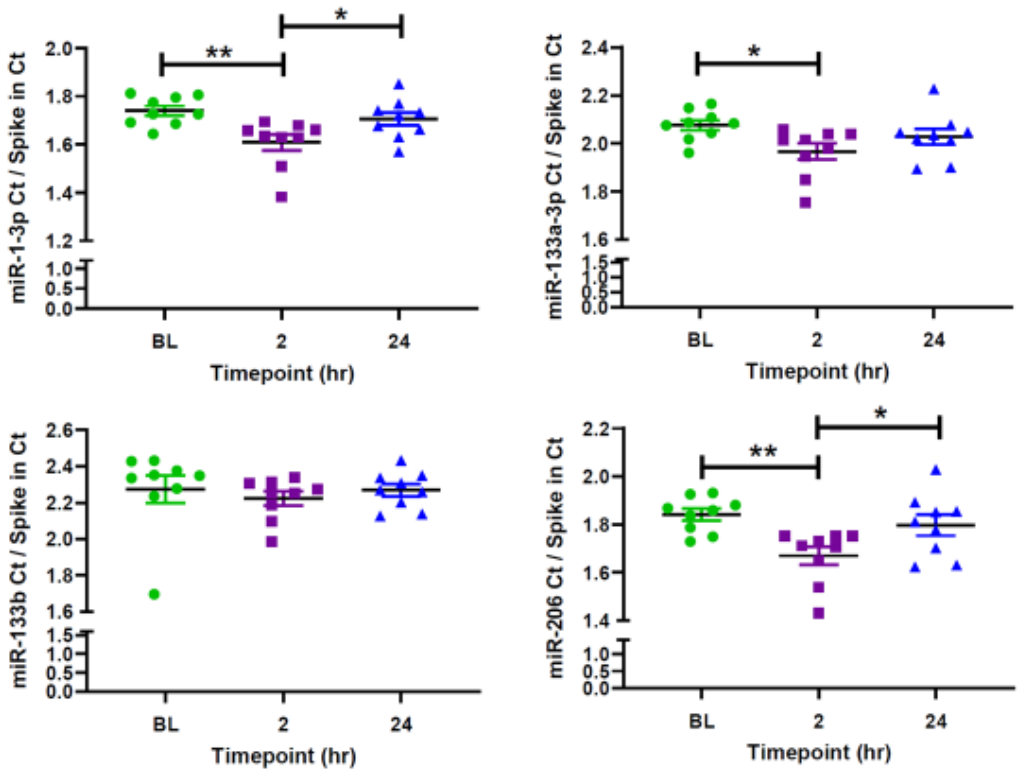

Figure 6.16. Abundance of four canonical myomiRs in 50 ul of plasma, normalised to the exogenous control, cel-miR-39. The exercise intervention had a significant effect on miR-1-3p, miR-133a-3p and miR-206. (One-way ANOVA with LSD posthoc test. Mean ± SEM. * $p < 0.05$ and **$p < 0.01$).

6.4.2 The effect of muscle-damaging exercise on plasma SkM-important miRs

Of the four SkM-important miRs analysed in plasma, only myomiR-208b-3p and myomiR-499-5p changed in response to the exercise intervention. Both exhibited an increase at 2 hr post-exercise when compared to BL (2.13 ± 0.04 vs 1.97 ± 0.05, p = 0.038671 and 2.25 ± 0.03 vs 2.13 ± 0.04, p = 0.041300, respectively). Similarly, both myomiR-208b-3p (2.13 ± 0.04 vs 1.99 ± 0.05, p = 0.055639) and myomiR-499-5p (2.25 ± 0.03 vs 2.14 ± 0.05, p = 0.054234) displayed a trend (i.e. $p < 0.1$) toward remaining at an increased abundance at 24 hr post-exercise. In a similar pattern to that seen in both small and large EV myomiR-486-5p abundances, plasma myomiR-486-5p was the most

abundant of the SkM-important miRs analysed (mean Ct = 21). Although these results are not comparable due to different volumes of starting material, the relative abundance of myomiR-486-5p compared to other miRs can be compared across different potential biomarker avenues i.e. plasma vs large EVs vs small EVs.

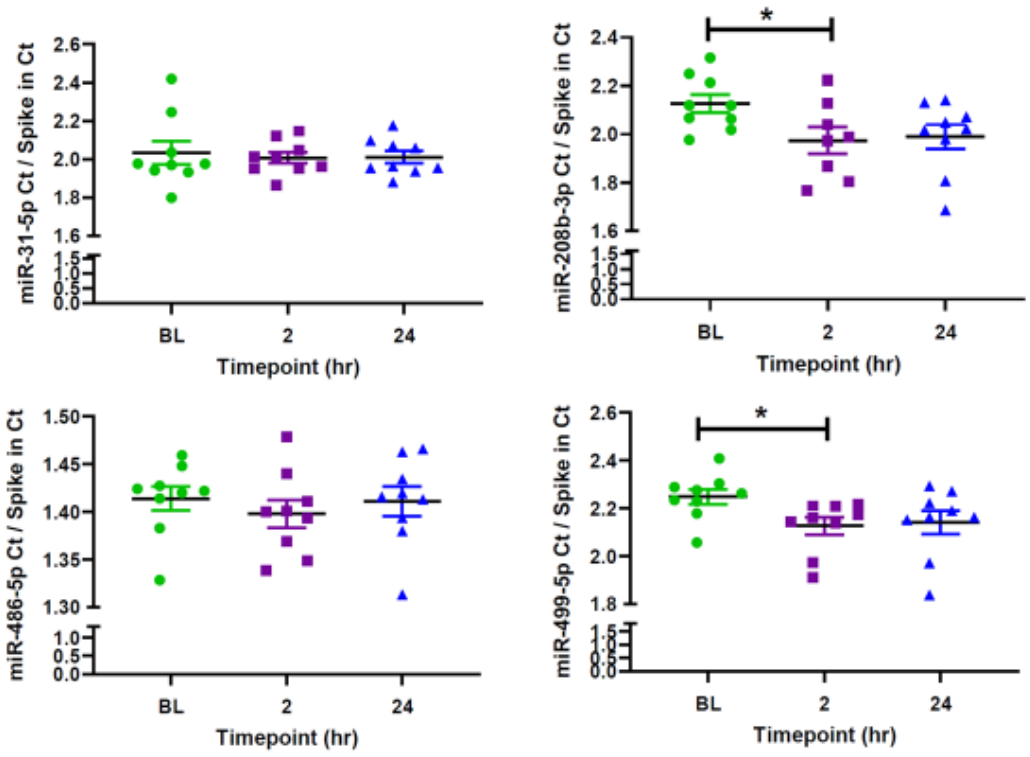

Figure 6.17. Abundance of four SkM-important miRs (including 3 non-canonical myomiRs) in 50 ul of plasma, normalised to the exogenous contro,l cel-miR-39. The exercise intervention had a significant effect on miR-208b-3p and miR-499-5p (One-way ANOVA with LSD posthoc test. Mean ± SEM. * $p < 0.05$).

6.4.3 The effect of muscle-damaging exercise on plasma immune miRs

Figure 6.18 shows results for the three immune miRs selected based on their involvement with immune cells. None of these miRs changed as a result of the exercise intervention. miR-146a-5p was the most highly expressed of all the miRs analysed in plasma (mean Ct = 18). The abundance of the three immune miRs remained remarkably stable after exercise.

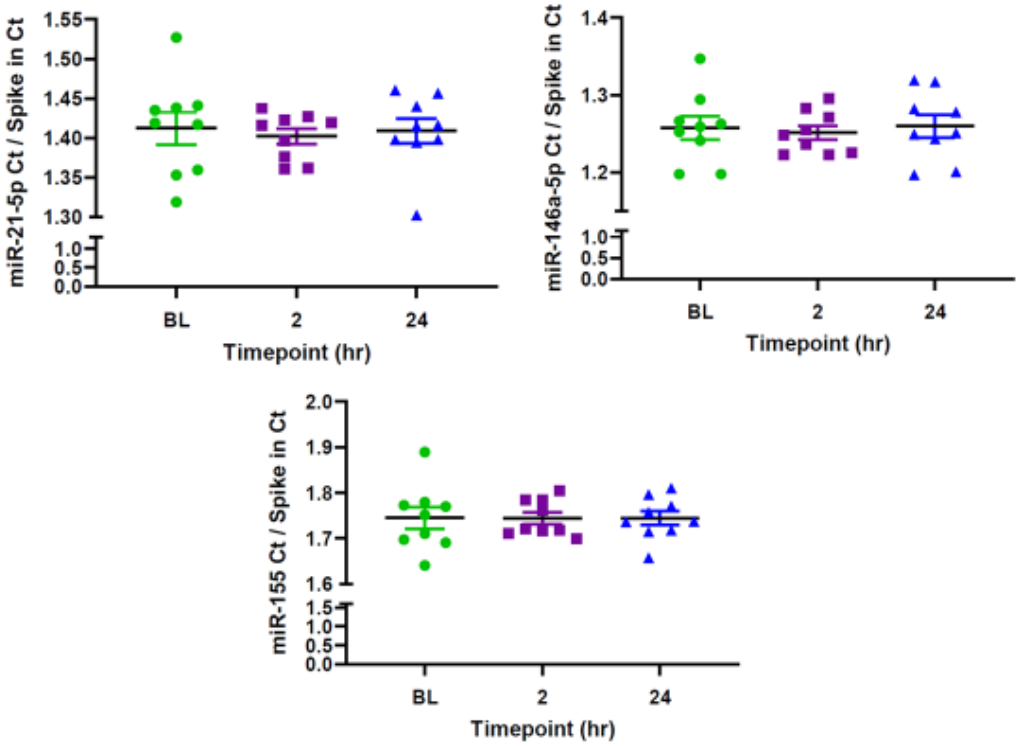

Figure 6.18. Abundance of three immune miRs in 50 ul of plasma, normalised to the exogenous control, cel-miR-39. The exercise intervention had no effect on the immune miRs (One-way ANOVA with LSD posthoc test. Mean ± SEM).

6.5 RNA sequencing of Total RNA associated with small EVs

To obtain a more comprehensive understanding of the RNA cargo present in small EVs before and after two consecutive bouts of muscle-damaging exercise, RNA sequencing technology was applied to a subset of participants' samples. Three participants were randomly selected to have their BL and corresponding 24 hr post-exercise timepoint small EV samples sequenced. The RNA sequencing protocol used in this study focused on sequencing fragments of 15 to 50 nucleotides in size i.e. small RNAs. Fragments larger than this would not be sequenced. Section of this RNA size range results in the following possible RNA subtypes being sequenced; microRNA, piwi-interacting RNA, circular RNA, transfer RNA and portions of protein coding RNA (whether in fragments or not). It is not possible within this thesis to address all these different types of RNA

in detail and therefore a focus will be placed on miR analysis, with a broad overview on the amount of other RNA present in the small EV samples.

6.5.1 Total RNA concentration present within small EVs pre and post-exercise

Prior to sequencing the quantity of RNA was determined using a small RNA chip (Bioanalyzer 2100, Agilent technologies). This chip makes use of fluorescent gel electrophoresis to determine a total RNA concentration, as well as the miR concentration specifically. No difference in small EV total RNA concentration was found between BL and 24 hr post-exercise (286 ± 32 vs 360 ± 6 pg / ul, p = 0.1958) or miR concentration (114 ± 27 vs 154 ± 8 pg / ul, p = 0.3470).

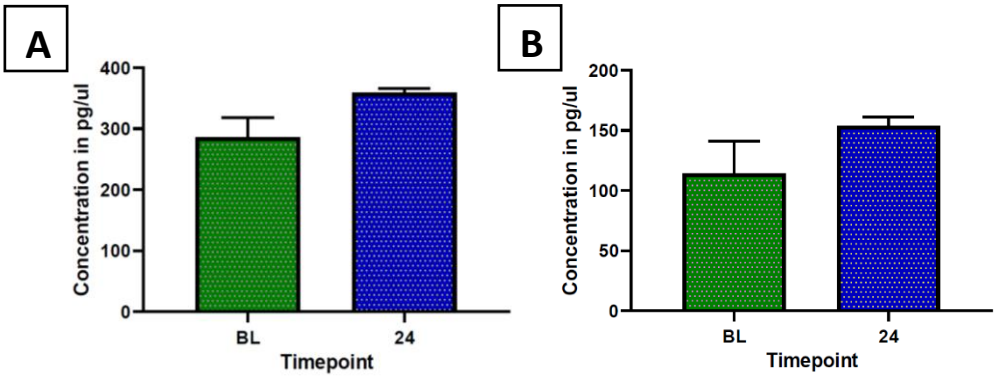

Figure 6.19. Small EV RNA concentrations (**A**) Total RNA (**B**) total miR. Values obtained from n = 3 participants at Baseline (BL) and 24 hr post-exercise (24). (Paired t-test).

6.5.2 RNA Biotype distribution in small EVs pre and 24 hr post-exercise

Qualitative analysis of total reads from RNA sequencing suggest that differences in concentrations of the various RNA biotypes in small EVs among people may exist. Participants 1 and 2 had miRs as their most about RNA biotype at both BL (53 % and 53 %, respectively) and 24 hr post-exercise (50 % and 51 %, respectively) (Figure 6.20 A & B). In contrast, participant 3 had miscRNA as their most abundant biotype with 44 % of reads at BL and 45 % at 24 hr. miR reads were the second most abundant biotype in this participant with 37 % of reads at BL and 37 % at 24 hr. The third most abundant RNA Biotype in all three participants was piRNA with some

apparent variation between participants. Participant 3 had somewhat higher levels of piRNA at both BL (15 %) and 24 hr (14 %) post-exercise. Lower levels of piRNA were found in participants 1 and 2 at both BL (12 % and 10 %, respectively) and at 24 hr post-exercise (13 % and 9 %, respectively). The other types of RNA, such as tRNA and protein coding RNA, were found to make up less than 10% in all participants. As the focus of this thesis is on miRs, it will be this RNA type that will be subsequently presented in more detail.

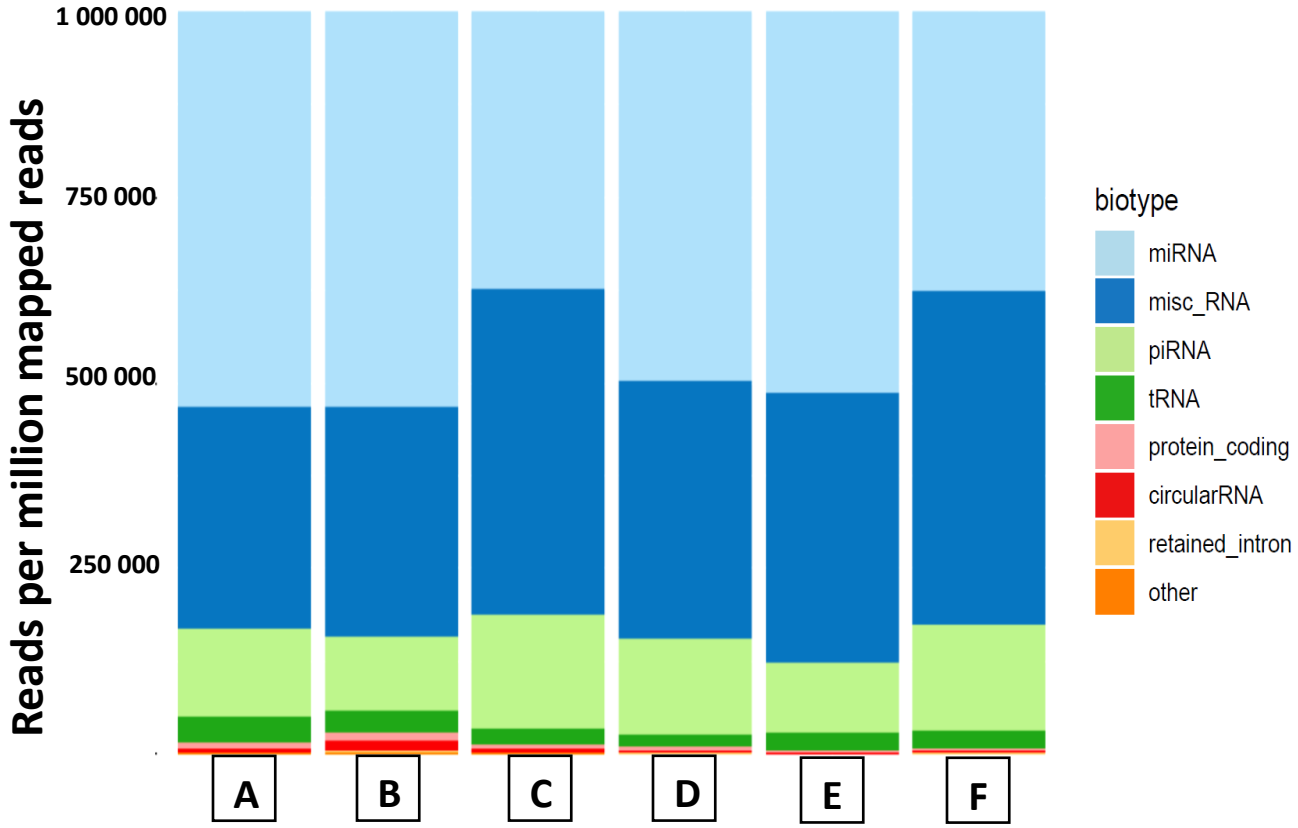

Figure 6.20. Biotype distribution of mapped small RNA reads per million reads for all 6 sequenced samples. **A** & **D** represent one participants' BL and 24 hr sample, respectively. **B** & **E** represent one participants' BL and 24 hr sample, respectively and **C** & **F** represent one participants' BL and 24 hr sample, respectively.

6.5.3 Total number of miRs identified in small EVs

RNA sequencing is a powerful big data technique that enables the investigation of many genes within a sample at the same time. By applying RNA sequencing technology to the study of small

EVs isolated from participant samples at BL and 24 hr post-exercise hundreds of different miRs were detected. Using a detection limit of at least one miR read per million in any sample at BL or at 24 hr post-exercise, 362 different miRs were detected. When considering miRs detected in every sample and at every timepoint, this number was reduced to 243 miRs. Therefore, 119 miRs showed variable detection between samples across timepoints. At a detection limit of at least 5 miRs per each sample at each timepoint 240 miRs were found, and these were used for later statistical analyses (appendix Table 1). These, as well as the following data, were generated using reads per million, normalised using the trimmed mean of M values (TMM) method.

6.5.4 The top 20 most abundant miRs in small EVs

The most abundant miR in all samples and at all timepoints was miR-26a-5p, with an average of 205 383 ± 12 186 and 261 005 ± 14 903 reads per million at BL and 24 hr post-exercise, respectively. The second most abundant miR in all samples and timepoints was miR-191-5p, with 83 922 ± 1 697 and 98 855 ± 4 396 reads per million at BL and 24 hr post-exercise, respectively. The top 20 most abundant miRs detected in BL and 24 hr samples are displayed in Table 6.3. Notably, nine of the top ten most abundant miRs were similar between both timepoints. For the other miRs, their ranking positions at each timepoint varied, but the general trend was a similar ranking between BL and 24 hr.

Table 6.3. Top 20 most abundant miRs at BL (**A**) and 24 hr (**B**). In column A, the number in brackets is the position of the miR at the 24 hr post-exercise timepoint.

A	miR	BL (Reads per million)
1 (1)	**miR-26a-5p**	205 383 ± 12185
2 (2)	**miR-191-5p**	83 922 ± 1697
3 (4)	**miR-423-5p**	61 178 ± 1315
4 (6)	**miR-486-5p**	60 400 ± 6805
5 (3)	**let-7f-5p**	54 708 ± 1048
6 (5)	**miR-151b**	49 298 ± 1290
7 (7)	**miR-146a-5p**	39 978 ± 2451

B	miR	24 hr (Reads per million)	>10%
1	**miR-26a-5p**	261 005 ± 14903	↑
2	**miR-191-5p**	98 855 ± 4396	↑
3	**let-7f-5p**	70 509 ± 5799	↑
4	**miR-423-5p**	57 328 ± 5873	
5	**miR-151b**	56 779 ± 3158	
6	**miR-486-5p**	42 356 ± 4608	↓
7	**miR-146a-5p**	40 212 ± 2627	

8 (8)	**miR-30d-5p**	26 219 ± 1871	8	**miR-30d-5p**	31 309 ± 1410	↑
9 (12)	**miR-10b-5p**	21 557 ± 9114 *	9	**let-7a-5p**	24 582 ± 1828	↑
10 (10)	**miR-21-5p**	20 500 ± 2614	10	**miR-21-5p**	23 320 ± 3654	↑
11 (9)	**let-7a-5p**	18 168 ± 998	11	**miR-92a-3p**	18 813 ± 721	
12 (13)	**miR-125a-5p**	16 903 ± 4157	12	**miR-10b-5p**	18 790 ± 6728 *	↑
13 (16)	**miR-146b-5p**	16 854 ± 1054	13	**miR-125a-5p**	18 702 ± 3999 *	↑
14 (15)	**miR-10a-5p**	15 422 ± 4589	14	**miR-30e-5p**	16 734 ± 502	
15 (11)	**miR-92a-3p**	14 895 ± 1089	15	**miR-10a-5p**	14 954 ± 4266 *	
16 (14)	**miR-30e-5p**	14 055 ± 1035	16	**miR-146b-5p**	14 919 ± 1546	
17 (18)	**miR-27b-3p**	11 748 ± 1564	17	**let-7b-5p**	13 393 ± 1761	↑
18 (17)	**let-7b-5p**	11 192 ± 1522	18	**miR-27b-3p**	12 297 ± 1773	↑
19	**miR-22-3p**	9 519 ± 381	19	**miR-1-3p**	9 889 ± 9495 *	
20	**miR-126-3p**	9 496 ± 1944	20	**miR-99b-5p**	9 864 ± 1225	

Footnote: "↑" & "↓" represent of greater than 10 % from BL, and "*" represents samples with high variation **(**for more detail see table 6.5**).**

6.5.5 miRs that displayed variable detection between samples

Notably, out of the 119 miRs that were variably detected three miRs were found to be present either in all BL samples and no post-exercise sample or *vice versa* (Table 6.4). miR-6513-3p was present in all BL samples at a mean read count of 13 ± 2.4 reads per million but absent from all 24 hr post-exercise samples. In contrast, miR-4511 and miR-3909 were present at mean read counts of 10 ± 0.3 and 9 ± 0.6 reads per million in all 24 hr post exercise samples, respectively, but absent from all BL samples.

Table 6.4. miRs that were detected in all participants at either baseline (BL) or 24 hr post-exercise (24) but not in both their timepoints.

	A (BL)	B (BL)	C (BL)	A (24)	B (24)	C (BL)
miR-6513-3p	10	18	12	0	0	0
miR-4511	0	0	0	10	11	10
miR-3909	0	0	0	9	8	10

6.5.6 miRs with a change between pre and post-exercise

Of the 240 miRs used for statistical analysis via paired t-tests, 28 displayed a significant change at 24 hr post-exercise when compared to BL (Table 6.5). Most (i.e. 18 of 28) displayed an increase post-exercise (Table 6.5 highlighted in green), whereas fewer (i.e. 10 of 28) showed a decrease post-exercise (Table 6.5 highlighted in red). Additionally, a total of 18 miRs were found to have a trend toward changing (i.e. $p < 0.1$) (Table 6.6).

Table 6.5. miRs that displayed a change due to the exercise intervention, represented as Mean ± SEM. (An increase post-exercise is highlighted in green, whereas a decrease is highlighted red)

	miR	BL (Reads per million)	24 (Reads per million)	P value
1	**miR-584-5p**	1627 ± 142	1839 ± 122	0,0009
2	**miR-199a-3p**	1814 ± 177	2216 ± 190	0,0043
3	**miR-185-5p**	4893 ± 161	3672 ± 77	0,0054
4	**miR-23b-3p**	1570 ± 229	1933 ± 248	0,0066
5	**miR-26a-5p** (1)	205383 ± 12185	261005 ± 14903	0,0077
6	**miR-126-5p**	3454 ± 594	4411 ± 696	0,0086
7	**miR-125a-5p** (12)	16903 ± 4157	18702 ± 3999	0,0107
8	**miR-92a-3p** (15)	14895 ± 1089	18813 ± 721	0,0119
9	**miR-505-5p**	155 ± 6	341 ± 21	0,0135
10	**miR-30c-5p**	4556 ± 374	5985 ± 197	0,0151
11	**miR-486-5p** (5)	60400 ± 6805	42356 ± 4608	0,0163
12	**miR-320c**	164 ± 11	97 ± 9	0,0166
13	**let-7e-5p**	1514 ± 211	2013 ± 278	0,0203
14	**miR-30d-5p** (8)	26219 ± 1871	31309 ± 1410	0,0212
15	**miR-106b-3p**	589 ± 62	301 ± 33	0,0224
16	**miR-24-3p**	2030 ± 40	1893 ± 53	0,0233
17	**miR-93-3p**	59 ± 6	31 ± 9	0,0252
18	**miR-145-3p**	55 ± 19	134 ± 9	0,0337
19	**miR-186-5p**	2959 ± 162	2173 ± 233	0,0340
20	**miR-151a-5p**	1695 ± 93	1973 ± 135	0,0373
21	**let-7d-5p**	3722 ± 147	4421 ± 279	0,0378
22	**miR-335-3p**	521 ± 130	816 ± 92	0,0395
23	**miR-28-5p**	504 ± 82	335 ± 47	0,0402
24	**miR-191-5p**	83922 ± 1697	98855 ± 4396	0,0412
25	**let-7a-5p** (11)	18168 ± 998	24582 ± 1828	0,0413
26	**miR-22-3p** (19)	9519 ± 381	8142 ± 232	0,0414
27	**miR-103a-3p**	1068 ± 34	1461 ± 114	0,0492
28	**miR-1301-3p**	1694 ± 150	1604 ± 157	0,0495

Footnote: Number in brackets indicates the rank for the number of reads per million (highest to lowest) as presented in table 6.3.

Table 6.6. miRs that displayed a trend toward change due to the exercise intervention, represented as Mean ± SEM. (An increase post-exercise is highlighted in green, whereas a decrease is highlighted red)

	miR	BL	24	P value
1	**miR-19b-3p**	24 ± 4	41 ± 6	0,0509
2	**let-7i-5p**	7547 ± 118	6871 ± 239	0,0521
3	**miR-192-5p**	2376 ± 394	1324 ± 164	0,0536
4	**miR-224-5p**	3236 ± 429	3774 ± 522	0,0540
5	**miR-181c-3p**	133 ± 5	93 ± 6	0,0582
6	**miR-4433b-5p**	497 ± 89	708 ± 112	0,0587
7	**miR-151b** (6)	49298 ± 1290	56779 ± 3158	0,0597
8	**miR-146b-5p** (13)	16854 ± 1054	14919 ± 1546	0,0649
9	**miR-451a**	3892 ± 525	1349 ± 271	0,0660
10	**miR-142-3p**	40 ± 1	99 ± 16	0,0680
11	**miR-125b-5p**	1248 ± 179	1051 ± 189	0,0707
12	**miR-494-3p**	386 ± 121	570 ± 172	0,0711
13	**miR-339-3p**	88 ± 10	45 ± 8	0,0794
14	**miR-30e-5p** (16)	14055 ± 1035	16734 ± 502	0,0830
15	**let-7f-5p** (5)	54708 ± 1048	70509 ± 5799	0,0883
16	**miR-150-5p**	1384 ± 378	1043 ± 393	0,0944
17	**miR-99a-5p**	2914 ± 424	2107 ± 249	0,0968
18	**miR-532-5p**	82 ± 18	47 ± 11	0,0981

6.5.7 Comparison of small EV qPCR data and sequence data

Eleven miRs were investigated in small EVs using qPCR (see section 6.8). Three of these same miRs (miR-486-5p, miR-146a-5p and miR-21-5p) were also detected in the top 20 most abundant miRs via sequencing (Figure 6.21). These miRs were found in differing abundances with sequencing when compared to qPCR. For sequencing the most abundant of these miRs was miR-215-5p followed by miR-146a-5p and miR-486-5p. In contrast the most abundant miR via qPCR was miR-486-5p followed by miR-146a-5p and miR-21-5p (see Figure 6.9 and 6.10).

Although detected using qPCR, miR-133b, miR-31-5p, miR-208b-3p, miR-499-5p and miR-155-5p were not detected in any sample at any timepoint with sequencing. Along similar variable

detection between sequencing and qPCR, miR-133a-3p was detected in all samples via qPCR but was detected in only 5 out of 6 samples via sequencing. A similar variable detection pattern was seen for miR-206 whereby it was detected in all samples via qPCR but only detected in 4 out of 6 samples via sequencing. Finally, it was found that miR-486-5p displayed a significant decrease post-exercise with sequencing (See Table 6.5), however no change using qPCR was found.

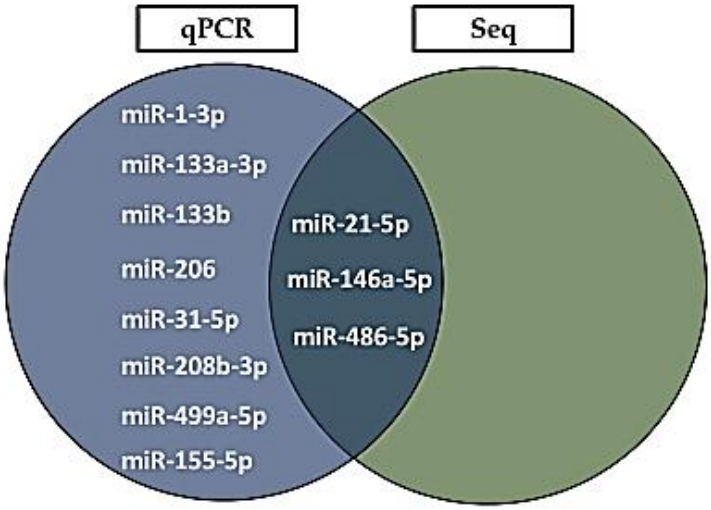

Figure 6.21. Venn diagram showing miRs that were detected using qPCR and were detected in all samples at all timepoints using small RNA sequencing.

Chapter 7: Discussion

The aim of this thesis was to determine the use of plasma, large EV and small EV associated miRs as potential biomarkers of SkM damage in healthy humans in response to a dynamic eccentric exercise intervention *in vivo*. Several miRs referred to as canonical myomiRs (n = 4) and other miRs important in SkM biology (n = 4), and miRs considered to be important in the immune cell response to tissue injury (n = 3), were measured. It was hypothesized that the response to the *in vivo* model of muscle-damaging exercise in human volunteers, consisting of two consecutive bouts of eccentrically-biased exercise, would result in substantial changes in these miRs at 24 hr after the intervention compared to BL. The 24 hr time was selected as important to investigate because it coincides with the delay in the onset of muscle soreness and the acute effects of exercise would not be a confounding factor. Nonetheless, the early post-exercise timepoint of 2 hr would represent the acute effects of exercise, with a relatively short duration of post-exercise rest. Additionally, it was hypothesized that changes in the miRs that were selected for analysis over time would be more likely in small EVs than larger EVs due to the possibility of selective packaging. Furthermore, using small RNA sequencing this study aimed to find miR changes in small EVs at 24 hr post-exercise when compared to BL.

To determine the effects of mild to moderate muscle damage, one first needs to establish evidence suggesting that muscle damage had indeed occurred. Indirect evidence for SkM damage was determined in this study by the large increase in serum CK levels and PMP scores following the exercise protocol. Notably, serum CK levels are the most widely used indirect marker of exercise-induced muscle damage [20]. The large elevation in serum CK levels observed in all participants reinforced the confidence that the chosen exercise intervention would have caused SkM injury and activated regeneration processes. Although direct evidence of damage was not assessed here, Macaluso *et al.* have visualised disruption of sarcomere ultrastructure following an acute bout of PMJ [9]. The number of plyometric jumps in their protocol was the same as that used here (10 sets of 10 jumps), however, maximal jump height was used as opposed to the 90% of maximum used

here. A novel aspect of the current study was that the protocol included the 2 -5 bouts of DHR following the PMJ. DHR alone was shown by van de Vyver *et al.* to result in a large peak in serum CK, with a concomitant increase in satellite cell activation 24 hr post-exercise [46]. The current data for the combined protocol indicates that the highest average perceived muscle pain scores were experienced at 24 hr. From these data, it was concluded that the model of muscle-damaging exercise induced by two consecutive eccentrically-biased exercise protocols was sufficient to induce significant changes in circulating EV cargo that might be specific to muscle damage.

As mentioned in the literature review of this thesis, SkM is the largest internal organ in the human body and is therefore likely to have a significant influence on the dynamics of circulating miRs, particularly after the perturbation of SkM through exercise. Here we show that myomiRs, miRs highly enriched in SkM, are abundant in plasma. There is a significant increase in most of the myomiRs 2 hr after two consecutive bouts of muscle-damaging exercise. Eccentrically-biased exercise is known to be frequently accompanied by disruption to the sarcolemma as a component of exercise-induced muscle damage [9]. These data therefore suggest that changes in plasma myomiRs may be a result of passive leakage from damaged membranes. Here, however, data on muscle myopathies (particularly muscular dystrophy) may help shed light on the dynamics of myomiR release into circulation with sarcolemmal disruption [188]. For example, it has also been shown that uniform sarcolemmal dystrophin expression (such as that absent in dystrophy patients) is needed to prevent increased abundances of myomiRs in circulation [188]. Indeed, the sera abundance of myomiRs has been shown to increase with dystrophy severity [189]. The abundance of myomiRs in circulation has been found to contrast the decrease in SkM tissue lysate abundances [190]. These data suggest that myomiRs, at least in dystrophic SkM, are actively secreted into circulation [191]. Indeed, similar to that seen in the case of dystrophy, tissue lysate myomiRs have been shown to decrease following downhill running, with a concomitant increase in plasma (such as that seen in this study) and EVs [118]. Therefore, the mechanisms of circulating myomiR release following muscle damage may not simply be passive in nature, and it remains for studies into the temporal release of myomiRs following damage to elucidate.

When considering miR abundances in circulation it is important to consider the rate of release and degradation. One or both dynamic parameters may differ depending on the predominance of certain nucleotides. Indeed, Roberts *et al.* have shown that miRs exhibit sequence-dependent stability, with GC content being correlated with more stable miRs [139]. Even within the myomiR family, different degradation kinetics have been shown. myomiR-208b (31%) and 499a (33%) have a lower GC content than myomiR-133a (54%) and 206 (45%) and yet the former two were found to exhibit a sustained increase in plasma at 24 hr post muscle-damaging exercise. This shows that either this stability does not hold true during our chosen physiological intervention, or there is a continued high release. Nevertheless, the differential abundance of canonical myomiRs (miR-1, 133a and 206) and SkM-important miRs (miR-208b and 499a) at 2 and 24 hr post-exercise highlights the importance of considering the temporal nature of miR abundances when choosing sample timepoints.

In a study by Mooren *et al.*, where myomiRs (miR-1, 133, 206, 499 and 208b) increased immediately after a marathon, only myomiR-208b and 499 returned to baseline abundances at 24 hr post-marathon [192]. This is in direct contrast to the pattern of myomiR-208b and 499a abundance in this thesis: myomiR-499a increased at 2 hr but trended toward remaining increased at 24 hr (Figure 9.17). MyomiR-208b also increased at 2hr, and had a trend toward staying increased at 24 hr. However, like the results of Mooren *et al.*, there was an acute increase in plasma myomiR-133a and 133b at 2 hr post-exercise, with a return to baseline levels at 24 hr. Also, myomiR-1 and 206 showed an increase at 2 hr, with a trend toward returning to baseline levels at 24 hr. However, myomiR-486 did not change in any of the three sample types. Taken together, these two studies show that different myomiRs show different temporal patterns in response to exercise and the temporal pattern may differ depending on the exercise intervention. These changes were exclusive to myomiRs.

Although the immune-important miRs were abundant in all three avenues of investigation (i.e. plasma, large EVs and small EVs), no change was seen due to the exercise intervention, despite the known immune cell involvement during early phases post-exercise and following muscle

damage [46] [26]. miR-21-5p, 146a-5p and 155-5p were chosen due to their known involvement with immune cells. Specifically, miR-21-5p and miR-155-5p have been shown to target the mRNA of transcription factors important in monocyte differentiation, thereby inhibiting this process [186]. These two miRs were not changed in abundance in circulation following a marathon [192]. miR-146a-5p has also been shown to increase immediately after a marathon, and return to baseline levels at 24 hr post [177]. miR-146a-5p, specifically, has been implicated in monocyte polarization, and also in inflammation [177] [187]. The timing of immune events after damage, however, is likely to result in a temporal different in immune miR abundances when compared to myomiRs and SkM-important miRs.

No change in the size or number of large EVs seen in EVs in this study. Similarly, the abundance of the selected miRs did not change due to the exercise intervention. However, all selected miRs were detected at reasonably high values in large EVs (e.g. miR-21-5p had an average Ct of 18 vs a Ct of 10 for 10 pM of spiked-in control). Indeed, all selected miRs were detected in all investigated avenues of potential biomarker i.e. plasma, large EVs and small EVs.

The increasing use of size exclusion chromatography (SEC) has been attributed to its speed and ease of use, as well as the passive nature of the isolation [90] [193]. The latter is important, since the testing of downstream effects of EVs applied to cells in culture has revealed that SEC derived EVs did not decrease cell viability when compared to chemical precipitation [193]. One can conclude from this, that even if the purpose is not to apply the EVs *in vitro,* the EVs would be less damaged and more similar in structure and nature to *in vivo.* The qEV columns used in this study have been shown to separate most EVs from abundant plasma proteins as shown by BCA assays [194]. The current results from both the Coomassie stain and BCA results confirm this. Nonetheless, a potential disadvantage of using SEC is the dilution of the sample, making some downstream analyses difficult. Despite this, miRs were successfully detected in small EV SEC-derived fractions using both qPCR and small RNA sequencing.

Small EV analysis of 15 fractions from 5 baseline samples revealed that fractions 7 to 9 were most enriched in particles, whereas fractions 8 to 10 had the lower diameters. Devoid of most proteins

(as shown by BCA and Coomassie stain) and showing an abundance of heterogeneously sized particles around the small EV range in STEM micrographs and NTA, fractions 7 - 10 were subsequently pooled for further analysis. These same fractions were determined as EV enriched by D'Souza *et al.* [148] and Stranska *et al.* [181] (as determined by western blot, NTA and TEM).

As seen in this thesis, circulating EV size and number do not change 24 hr post-exercise, a finding that has been noted previously [51] [117]. Different exercise modalities, e.g. aerobic [114] or muscle-damaging [51] (similar to this study) also appear to have no major impact on circulating EV number when assessed more than 1 hr post-performance of the exercise bout. However, if EV number is assessed immediately after performance of an aerobically based exercise intervention a significant increase in EV number has been reported, which returns to baseline levels 90 min post-exercise [114]. We did not assess EV number immediately post the muscle-damaging exercise intervention and hence whether the same temporal increase occurs with muscle-damaging exercise remains to be determined. In the current investigation, blood draw timepoints were chosen in accordance with concentrations changes of circulating molecules which have been investigated on a regular basis, such as CK, Mb, IL-6 and which have been related to intramuscular events. The 2 hr post-exercise timepoint was chosen in accordance with peak elevation in the inflammatory cytokine, IL-6, from a similar DHR protocol [22]. Similarly, the 24 hr timepoint was chosen as this has been shown to be when the largest CK response occurs [21]. Additionally, peak satellite cell activation, as shown by an increase in Pax 7^{+} cells, in muscle biopsies taken after a similar DHR regimen is seen at this timepoint [21].

Although four muscle-important miRs were assessed in the pooled small EVs only one, miR-31-5p, displayed a decrease in abundance at 24 hr post-exercise when compared to BL, with a similar decrease at 24 hr when compared to 2 hr. No change in plasma nor large EV miR-31-5p was seen, showing that the change was specific to small EVs and specific as a delayed response to the exercise intervention. Despite not fitting the classic definition of being a myomiR i.e. existing ≥ 20-fold abundance in SkM when compared to other tissues, miR-31-5p has been reported as muscle-important [32] [195] [196] [197]. Indeed, with regard to SkM, a study by Crist *et al.* [32] showed that

miR-31-5p sequesters the mRNA transcript of Myf5. This was found by in situ hybridization, which showed that both miR-31 and Myf5 were co-located in messenger ribonucleoprotein (mRNP) granules in quiescent satellite cells. miR-31-5p causes the transient repression of translation of the Myf5 mRNA transcript into the Myf5 protein. Myf5 is a transcription factor in myogenesis and is part of a group of transcription factors known as Myogenic Regulatory Factors (MRF) [198]. Its presence in the protein form is key for myogenic progenitor cell proliferation, and the inhibition of differentiation [32]. The premise that miR-31-5p is involved in myogenesis was further supported by Dmitriev *et al.* [196] using miR profiling of $CD56^{+}$ myoblast undergoing differentiation, these authors showed that miR-31-5p decreased throughout this process, hence decreasing the inhibition of the relevant proteins' translation. Yet another study alluded to the involvement of miR-31-5p in regeneration, particularly with regard to muscular dystrophy [197]. This study used a model of hindlimb ischemia in mdx mice, where an experimental treatment of endothelial nitric oxide synthase was used for the model of regeneration, to establish that miR-31-5p was increased in lysates during regeneration. In human volunteers, miR-31-5p has also been shown to decrease in muscle lysates 3 hr after an acute bout of moderate intensity aerobic exercise [199]. This study suggests that miR-31-5p is not only responsive to muscle damage, but also metabolic demand or mechanical stress without damage. Nevertheless, taken together the data suggest that this specific component of EV cargo represents a change in the internal nature of SkM tissue. The results of the study in this thesis found no change in small EV miR-31-5p at 2 hr post muscle-damaging exercise. The aforementioned study, where the 3 hr timepoint was after an acute bout of moderate-intensity endurance cycling, suggests that the metabolic demand of the eccentric exercise protocol in this study, despite its consecutive nature, was not similarly high. Although both studies were in untrained individuals, these combined findings would seem to indicate that miR-31-5p plays multiple roles in multiple systems.

The decrease in small EV miR-31-5p suggests that small EVs are actively released following muscle-damaging exercise. Western blotting for ESCRT or RNA loading associated proteins may aid the determination of whether these small EVs are selectively packaged and actively secreted. However, the tissue origin of this miR cannot be explicitly attributed to SkM in this study. The

addition of immune capture techniques against SkM specific proteins would help clarify this. Nevertheless, no change in large EV miRs implicates passive release in this EV subtype's response, or lack thereof, to muscle-damaging exercise.

The question as to whether the amount of myomiRs in EVs is enough to cause significant changes in the recipient cell is yet to be determined. The existence of specific EV miR changes (i.e. miR-31-5p) in response to a physiological stimulus (i.e. muscle-damaging exercise) might suggest a role for EV miRs in intercellular/inter-organ communication. Recently, EV myomiR-206 has been associated with muscle to heart communication (perhaps explaining a mode whereby heart defects are manifested during muscular disorders) [200]. This aids the notion that myomiR-206 is not only SkM specific but is actively involved in inter-striated muscle communication, and it is through its association with EVs that this occurs.

It is important to consider that EV-free (i.e. complexed with RISC proteins, HDL or with unknown proteins) and EV-transported miRs may have different physiological roles *in vivo*. Indeed, subgrouping miR analyses according to their carrier may help better elucidate the exact role of circulating miRs. EVs exist as an easy explanation for how miRs are protected from degradation by circulating RNases, however, more circulating miR carriers have been established [147]. The exact physiological roles of these different miR carriers and their miRs remains to be determined.

Small RNA sequencing allows for a global investigation of miRs, rather than a targeted approach; thereby screening all candidate miRs for potential changes. RNA sequencing, and other "omic" approaches, are increasingly being used to investigate EVs [98 180 201].

In this study, small RNA sequencing of pooled small EV fractions (F7 - 10, derived from SEC) revealed the following general results:

- An abundance of miRs and small miscellaneous RNAs.
- Although less abundant, piwi RNA and tRNA were detected, but were not focused on for this thesis

- Of the 240 miRs that were detected greater than 5 times in all samples at BL and 24 hr post-exercise, by far the most abundant miR was miR-26a-5p, constituting 23 % of all reads when considering all samples analysed.
- As determined by sequencing, 28 miRs changed in abundance due to the exercise intervention, of which 18 increased and 10 decreased 24 hr post-exercise.
- Many miRs displayed considerable variability, and therefore no change was found.

When comparing the most abundant miRs in the current results with those reported in the literature, some consistency was seen. Of the top 27 most abundant miRs detected in this study, 15 were similar to those detected by Zhao *et al.* [202], who sequenced small EVs from human serum (for a comparison see Table 7.1).

miRs are known to target multiple mRNA. Of the 18 miRs that increased post-exercise in the current study, 10 have previously been shown to change in SkM under varying conditions, or in circulation in response to exercise. For example, miR-584-5p had approximately a 52-fold greater abundance in the plasma of trained athletes under resting conditions when compared to sedentary individuals [203]. miR-584-5p has been shown to target the matrix metalloproteinase 14 promoter in neuroblastoma cells [204]. miR-199a-3p (which has been termed a "dystromiR" [190]) has been shown to be increased in the diaphragm and quadriceps of mdx when compared to wildtype mice [190]. Conversely, following 10 days of bed rest, miR-199a-3p has been shown to decrease in human *V.L.* lysates when compared to healthy controls [205]. Additionally, this miR has also been shown to decrease in the *V.L.* lysates of old individuals at BL when compared to young individuals [159]. These results suggest that this miR is expressed under conditions when muscle is damaged, but not when the abnormal condition is atrophy. miR-199a-3p has been shown to decrease Caveolin-2 expression [206]. Caveolin-2 is a scaffolding protein with important roles in endocytosis and signalling [206]. miR-26a-5p has been found to be decreased in SkM under experimental conditions of chronic kidney disease-associated SkM atrophy in mice [207]. Overexpression of miR-26a-5p in EVs targeted toward SkM, through expression of a muscle specific peptide, has been shown to result in an increase in SkM cross-sectional area [207]. In the

current study miR-26a-5p increased in small EVs following muscle-damaging exercise. Whereas plasma miR-26a-5p has been shown to decrease after a marathon in elite runners specifically [208]. This suggests that metabolic stress and mechanical loading have opposite effects. Following a 10 km or marathon run, neither miR-125a-5p, miR-30c-5p, let-7d-5p nor let-7a-5p changed in plasma abundances when compared to baseline levels [178]. This also suggests the muscle damaging exercise is a stressor that varies significantly from a metabolically stressful form.

When considering the chronic effect of exercise as opposed to the effect of an acute intervention, plasma miR-30c-5p has been shown to be downregulated in trained vs sedentary individuals [203]. Although miR-151a-5p has been determined as one of the top most abundant miRs in small EVs derived from human serum [202], the trained state reflected a decrease in miR-151a-5p content of EVs of trained individuals (taking part in endurance activities for ≥ 5 years) at rest when compared to sedentary individuals [209]. Similarly, let-7a-5p is downregulated in trained individuals [203]. miR-103a-3p is downregulated in trained vs sedentary individuals [203] although it has been shown to be downregulated during myogenic differentiation *in vitro* [196]. Aerobic fitness does not necessarily result in increased muscle size. miR-191-5p has been shown to be correlated with isokinetic knee extension strength and muscle cross-sectional area in healthy middle-aged males [210]. Of the 18 miRs increased post-exercise 8 have not been reported to be involved in SkM or a response to exercise (miR-335-3p, miR-145-3p, miR-30d-5p, let-7e-5p, miR-505-5p, miR-92a-3p, miR-126-5p and miR-23b-3p).

Of the 10 miRs decreased post-exercise 8 have not been reported to be involved in SkM or a response to exercise (miR-106b-3p, miR-24-3p, miR-93-3p, miR-186-5p, miR-28-5p, miR-22-3p, miR-1301-3p). The other 2 have previously been shown to change in SkM under varying conditions, or in circulation in response to exercise. Sequencing revealed a decrease in miR-486-5p at 24 hr post-exercise in the current study. Similar to this study, miR-486-5p has been detected as the most abundant miR in SkM and plasma in previous studies using sequencing [210] [144]. Although no change was determined with this miR through the use of qPCR, and no change was found in EVs in our previous study [51], two separate studies have shown a decrease in plasma

miR-486-5p following immediately after [179] and 4 hr after [148] aerobic exercise. In contrast to the circulating changes in miR-486-5p, abundances in *V.L.* lysates increased 4 hr post-exercise when compared to BL [211]. These findings highlight the common result of tissue miR abundances being opposite to circulating abundances i.e. if tissue abundance increases, then circulating abundance decreases [148] [191]. In regard to exercise-induced changes in EV miR-486-5p, an increase in abundance immediately after an acute bout of high-intensity interval exercise has been reported [148]. A return to baseline abundances, however, was noted at 4 hr post-exercise. Interestingly, in a separate study, EV miR-486-5p was shown to decrease immediately after an acute bout of aerobic exercise in trained individuals. EV miR-486-5p was higher in old trained individuals when compared to old sedentary individuals at baseline [209]. These varying responses, depending on study design, may be reflective of a variety of different roles that miR-486-5p plays. For example, miR-486-5p is predicted to control PI3K/Akt signalling through the repression of PTEN and FoxO1a [212]. Additionally, the transcription of miR-486-5p is controlled by MyoD, suggesting a role in myogenesis. In a different study miR-486-5p it has been shown to be upregulated during myoblast differentiation via the binding to the 3′ UTR of Pax7; a transcription factor highly expressed in satellite cells [184]. Another miR that may play a role in myogenesis is miR-320c which is decreased in quiescent compared to activated satellite cells [213].

Table 7.1. A comparison of the top 27 most detected miRs in the study by Zhao *et al*. [202] compared with the current study. The corresponding rank in this study is in brackets next to the rank for the Zhao *et al*. study. Counts are represented in reads per million.

	miR	Zhao et al	This study
1 (4)	**miR-486-5p**	360870	60400
2 (15)	**miR-92a-3p**	44958	14895
3	**miR-451a**	24460	
4 (3)	**miR-423-5p**	23392	61178
5 (2)	**miR-191-5p**	8452	83922
6 (18)	**let-7b-5p**	5222	11192
7 (1)	**miR-26a-5p**	5138	205383
8 (9)	**miR-10b-5p**	3796	21557
9 (14)	**miR-10a-5p**	2990	15422
10	**miR-125b-5p**	2984	
11	**miR-99a-5p**	2537	
12 (7)	**miR-146a-5p**	2270	39978
13 (12)	**miR-125a-5p**	2214	16903
14 (19)	**miR-22-3p**	1927	9519
15 (8)	**miR-30d-5p**	1903	26219
16	**miR-25-3p**	1687	
17	**miR-100-5p**	1561	
18	**miR-122-5p**	1213	
19 (22)	**miR-99b-5p**	1187	9017
20	**let-7a-5p**	1178	
21	**miR-484**	1148	
22	**miR-363-3p**	1129	
23	**miR-320a**	1030	
24 (5)	**let-7f-5p**	971	54708
25 (6)	**miR-151a-5p**	963	49298
26	**let-7d-3p**	738	
27	**miR-96-5p**	609	

7.1 Conclusion

Systemic intercellular communication is not a new concept. A plethora of information on the dynamics of circulating hormones, cytokines and peptides is available for a host of different states *in vivo*. In contrast, sparse information on EV and miR dynamics in response to exercise or muscle damage exists. The current study brings much information on EVs and miRs to light, whilst raising questions as to their temporal release following muscle-damaging exercise.

Although no change in large EVs was seen, both small EV and plasma miRs changed in response to muscle-damaging exercise and may be potential biomarkers of SkM damage. Each exhibited distinct miR changes, and timing of changes as shown by targeted qPCR. miR-31-5p, for example, decreased only in small EVs post-exercise, whereas most myomiRs increased only in plasma post-exercise. RNA Sequencing revealed more small EV miR changes. However, where comparison with qPCR was made, correspondence was lacking. This thesis helps solidify the role of EVs and miRs as exerkines, whilst showing that the use of both small EV and plasma miRs as biomarkers is promising.

Chapter 8: Limitations and future directions

Future studies would benefit from a greater number of exercising participants. More participants would increase the statistical analysis power, thereby potentially resolving changes that may have been too variable to resolve with n = 9 participants. This is particularly important in studies where the biological response is known to be variable, such as for plyometric exercise. Similarly, small RNA sequencing results would also benefit from a greater number of samples analysed, although costly. However, typically, other studies analysing EV miRs in response to an acute exercise intervention have used samples from ± 10 subjects [148] [116] [214] [209].

The combined exercise modalities utilized in this study were implemented to maximize the potential for mild exercise-induced muscle damage to occur. Both PMJ and DHR have been shown by our research group to induce mild muscle damage in humans, and therefore our intervention is a useful model for the study of changes in circulating EVs post muscle-damaging exercise [9] [22]. However, it should be noted that the DHR portion of the intervention used here has a relatively large aerobic component, and therefore the observations cannot be solely attributed to SkM damage. Previously it has been shown that the choice of exercise modality does appear to influence circulating miRs in plasma [113]. Therefore, pure eccentric/muscle-damaging exercise should be considered in the future, in order to remove any influence of aerobic exercise. Alternatively, a control group doing only the running part of the protocol could complete the study on a flat gradient.

Briefly mentioned in the introduction section of this thesis, no single indirect indicator of muscle damage can be taken as an absolute measure. Visualisation of sarcomere damage from muscle biopsies can be used to directly indicate damage [9]. A combination of strategies may be preferable for indirect measures. Here, the use of serum CK activity and PMP could be improved upon with the addition of circulating inflammatory marker analysis. For example, IL-6 has been used [26]. However, if this marker is used, the flat running group would be imperative because IL-6 has

been shown to respond to aerobic exercise [43]. Additionally, measurement of isometric force loss would aid as an indirect measure of muscle damage. However, it remains true that muscle damage can only be accurately validated in muscle biopsies themselves or through the use of scanning technologies (i.e. ultrasound and MRI) [7].

An overlap in diameters between some lipoproteins and EVs has been noted in a study by Karimi *et al.* [201]. Size similarities need to be considered when EV isolation involves size exclusion; a technique that does remove HDL (5 -12 nm), LDL (18 – 25 nm), IDL (25 – 35 nm) and 90 % of plasma proteins (e.g. Albumin), but does not address the overlap between VLDL (30 – 80 nm) and Exo (30 – 150 nm) and between chylomicrons (75 – 1200 nm) and MVs (100 – 1000 nm) . These overlapping particles can be successfully separated by using density gradients, as most lipoproteins are of a lesser density than EVs; all lipoproteins barring HDL [201]. These considerations are important for the isolation of pure EVs. When considering downstream miR analyses, however, the removal of HDL is of most importance due to its ability to carry circulating miRs [137]. This issue, to the best of our knowledge, does not seem to be the case with the co-isolation of VLDL with EVs via SEC. Given the potential influence of lipoproteins on EV analysis, however, it is likely that taking blood in a fasted state may simplify downstream analyses. This has been shown by Brahmer *et al*. who found that a high fat meal before blood sampling can cloud epitopes for western blotting analysis [42].

Using antibodies targeted to specific proteins it is possible to immune-capture tissue specific circulating EVs. As mentioned in the literature review of this thesis, Guescini *et al* have used this technique to analyse the miR content of $SGCA^{+}$ (a muscle specific protein) EVs [50]. Similarly, Brahmer et al have determined that the majority of EVs released in response to aerobic exercise are from leukocytes, platelets and endothelial cells [42]. It is likely, however, that the absolute confirmation of a tissue specific EV will involve the analysis of more than one protein.

In this study we made use of a general protein detection method through coomassie-stained gels. However, a targeted antibody approach would aid in the exact determination of EV-associated proteins and for some cell types the EV origin may include a tissue-specific protein. One could include negative markers such as Calnexin, an endoplasmic reticulum protein.

Tissue lysates and blood analysis often show opposite miR results following an intervention [148]. This may be due to the biological process of EV release being higher than synthesis rate, or due to technical issues. However, new techniques have improved upon the analysis of tissue lysates and have begun to delineate EVs derived from tissues rather than blood. Although this would be invasive, it may be of particular importance in miR analyses as it has been hypothesised that a large proportion of miRs exist within the interstitium when compared to circulation [191]. As seen in a study by D'Souza *et al*. who analysed muscle biopsy lysates, plasma and EV miRs, in future it may be worth considering the additional analysis of tissue EVs [148].

The emergence of more sensitive EV separation techniques, as well as a more accurate description of EV characteristics, has helped resolve more subgroups of vesicles. Exomeres (<50 nm), for example, have been isolated through high speed ultracentrifugation (i.e. 167 000 G), and have also been shown to transfer functional cargo [215]. Although their biogenesis is currently unknown, future studies would benefit from separating subgroups of EVs to determine which may be applicable to their hypothesis.

Efforts have been made to understand the identification of circulating SkM-derived EVs specifically [50]. As mentioned before, myomiR-206 (a SkM specific miR) is consistently detected in baseline plasma samples in this study. This is despite the hurdle of having to cross the borders of a highly organized, yet evidently plastic tissue. In order to derive SkM information in the milieu of blood it should be known what proportion of circulating EVs were released by muscle as opposed to other cells that may become activated to release more EVs during and after exercise.

A study by Fruhbeis *et al.* revealed a large increase in small EV numbers immediately following an acute bout of aerobic exercise, a timepoint that was not used in this study [214]. Additionally, Banzet *et al.* found an increase in circulating myomiRs at 6 hr after an acute bout of eccentrically-biased exercise. However, EVs were not taken into account with these myomiR changes. Although the two aforementioned studies cannot directly be translated into the context of this study i.e. use of aerobic exercise and non-EV related myomiRs changes, respectively, it is nonetheless important for researchers to consider additional timepoints to more comprehensively determine the dynamics of circulating EVs and the temporal nature of their miR cargo e.g. BL,

immediately post-exercise, and at 1, 2, 6, 24 and 48 hr post-exercise. Contrary to previous studies, and our previous study, myomiR-206 was reliably detected in all participants at baseline [148] [113]. It has been noted that immature regenerating muscle fibers exhibit increases in myomiR-206 [191]. However, in this study, no difference in myomiR-206 levels was seen following muscle-damaging exercise; suggesting that our timepoints may not have been extended enough to detect the regeneration process. Therefore, future studies should consider sampling at extended timepoints post-exercise.

A leading issue in the study of miRs from biofluids is the lack of an available endogenous miR control. Many studies make us of an exogenous "spike-in" control (e.g. cel-miR-39), which can help determine RNA isolation and reverse transcription efficiency. Disparate normalization strategies across different studies makes translation of results difficult.

qPCR still exists as the gold standard in miR analysis. It is problematic for the field, that qPCR of selected miRs might not (in our case, often did not) concur with data on change of levels of circulating miRs gained from sequencing data. More publications on methodological issues might allow for more standardized procedures/guidelines. Additionally, greater sample numbers may resolve differences between sequencing and qPCR results, as the randomly chosen participant samples may not fit the trend of the whole sample group analysed.

Here we selected Illumina HiSeq 500 small RNA sequencing due to its ability to detect low concentrations of RNA. As technologies have evolved small RNA sequencing has increasingly become more cost effective than miR arrays, and many technologies exist e.g. nanostring, Illumina and oxford nanopore. However, perhaps the most established are the Illumina sequencing systems (www.illumina.com) which make use of conversion into cDNA and library construction. Non-targeted approaches such as this allow for the detection of multiple small RNA subtypes.

List of references

1. Rolfe, D. F. S. & Brown, G. C. Cellular energy utilization and molecular origin of standard metabolic rate in mammals. *Physiol. Rev.* **77**, 731–758 (1997).

2. Ekstrand, J., Hägglund, M. & Waldén, M. Epidemiology of muscle injuries in professional football (soccer). *Am. J. Sports Med.* **39**, 1226–1232 (2011).

3. Niesler, C. U., Van de Vyver, M. & Myburgh, K. H. Cellular regenerative therapy for acquired noncongenital musculoskeletal disorders. *S. Afr. Med. J.* **109**, 58–63 (2019).

4. Nomura, T., Kawae, T., Kataoka, H. & Ikeda, Y. Assessment of lower extremity muscle mass, muscle strength, and exercise therapy in elderly patients with diabetes mellitus. *Environ. Health Prev. Med.* **23**, 1–7 (2018).

5. Mu, X. *et al.* Notch Signaling Mediates Skeletal Muscle Atrophy in Cancer Cachexia Caused by Osteosarcoma. *Sarcoma* **2016**, (2016).

6. Zhang, A. *et al.* miRNA-23a/27a attenuates muscle atrophy and renal fibrosis through muscle-kidney crosstalk. *J. Cachexia. Sarcopenia Muscle* **9**, 755–770 (2018).

7. Flores, D. V., Gómez, C. M., Estrada-Castrillón, M., Smitaman, E. & Pathria, M. N. MR imaging of muscle trauma: Anatomy, biomechanics, pathophysiology, and imaging appearance. *Radiographics* **38**, 124–148 (2018).

8. Volpi, P., Chamari, K. & Bisciotti, G. N. Risk diagnosis of minor muscle injuries in professional football players: When imaging cannot help out biology might. *BMJ Open Sport Exerc. Med.* **5**, 2018–2019 (2019).

9. Macaluso, F., Isaacs, A. W., Di Felice, V. & Myburgh, K. H. Acute change of titin at mid-sarcomere remains despite 8 wk of plyometric training. *J. Appl. Physiol.* **116**, 1512–1519 (2014).

10. Buono, D. & Via, G. Muscle injuries: A brief guide to classification and management. *Transl. Med.* **12**, 14–18 (2015).

11. Kanda, K. *et al.* Eccentric exercise-induced delayed-onset muscle soreness and changes in markers of muscle damage and inflammation. *Exerc. Immunol. Rev.* **19**, 72–85 (2013).

12. Morgan, D. L. New insights into the behavior of muscle during active lengthening. *Biophys. J.* **57**, 209–221 (1990).

13. Morgan, D. L. & Proske, U. Popping sarcomere hypothesis explains stretch-induced muscle damage. *Clin. Exp. Pharmacol. Physiol.* **31**, 541–545 (2004).

14. Scime, A., Caron, A. Z. & Grenier, G. Advances in myogenic cell transplantation and skeletal muscle tissue engineering. *Front. Biosci.* **14**, 3012–3023 (2009).

15. Dobek, G. L., Fulkerson, N. D., Nicholas, J. & Schneider, B. S. P. Mouse model of muscle crush injury of the legs. *Comp. Med.* **63**, 227–232 (2013).

16. Zanotti, S., Gibertini, S., Blasevich, F. & Bragato, C. Exosomes and exosomal miRNAs from muscle-derived fibroblasts promote skeletal muscle fibrosis. *Matrix Biol.* (2018) doi:10.1016/j.matbio.2018.07.003.

17. Hubal, M. J., Rubinstein, S. R. & Clarkson, P. M. Mechanisms of variability in strength loss after muscle-lengthening actions. *Med. Sci. Sports Exerc.* **39**, 461–468 (2007).

18. Potvin, J. R. & Fuglevand, A. J. A motor unit-based model of muscle fatigue. *PLoS Comput. Biol.* **13**, 1–30 (2017).

19. Lee, S. S. M., De Boef Miara, M., Arnold, A. S., Biewener, A. A. & Wakeling, J. M. Recruitment of faster motor units is associated with greater rates of fascicle strain and rapid changes in muscle force during locomotion. *J. Exp. Biol.* **216**, 198–207 (2013).

20. Clarkson, P. M. & Hubal, M. J. Exercise-induced muscle damage in humans. *Am. J. Phys. Med. Rehabil.* **81**, S52–S69 (2002).

21. Van De Vyver, M. & Myburgh, K. H. Cytokine and satellite cell responses to muscle damage: Interpretation and possible confounding factors in human studies. *J. Muscle Res. Cell Motil.* **33**, 177–185 (2012).

22. Van de Vyver, M. & Myburgh, K. H. Variable inflammation and intramuscular STAT3 phosphorylation and myeloperoxidase levels after downhill running. *Scand. J. Med. Sci. Sport.* **24**, e360–e371 (2014).

23. Zhang, C. *et al.* Interleukin-6/signal transducer and activator of transcription 3 (STAT3) pathway is essential for macrophage infiltration and myoblast proliferation during muscle regeneration. *J. Biol. Chem.* **288**, 1489–1499 (2013).

24. Totsuka, M., Nakaji, S., Suzuki, K., Sugawara, K. & Sato, K. Break point of serum creatine kinase release after endurance exercise. *J. Appl. Physiol.* **93**, 1280–1286 (2002).

25. Nieman, D. C. *et al.* Cytokine changes after a marathon race. *J Appl Physiol* **91**, 109–114 (2001).

26. Smith, L. L. *et al.* Changes in serum cytokines after repeated bouts of downhill running. *Appl. Physiol. Nutr. Metab.* **32**, 233–240 (2007).

27. Mauro, A. Satellite cell of skeletal muscle fibers. *J. Biophys. Biochem. Cytol.* **9**, 493–495 (1961).

28. Morozov, V. I., Tsyplenkov, P. V., Golberg, N. D. & Kalinski, M. I. The effects of high-intensity exercise on skeletal muscle neutrophil myeloperoxidase in untrained and trained rats. *Eur. J. Appl. Physiol.* **97**, 716–722 (2006).

29. Tidball, J. G. & Villalta, S. A. Regulatory interactions between muscle and the immune system during muscle regeneration. *Am J Physiol Regul Integr Comp Physiol* **298**, R1173-87 (2010).

30. Collins, C. A. *et al.* Stem cell function, self-renewal, and behavioral heterogeneity of cells from the adult muscle satellite cell niche. *Cell* **122**, 289–301 (2005).

31. Weintraub, H. *et al.* Activation of muscle-specific genes in pigment, nerve, fat, liver, and fibroblast cell lines by forced expression of MyoD. *Proc. Natl. Acad. Sci. U. S. A.* **86**, 5434–5438 (1989).

32. Crist, C. G., Montarras, D. & Buckingham, M. Muscle satellite cells are primed for myogenesis but maintain quiescence with sequestration of Myf5 mRNA targeted by microRNA-31 in mRNP granules. *Cell Stem Cell* **11**, 118–126 (2012).

33. Füchtbauer, E. M. & Westphal, H. MyoD and myogenin are coexpressed in regenerating skeletal muscle of the mouse. *Dev. Dyn.* **193**, 34–39 (1992).

34. Rebalka, I. A. & Hawke, T. J. Potential biomarkers of skeletal muscle damage. *Biomark. Med.* **8**, 375–378 (2014).

35. Lässer, C. *et al.* Human saliva, plasma and breast milk exosomes contain RNA: Uptake by macrophages. *J. Transl. Med.* **9**, 9 (2011).

36. Lindsay, A. & Costello, J. T. Realising the Potential of Urine and Saliva as Diagnostic Tools in Sport and Exercise Medicine. *Sport. Med.* **47**, 11–31 (2017).

37. Baskin, K. K., Winders, B. R. & Olson, E. N. Muscle as a 'mediator' of systemic metabolism. *Cell Metab.* **21**, 237–248 (2015).

38. Koutsoulidou, A. *et al.* Identification of Exosomal Muscle-Specific miRNAs in Serum of Myotonic Dystrophy Patients Relating to Muscle Disease Progress. *Oxford Univ. Press* (2017).

39. Pedersen, B. K. & Febbraio, M. A. Muscles, exercise and obesity: skeletal muscle as a secretory organ. *Nat. Rev. Endocrinol.* **8**, (2012).

40. Steensberg, A., Philip, C. & Fischer, P. Searching for the exercise factor : Is IL-6 a candidate ? (2003) doi:10.1023/A.

41. Safdar, A. & Tarnopolsky, M. A. Exosomes as mediators of the systemic adaptations to endurance exercise. *Cold Spring Harb. Perspect. Med.* **8**, 1–24 (2018).

42. Brahmer, A. *et al.* Platelets, endothelial cells and leukocytes contribute to the exercise-triggered release of extracellular vesicles into the circulation. *J. Extracell. Vesicles* **8**, (2019).

43. Pedersen, B. K. & Febbraio, M. A. Muscle as an endocrine organ: Focus on muscle-derived interleukin-6. *Physiol. Rev.* **88**, 1379–1406 (2008).

44. Muñoz-Cánoves, P., Scheele, C., Pedersen, B. K. & Serrano, A. L. Interleukin-6 myokine signaling in skeletal muscle: A double-edged sword? *FEBS J.* **280**, 4131–4148 (2013).

45. Rodríguez, A., Becerril, S., Ezquerro, S., Méndez-Giménez, L. & Frühbeck, G. Crosstalk between adipokines and myokines

in fat browning. *Acta Physiol.* **219**, 362–381 (2017).

46. Van De Vyver, M. & Myburgh, K. H. Cytokine and satellite cell responses to muscle damage: Interpretation and possible confounding factors in human studies. *J. Muscle Res. Cell Motil.* **33**, 177–185 (2012).

47. Rome, S., Forterre, A., Mizgier, M. L. & Bouzakri, K. Skeletal muscle-released extracellular vesicles: State of the art. *Front. Physiol.* **10**, (2019).

48. Vechetti, I. J., Valentino, T., Mobley, C. B. & McCarthy, J. J. The role of extracellular vesicles in skeletal muscle and systematic adaptation to exercise. *J. Physiol.* 1–39 (2020) doi:10.1113/JP278929.

49. Murphy, C. *et al.* Emerging role of extracellular vesicles in musculoskeletal diseases. *Mol. Aspects Med.* **60**, 123–128 (2018).

50. Guescini, M. *et al.* Muscle releases alpha-sarcoglycan positive extracellular vesicles carrying miRNAs in the bloodstream. *PLoS One* **10**, 1–19 (2015).

51. Lovett, J. A. C., Durcan, P. J. & Myburgh, K. H. Investigation of circulating extracellular vesicle microRNA following two consecutive bouts of muscle-damaging exercise. *Front. Physiol.* **9**, (2018).

52. Yáñez-Mó, M. *et al.* Biological properties of extracellular vesicles and their physiological functions. *J. Extracell. Vesicles* **4**, 1–60 (2015).

53. Kakarla, R., Hur, J., Kim, Y. J., Kim, J. & Chwae, Y. J. Apoptotic cell-derived exosomes: messages from dying cells. *Exp. Mol. Med.* **52**, 1–6 (2020).

54. Pike, L. J. Lipid rafts: Bringing order to chaos. *J. Lipid Res.* **44**, 655–667 (2003).

55. Valadi, H. Ekstrom, K. Bossios, A. Sjostrand, M. Lee, J. Lotvall, J. *et al.* Exosome-mediated transfer of mRNAs and microRNAs is a novel mechanism of genetic exchange between cells. *Nat. Cell Biol.* **9**, 654–659 (2007).

56. Record, M., Carayon, K., Poirot, M. & Silvente-Poirot, S. Exosomes as new vesicular lipid transporters involved in cell-cell communication and various pathophysiologies. *Biochim. Biophys. Acta - Mol. Cell Biol. Lipids* **1841**, 108–120 (2014).

57. Skotland, T. *et al.* Molecular lipid species in urinary exosomes as potential prostate cancer biomarkers. *Eur. J. Cancer* **70**, 122–132 (2017).

58. Lakhter, A. J. & Sims, E. K. Minireview: Emerging roles for extracellular vesicles in diabetes and related metabolic disorders. *Mol. Endocrinol.* **29**, 1535–1548 (2015).

59. Melo, S. a. *et al.* Glypican-1 identifies cancer exosomes and detects early pancreatic cancer. *Nature* **523**, 177–182 (2015).

60. Witwer, K. W. *et al.* Standardization of sample collection, isolation and analysis methods in extracellular vesicle research. *J. Extracell. Vesicles* **2**, 1–25 (2013).

61. Chargaff, E. *et al.* The biological significance of the thromboplastic protein of blood. *J. Biol. Chem.* 189–197 (1946).

62. Wolf, P. The nature and significance of platelet products in human plasma. *Br. J. Haematol.* **5**, (1967).

63. Pan, B. T. & Johnstone, R. M. Fate of the transferrin receptor during maturation of sheep reticulocytes in vitro: Selective externalization of the receptor. *Cell* **33**, 967–978 (1983).

64. G Raposo, H W Nijman, W Stoorvogel, R Liejendekker, C V Harding, C J Melief, and H. J. G. B Lymphocytes Secrete Antigen-presentingVesicles. *J. Exp. Med.* **183**, 1161–1172 (1996).

65. Ratajczak, J. *et al.* Embryonic stem cell-derived microvesicles reprogram hematopoietic progenitors: Evidence for horizontal transfer of mRNA and protein delivery. *Leukemia* **20**, 847–856 (2006).

66. Valadi, H. Ekstrom, K. Bossios, A. Sjostrand, M. Lee, J. Lotvall, J. Exosome-mediated transfer of mRNAs and microRNAs is a novel mechanism of genetic exchange between cells. *Nat. Cell Biol.* **9**, (2007).

67. Ekström, K. *et al.* Characterization of mRNA and microRNA in human mast cell-derived exosomes and their transfer to other mast cells and blood CD34 progenitor cells. *J. Extracell. Vesicles* **1**, 1–12 (2012).

68. Pan, B. T., Teng, K., Wu, C., Adam, M. & Johnstone, R. M. Electron microscopic evidence for externalization of the transferrin receptor in vesicular form in sheep reticulocytes. *J. Cell Biol.* **101**, 942–948 (1985).

69. Colombo, M., Raposo, G. & Théry, C. Biogenesis, Secretion, and Intercellular Interactions of Exosomes and Other Extracellular Vesicles. *Annu. Rev. Cell Dev. Biol.* **30**, 255–289 (2014).

70. Colombo, M. *et al.* Analysis of ESCRT functions in exosome biogenesis, composition and secretion highlights the heterogeneity of extracellular vesicles. *J. Cell Sci.* **126**, 5553–5565 (2013).

71. Mayers, J. R. *et al.* ESCRT-0 assembles as a heterotetrameric complex on membranes and binds multiple ubiquitinylated cargoes simultaneously. *J. Biol. Chem.* **286**, 9636–9645 (2011).

72. Romancino, D. P. *et al.* Identification and characterization of the nano-sized vesicles released by muscle cells. *FEBS Lett.* **587**, 1379–1384 (2013).

73. Stuffers, S., Sem Wegner, C., Stenmark, H. & Brech, A. Multivesicular endosome biogenesis in the absence of ESCRTs. *Traffic* **10**, 925–937 (2009).

74. Theos, A. C. *et al.* A novel pathway for sorting to intralumenal vesicles of multivesicular endosomes involved in organelle morphogenesis Alexander. *Dev. Cell* **10**, 343–354 (2007).

75. Zhang, G. *et al.* Tumor induces muscle wasting in mice through releasing extracellular Hsp70 and Hsp90. *Nat. Commun.* **8**, (2017).

76. Kaushik, Susmita. Cuervo, A. Chaperone-Mediated Autophagy. *Methods Mol. Biol.* **445**, 1–9 (2008).

77. Mulcahy, L. A., Pink, R. C. & Carter, D. R. F. Routes and mechanisms of extracellular vesicle uptake. *J. Extracell. Vesicles* **3**, 1–14 (2014).

78. Morelli, A. E. *et al.* Endocytosis, intracellular sorting, and processing of exosomes by dendritic cells. *Blood* **104**, 3257–3266 (2004).

79. Chen, C. *et al.* Imaging and Intracellular Tracking of Cancer Derived Exosomes Using Single Molecule Localization Based Super Resolution Microscope. *ACS Appl. Mater. Interfaces* (2016) doi:10.1021/acsami.6b09442.

80. Doherty, G. J. & McMahon, H. T. Mechanisms of Endocytosis. *Annu. Rev. Biochem.* **78**, 857–902 (2009).

81. Barrès, C. *et al.* Galectin-5 is bound onto the surface of rat reticulocyte exosomes and modulates vesicle uptake by macrophages. *Blood* **115**, 696–705 (2010).

82. Svensson, K. J. *et al.* Exosome uptake depends on ERK1/2-heat shock protein 27 signaling and lipid raft-mediated endocytosis negatively regulated by caveolin-1. *J. Biol. Chem.* **288**, 17713–17724 (2013).

83. Mathieu, M., Martin-Jaular, L., Lavieu, G. & Théry, C. Specificities of secretion and uptake of exosomes and other extracellular vesicles for cell-to-cell communication. *Nat. Cell Biol.* **21**, 9–17 (2019).

84. Denzer, K. *et al.* Follicular dendritic cells carry MHC class II-expressing microvesicles at their surface. *J. Immunol.* **165**, 1259–1265 (2000).

85. Alvarez-Erviti, L. & Seow, Y. Delivery of siRNA to the mouse brain by systemic injection of targeted exosomes. *Nat. biotecjnology* (2010).

86. Andreu, Z. *et al.* Comparative analysis of EV isolation procedures for miRNAs detection in serum samples. *J. Extracell. Vesicles* **5**, 1–10 (2016).

87. Gámez-Valero, A. *et al.* Size-Exclusion Chromatography-based isolation minimally alters Extracellular Vesicles' characteristics compared to precipitating agents. *Sci. Rep.* **6**, 33641 (2016).

88. Baranyai, T. *et al.* Isolation of exosomes from blood plasma: Qualitative and quantitative comparison of ultracentrifugation and size exclusion chromatography methods. *PLoS One* **10**, 1–13 (2015).

89. Crossland, R. E., Norden, J., Bibby, L. A., Davis, J. & Dickinson, A. M. *Evaluation of optimal extracellular vesicle small RNA isolation and qRT-PCR normalisation for serum and urine*. *Journal of Immunological Methods* vol. 429 (Elsevier B.V., 2016).

90. Gardiner, C. *et al.* Techniques used for the isolation and characterization of extracellular vesicles: Results of a worldwide survey. *J. Extracell. Vesicles* **5**, 1–6 (2016).

91. Chargaff, E. & West, R. The biological significance of the thromboplastic protein of blood. *J. Biol. Chem.* 189–197 (1946).

92. Mateescu, B. *et al.* Obstacles and opportunities in the functional analysis of extracellular vesicle RNA - An ISEV position paper. *J. Extracell. Vesicles* **6**, (2017).

93. Théry, C. *et al.* Minimal information for studies of extracellular vesicles 2018 (MISEV2018): a position statement of the International Society for Extracellular Vesicles and update of the MISEV2014 guidelines. *J. Extracell. Vesicles* **7**, (2018).

94. Wubbolts, R. *et al.* Proteomic and biochemical analyses of human B cell-derived exosomes: Potential implications for their function and multivesicular body formation. *J. Biol. Chem.* **278**, 10963–10972 (2003).

95. Hildonen, S. *et al.* Isolation and mass spectrometry analysis of urinary extraexosomal proteins. *Sci. Rep.* **6**, 1–14 (2016).

96. de Menezes-Neto, A. *et al.* Size-exclusion chromatography as a stand-alone methodology identifies novel markers in mass spectrometry analyses of plasma-derived vesicles from healthy individuals. *J. Extracell. Vesicles* **4**, 1–14 (2015).

97. Vagner, T. *et al.* Protein Composition Reflects Extracellular Vesicle Heterogeneity. *Proteomics* **19**, 1–32 (2019).

98. Chen, S. *et al.* Lipidomic characterization of extracellular vesicles in human serum. *J. Circ. Biomarkers* **8**, 1–12 (2019).

99. Brown, D. A. & London, E. Structure and function of sphingolipid- and cholesterol-rich membrane rafts. *J. Biol. Chem.* **275**, 17221–17224 (2000).

100. Subra, C. *et al.* Exosomes account for vesicle-mediated transcellular transport of activatable phospholipases and prostaglandins. *J. Lipid Res.* **51**, 2105–2120 (2010).

101. Madison, R. D., McGee, C., Rawson, R. & Robinson, G. A. Extracellular vesicles from a muscle cell line (C2C12) enhance cell survival and neurite outgrowth of a motor neuron cell line (NSC-34). *J. Extracell. Vesicles* **3**, 1–9 (2014).

102. Guescini, M. *et al.* C2C12 myoblasts release micro-vesicles containing mtDNA and proteins involved in signal transduction. *Exp. Cell Res.* **316**, 1977–1984 (2010).

103. Le Bihan, M. C. *et al.* In-depth analysis of the secretome identifies three major independent secretory pathways in differentiating human myoblasts. *J. Proteomics* **77**, 344–356 (2012).

104. Forterre, A. *et al.* Proteomic analysis of C2C12 myoblast and myotube exosome-like vesicles: A new paradigm for myoblast-myotube cross talk? *PLoS One* **9**, (2014).

105. Id, M. G., Maggio, S., Ceccaroli, P., Battistelli, M. & Annibalini, G. Extracellular Vesicles Released by Oxidatively Injured or Intact C2C12 Myotubes Promote Distinct Responses Converging toward Myogenesis. (2017) doi:10.3390/ijms18112488.

106. Qin, Y. *et al.* Myostatin inhibits osteoblastic differentiation by suppressing osteocyte-derived exosomal microRNA-218: A novel mechanism in muscle-bone communication. *J. Biol. Chem.* **292**, 11021–11033 (2017).

107. Xu, Q. *et al.* Exosomes from C2C12 myoblasts enhance osteogenic differentiation of MC3T3-E1 pre-osteoblasts by delivering miR-27a-3p. *Biochem. Biophys. Res. Commun.* **498**, 32–37 (2018).

108. Nakamura, Y. *et al.* Mesenchymal-stem-cell-derived exosomes accelerate skeletal muscle regeneration. *FEBS Lett.* **589**, 1257–1265 (2015).

109. Matsuzaka, Y. *et al.* Characterization and functional analysis of extracellular vesicles and muscle-abundant miRNAs (miR-1, miR-133a, and miR-206) in C2 C12 myocytes and mdx Mice. *PLoS One* **11**, 1–23 (2016).

110. Frattini, P. *et al.* Autologous intramuscular transplantation of engineered satellite cells induces exosome-mediated systemic expression of Fukutin-related protein and rescues disease phenotype in a murine model of limb-girdle muscular dystrophy type 2I. *Hum. Mol. Genet.* **26**, 3682–3698 (2017).

111. Choi, J. S. *et al.* Exosomes from differentiating human skeletal muscle cells trigger myogenesis of stem cells and provide biochemical cues for skeletal muscle regeneration. *J. Control. Release* **222**, 107–115 (2016).

112. Fry, C. S., Kirby, T. J., Kosmac, K., McCarthy, J. J. & Peterson, C. A. Myogenic Progenitor Cells Control Extracellular Matrix Production by Fibroblasts during Skeletal Muscle Hypertrophy. *Cell Stem Cell* **20**, 56–69 (2017).

113. Banzet, S. *et al.* Changes in circulating microRNAs levels with exercise modality. *J. Appl. Physiol.* **115**, 1237–1244 (2013).

114. Kramers, E.-M. Physical exercise induces rapid release of small extracellular vesicles into the circulation. *J. Extracell. Vesicles* **1**, 1–11 (2015).

115. Helmig, S., Frühbeis, C., Krämer-Albers, E. M., Simon, P. & Tug, S. Release of bulk cell free DNA during physical exercise occurs independent of extracellular vesicles. *Eur. J. Appl. Physiol.* **115**, 2271–2280 (2015).

116. Whitham, M. *et al.* Extracellular Vesicles Provide a Means for Tissue Crosstalk during Exercise. *Cell Metab.* **27**, 237-251.e4 (2018).

117. Hou, Z. *et al.* Longterm Exercise-Derived Exosomal miR-342-5p: A Novel Exerkine for Cardioprotection. *Circ. Res.* **124**, 1386–1400 (2019).

118. Yin, X. *et al.* Time-Course Responses of Muscle-Specific MicroRNAs Following Acute Uphill or Downhill Exercise in Sprague-Dawley Rats. *Front. Physiol.* **10**, (2019).

119. Lagos-Quintana, M., Rauhut, R., Lendeckel, W. & Tuschl, T. Identification of novel genes coding for small expressed RNAs. *Science (80-.).* **294**, 853–858 (2001).

120. Feinbaum, R., Ambros, V. & Lee, R. The C. elegans Heterochronic Gene lin-4 Encodes Small RNAs with Antisense Complementarity to lin-14. *Cell* **116**, 843–854 (2004).

121. Wightman, B., Biirglin, R., Gatto, J., Arasu, P. & Ruvkun, G. Negative regulatory sequences in the lin-14 3′ -untranslated region are necessary to generate a temporal switch during Caenorhabditis elegans development. *Genes Dev.* 1813–1824 (1991).

122. Wightman, B. Posttranscriptional Regulation of the Heterochronic Gene lin-14 by W -4 Mediates Temporal Pattern Formation in C . elegans. *cell Press* **75**, 855–862 (1993).

123. Reinhart, B. J., Slack, F. J. & Basson, M. The 21-nucleotide let-7 RNA regulates developmental timing in Caenorhabditis elegans. 901–906 (2000).

124. Lagos-Quintana, M., Rauhut, R., Meyer, J., Borkhardt, A. & Tuschl, T. New microRNAs from mouse and human. *Rna* **9**, 175–179 (2003).

125. Teeple E, Collins J, Shrestha S, Dennerlein J, et al. An integrated expression atlas of miRNAs and their promoters in human and mouse. *Physiol. Behav.* **176**, 139–148 (2018).

126. Bartel, D. P. MicroRNA target recognition and regulatory functions. *Trop. Grasslands* **44**, 141–157 (2010).

127. Vasudevan, S. Posttranscriptional Upregulation by MicroRNAs. *Wiley Interdiscip. Rev. RNA* **3**, 311–330 (2012).

128. Catalanotto, C., Cogoni, C. & Zardo, G. MicroRNA in control of gene expression: An overview of nuclear functions. *Int. J. Mol. Sci.* **17**, (2016).

129. Perera, R. J. & Ray, A. MicroRNAs in the Search for Understanding Human Diseases. *Biodrugs* **21**, 97–104 (2007).

130. Friedman, R. C., Farh, K. K., Burge, C. B. & Bartel, D. P. Most mammalian mRNAs are conserved targets of microRNAs. *Methods* 92–105 (2009) doi:10.1101/gr.082701.108.

131. Grey, F., Meyers, H., White, E. A., Spector, D. H. & Nelson, J. A human cytomegalovirus-encoded microRNA regulates expression of multiple viral genes involved in replication. *PLoS Pathog.* **3**, 1593–1602 (2007).

132. Rooij, E. Van *et al.* Expression and Muscle Performance. *Dev. Cell* **17**, 662–673 (2009).

133. Kim, Y. K., Kim, B. & Kim, V. N. Re-evaluation of the roles of DROSHA, Exportin 5, and DICER in microRNA biogenesis. *Proc. Natl. Acad. Sci. U. S. A.* **113**, E1881–E1889 (2016).

134. Chendrimada, T. P. *et al.* TRBP recruits the Dicer complex to Ago2 for microRNA processing and gene silencing. *Nature* **436**, 740–744 (2010).

135. Tomari, Y. Sorting of Drosophila small silencing RNAs Yukihide. **130**, 299–308 (2010).

136. Turchinovich, A. & Burwinkel, B. Distinct AGO1 and AGO2 associated miRNA profiles in human cells and blood plasma. *RNA Biol.* **9**, 1066–1075 (2012).

137. Vickers, K., Palmisano, B., Shoucri, B., Shamburek, R. & Alan, R. MicroRNAs can be transported in plasma and delivered to recipient cells by high-density lipoproteins. *Nat. Cell Biol.* **13**, (2011).

138. Khvorova, A., Reynolds, A. & Jayasena, S. D. Functional siRNAs and miRNAs exhibit strand bias. *Cell* **115**, 209–216 (2003).

139. Coenen-Stass, A. M. L. *et al.* Extracellular microRNAs exhibit sequence-dependent stability and cellular release kinetics. *RNA Biol.* **16**, 696–706 (2019).

140. Mccarthy, J. J. The MyomiR Network in Skeletal Muscle Plasticity. *Exerc. Sport Sci. Rev.* **39**, 150–154 (2016).

141. Drummond, M. J., McCarthy, J. J., Fry, C. S., Esser, K. A. & Rasmussen, B. B. Aging differentially affects human skeletal muscle microRNA expression at rest and after an anabolic stimulus of resistance exercise and essential amino acids. *Am. J. Physiol. - Endocrinol. Metab.* **295**, 1333–1340 (2008).

142. Eun, J. L. *et al.* Systematic evaluation of microRNA processing patterns in tissues, cell lines, and tumors. *Rna* **14**, 35–42 (2008).

143. Sempere, L. F. *et al.* Expression profiling of mammalian microRNAs uncovers a subset of brain-expressed microRNAs with possible roles in murine and human neuronal differentiation. *Genome Biol.* **5**, (2004).

144. El-Mogy, M. *et al.* Diversity and signature of small RNA in different bodily fluids using next generation sequencing. *BMC Genomics* **19**, 1–24 (2018).

145. Monguió-Tortajada, M. *et al.* Extracellular-Vesicle Isolation from Different Biological Fluids by Size-Exclusion Chromatography. *Curr. Protoc. Stem Cell Biol.* **49**, 1–24 (2019).

146. Coenen-Stass, A. M. L. *et al.* Selective release of muscle-specific, extracellular microRNAs during myogenic differentiation. *Hum. Mol. Genet.* **25**, 3960–3974 (2016).

147. Lässer, C. Mapping Extracellular RNA Sheds Lights on Distinct Carriers. *Cell* **177**, 228–230 (2019).

148. D'souza, R. F. *et al.* Circulatory exosomal miRNA following intense exercise is unrelated to muscle and plasma miRNA abundances. *Am. J. Physiol. - Endocrinol. Metab.* **315**, E723–E733 (2018).

149. McCarthy, J. J. & Esser, K. A. MicroRNA-1 and microRNA-133a expression are decreased during skeletal muscle hypertrophy. *J. Appl. Physiol.* **102**, 306–313 (2007).

150. Drummond, M. J., McCarthy, J. J., Fry, C. S., Esser, K. A. & Rasmussen, B. B. Aging differentially affects human skeletal muscle microRNA expression at rest and after an anabolic stimulus of resistance exercise and essential amino acids. *AJP Endocrinol. Metab.* **295**, E1333–E1340 (2008).

151. Safdar, A., Abadi, A., Akhtar, M., Hettinga, B. P. & Tarnopolsky, M. A. miRNA in the regulation of skeletal muscle adaptation to acute endurance exercise in C57Bl/6J male mice. *PLoS One* **4**, 19–22 (2009).

152. Mitchell, P. S. *et al.* Circulating microRNAs as stable blood-based markers for cancer detection. *Proc. Natl. Acad. Sci. U. S. A.* **105**, 10513–10518 (2008).

153. Mizuno, H. *et al.* Identification of muscle-specific MicroRNAs in serum of muscular dystrophy animal models: Promising novel blood-based markers for muscular dystrophy. *PLoS One* **6**, 14–19 (2011).

154. Roberts, T. C., Coenen-Stass, A. M. L. & Wood, M. J. A. Assessment of RT-qPCR normalization strategies for accurate quantification of extracellular microRNAs in murine Serum. *PLoS One* **9**, (2014).

155. Koutsoulidou, A. *et al.* Identification of exosomal muscle-specific miRNAs in serum of myotonic dystrophy patients relating to muscle disease progress. *Hum. Mol. Genet.* **26**, 3285–3302 (2017).

156. Baggish, A. L. *et al.* Dynamic regulation of circulating microRNA during acute exhaustive exercise and sustained aerobic exercise training. *J. Physiol.* **589**, 3983–3994 (2011).

157. Uhlemann, M. *et al.* Circulating microRNA-126 increases after different forms of endurance exercise in healthy adults. *Eur. J. Prev. Cardiol.* **21**, 484–491 (2014).

158. Aoi, W. *et al.* Muscle-enriched micro RNA miR-486 decreases in circulation in response to exercise in young men. *Front. Physiol.* **4 APR**, 1–7 (2013).

159. Rivas, D. A. *et al.* Diminished skeletal muscle microRNA expression with aging is associated with attenuated muscle plasticity and inhibition of IGF-1 signaling. *FASEB J.* **28**, 4133–4147 (2014).

160. Camera, D. M., Ong, J. N., Coffey, V. G. & Hawley, J. A. Selective modulation of microRNA expression with protein ingestion following concurrent resistance and endurance exercise in human skeletal muscle. *Front. Physiol.* **7**, 1–8 (2016).

161. Cui, S. F. *et al.* Acute responses of circulating microRNAs to low-volume sprint interval cycling. *Front. Physiol.* **6**, 1–7 (2015).

162. Cui, S. F. *et al.* Similar responses of circulating microRNAs to acute high-intensity interval exercise and vigorous-intensity continuous exercise. *Front. Physiol.* **7**, 1–8 (2016).

163. Cui, S. *et al.* Time-course responses of circulating microRNAs to three resistance training protocols in healthy young men. *Sci. Rep.* **7**, 1–13 (2017).

164. Wardle, S. L. *et al.* Plasma microRNA levels differ between endurance and strength athletes. *PLoS One* **10**, 1–15 (2015).

165. Denham, J. & Prestes, P. R. Muscle-enriched MicroRNAs isolated from whole blood are regulated by exercise and are potential biomarkers of cardiorespiratory fitness. *Front. Genet.* **7**, 1–8 (2016).

166. Davidsen, P. K. K. *et al.* High responders to resistance exercise training demonstrate differential regulation of skeletal muscle microRNA expression. *J. Appl. Physiol.* **110**, 309–317 (2011).

167. Zhang, T. *et al.* Improved knee extensor strength with resistance training associates with muscle specific miRNAs in older adults. *Exp. Gerontol.* **62**, 7–13 (2015).

168. Lee, D. E. *et al.* microRNA-16 Is Downregulated During Insulin Resistance and Controls Skeletal Muscle Protein Accretion. *J. Cell. Biochem.* **117**, 1775–1787 (2016).

169. Nielsen, S. *et al.* Muscle specific microRNAs are regulated by endurance exercise in human skeletal muscle. *J. Physiol.* **588**, 4029–4037 (2010).

170. Denham, J., Gray, A., Scott-Hamilton, J. & Hagstrom, A. D. Sprint Interval Training Decreases Circulating MicroRNAs Important for Muscle Development. *Int. J. Sports Med.* **39**, 67–72 (2018).

171. Nie, Y. *et al.* Impaired exercise tolerance, mitochondrial biogenesis, and muscle fiber maintenance in miR-133a-deficient mice. *FASEB J.* **30**, 3745–3758 (2016).

172. Egawa, T. *et al.* Involvement of AMPK in regulating slow-twitch muscle atrophy during hindlimb unloading in mice. *Am. J. Physiol. - Endocrinol. Metab.* **309**, E651–E662 (2015).

173. Gomes, C. P. C. *et al.* Circulating miR-1, miR-133a, and miR-206 levels are increased after a half-marathon run. *Biomarkers* **19**, 585–589 (2014).

174. Mooren, F. C., Viereck, J., Kruger, K. & Thum, T. Circulating micrornas as potential biomarkers of aerobic exercise capacity. *AJP Hear. Circ. Physiol.* **306**, H557–H563 (2014).

175. Clauss, S., Wakili, R., Hildebrand, B., Kääb, S. & Hoster, E. MicroRNAs as Biomarkers for Acute Atrial Remodeling in Marathon Runners (The miRathon Study – A Sub-Study of the Munich Marathon Study). 1–23 (2016) doi:10.1371/journal.pone.0148599.

176. Min, P. K. *et al.* Influence of statins on distinct circulating microRNAs during prolonged aerobic exercise. *J. Appl. Physiol.* **120**, 711–720 (2016).

177. Baggish, A. L. *et al.* Rapid upregulation and clearance of distinct circulating microRNAs after prolonged aerobic exercise. *J. Appl. Physiol.* **116**, 522–531 (2014).

178. De Gonzalo-Calvo, D. *et al.* Circulating inflammatory miRNA signature in response to different doses of aerobic exercise. *J. Appl. Physiol.* **119**, 124–134 (2015).

179. Aoi, W. *et al.* Muscle-enriched microRNA miR-486 decreases in circulation in response to exercise in young men. *Front. Physiol.* **4**, 1–7 (2013).

180. Buschmann, D. *et al.* Evaluation of serum extracellular vesicle isolation methods for profiling miRNAs by next-generation sequencing. *J. Extracell. Vesicles* **7**, (2018).

181. Stranska, R. *et al.* Comparison of membrane affinity-based method with size-exclusion chromatography for isolation of exosome-like vesicles from human plasma. *J. Transl. Med.* **16**, 1–9 (2018).

182. Zaborowski, M. P. *et al.* Membrane-bound Gaussia luciferase as a tool to track shedding of membrane proteins from the surface of extracellular vesicles. *Sci. Rep.* **9**, 17387 (2019).

183. Siracusa, J. *et al.* Phenotype-specific response of circulating miRNAs provides new biomarkers of slow or fast muscle damage. *Front. Physiol.* **9**, (2018).

184. Dey, B. K., Gagan, J. & Dutta, A. miR-206 and -486 Induce Myoblast Differentiation by Downregulating Pax7. *Mol. Cell. Biol.* **31**, 1329–1329 (2011).

185. Soci, U. P. R. *et al.* Epigenetic control of exercise training-induced cardiac hypertrophy by miR-208. *Clin. Sci.* **130**, 2005–2015 (2016).

186. Schmeier, S. *et al.* Deciphering the transcriptional circuitry of microRNA genes expressed during human monocytic differentiation. *BMC Genomics* **10**, 1–18 (2009).

187. Li, D. *et al.* MiR-146a modulates macrophage polarization in systemic juvenile idiopathic arthritis by targeting INHBA. *Mol. Immunol.* **77**, 205–212 (2016).

188. Westering, T. L. E. Van, Lomonosova, Y., Coenen-stass, A. M. L., Betts, C. A. & Bhomra, A. Uniform sarcolemmal dystrophin expression is required to prevent extracellular microRNA release and improve dystrophic pathology. *J. Cachexia. Sarcopenia Muscle* (2019) doi:10.1002/jcsm.12506.

189. Cacchiarelli, D. *et al.* miRNAs as serum biomarkers for Duchenne muscular dystrophy. *EMBO Mol. Med.* **3**, 258–265 (2011).

190. Roberts, T. C. *et al.* Expression analysis in multiple muscle groups and serum reveals complexity in the MicroRNA transcriptome of the mdx mouse with implications for therapy. *Mol. Ther. - Nucleic Acids* **1**, e39 (2012).

191. Coenen-Stass, A. M. L., Wood, M. J. A. & Roberts, T. C. Biomarker Potential of Extracellular miRNAs in Duchenne Muscular Dystrophy. *Trends Mol. Med.* **23**, 989–1001 (2017).

192. Mooren, F. C. *et al.* Circulating micrornas as potential biomarkers of aerobic exercise capacity. *Am. J. Physiol. - Hear. Circ. Physiol.* **306**, H557–H563 (2014).

193. Monguió-Tortajada, M., Gálvez-Montón, C., Bayes-Genis, A., Roura, S. & Borràs, F. E. Extracellular vesicle isolation methods: rising impact of size-exclusion chromatography. *Cell. Mol. Life Sci.* (2019) doi:10.1007/s00018-019-03071-y.

194. Gámez-Valero, A. *et al.* Size-Exclusion Chromatography-based isolation minimally alters Extracellular Vesicles' characteristics compared to precipitating agents. *Sci. Rep.* **6**, 1–9 (2016).

195. Sharma, M., Juvvuna, P. K., Kukreti, H. & McFarlane, C. Mega roles of microRNAs in regulation of skeletal muscle health and disease. *Front. Physiol.* **5 JUN**, 1–9 (2014).

196. Dmitriev, P. *et al.* Simultaneous miRNA and mRNA transcriptome profiling of human myoblasts reveals a novel set of myogenic differentiation-associated miRNAs and their target genes. *BMC Genomics* **14**, (2013).

197. Greco, S. *et al.* Common micro-RNA signature in skeletal muscle damage and regeneration induced by Duchenne muscular dystrophy and acute ischemia. *FASEB J.* **23**, 3335–3346 (2009).

198. Rao, P. K., Kumar, R. M., Farkhondeh, M., Baskerville, S. & Lodish, H. F. Myogenic factors that regulate expression of muscle-specific microRNAs. *Proc. Natl. Acad. Sci. U. S. A.* **103**, 8721–8726 (2006).

199. Russell, A. P. *et al.* Regulation of miRNAs in human skeletal muscle following acute endurance exercise and short-term endurance training. *J. Physiol.* **591**, 4637–4653 (2013).

200. Zaglia, T., Prando, V., Bertoli, S. & Favaro, G. Circulating muscle-derived mir-206 links skeletal muscle dysfunction to cardiac autonomic denervation. *Rapid fire Abstr.* 2019 (2019).

201. Karimi, N. *et al.* Detailed analysis of the plasma extracellular vesicle proteome after separation from lipoproteins. *Cell. Mol. Life Sci.* **75**, 2873–2886 (2018).

202. Zhao, F. *et al.* Characterization of serum small extracellular vesicles and their small RNA contents across humans , rats , and mice. *Sci. Rep.* 1–16 (2020) doi:10.1038/s41598-020-61098-9.

203. Faraldi, M. *et al.* Normalization strategies differently affect circulating miRNA profile associated with the training status. *Sci. Rep.* **9**, 1–13 (2019).

204. Xiang, X. *et al.* miRNA-584-5p exerts tumor suppressive functions in human neuroblastoma through repressing transcription of matrix metalloproteinase 14. *Biochim. Biophys. Acta - Mol. Basis Dis.* **1852**, 1743–1754 (2015).

205. Režen, T., Kovanda, A., Eiken, O., Mekjavic, I. B. & Rogelj, B. Expression changes in human skeletal muscle miRNAs following 10 days of bed rest in young healthy males. *Acta Physiol.* **210**, 655–666 (2014).

206. Shatseva, T., Lee, D. Y., Deng, Z. & Yang, B. B. MicroRNA miR-199a-3p regulates cell proliferation and survival by targeting caveolin-2. *J. Cell Sci.* **124**, 2826–2836 (2011).

207. Wang, B. *et al.* miR-26a limits muscle wasting and cardiac fibrosis through exosome-mediated microRNA transfer in chronic kidney disease. *Theranostics* **9**, 1864–1877 (2019).

208. Clauss, S. *et al.* MicroRNAs as biomarkers for acute atrial remodeling in marathon runners (The miRathon study - A sub-study of the Munich marathon study). *PLoS One* **11**, 1–23 (2016).

209. Nair, V. D. *et al.* Sedentary and Trained Older Men Have Distinct Circulating Exosomal microRNA Profiles at Baseline and in Response to Acute Exercise. *Front. Physiol.* **11**, 1–15 (2020).

210. Mitchell, C. J. *et al.* Identification of human skeletal muscle miRNA related to strength by high-throughput sequencing. *Physiol. Genomics* **50**, 416–424 (2018).

211. D'Souza, R. F. *et al.* Acute resistance exercise modulates microRNA expression profiles: Combined tissue and circulatory targeted analyses. *PLoS One* **12**, 1–15 (2017).

212. Small, E. M. *et al.* Regulation of PI3-kinase/Akt signaling by muscle-enriched microRNA-486. *Proc. Natl. Acad. Sci. U. S. A.* **107**, 4218–4223 (2010).

213. Koning, M., Werker, P. M. N., van Luyn, M. J. A., Krenning, G. & Harmsen, M. C. A global downregulation of microRNAs occurs in human quiescent satellite cells during myogenesis. *Differentiation* **84**, 314–321 (2012).

214. Kramers, E.-M. *et al.* Physical exercise induces rapid release of small extracellular vesicles into the circulation. *J. Extracell. Vesicles* **4**, 1–11 (2015).

215. Zhang, Q. *et al.* Transfer of Functional Cargo in Exomeres. *Cell Rep.* **27**, 940-954.e6 (2019).

Appendix 1

Appendix table 1. miRs detected ≥ 5 times in every sample at every timepoint.

	miRNA	A	B	C	D	E	F
1	miR-26a-5p	195405	229628	191116	257509	288388	237119
2	miR-191-5p	81512	87197	83055	97108	107192	92266
3	miR-486-5p	71049	47734	62416	50303	34342	42423
4	miR-423-5p	60599	63690	59245	45581	63175	63227
5	let-7f-5p	54053	56759	53311	60693	80768	70066
6	miR-151b	48845	51723	47325	54410	63033	52893
7	miR-146a-5p	44099	35618	40218	45246	36394	38996
8	miR-10b-5p	39137	16937	8597	31170	17167	8032
9	miR-125a-5p	24449	16152	10107	26042	17783	12281
10	miR-10a-5p	23687	14744	7835	22194	15246	7424
11	miR-30d-5p	23222	29657	25777	29810	34127	29988
12	let-7a-5p	19442	18863	16200	24167	27934	21644
13	miR-21-5p	16938	25594	18967	19570	30626	19764
14	miR-92a-3p	15133	16651	12900	18606	20152	17680
15	miR-146b-5p	15100	18742	16719	12584	17842	14332
16	let-7b-5p	13983	10846	8746	15011	15294	9875
17	miR-27b-3p	13399	13223	8621	13619	14484	8787
18	miR-126-3p	13035	9119	6334	12019	9344	6630
19	miR-30e-5p	12263	15847	14056	16589	17667	15945
20	miR-99b-5p	9822	10310	6918	9715	12056	7820
21	miR-22-3p	9483	8878	10197	7777	8077	8573
22	miR-423-3p	7950	10093	9526	8714	8552	9929
23	let-7i-5p	7593	7324	7725	6666	6599	7349
24	miR-181a-5p	6736	4599	5776	7122	3604	4838
25	miR-151a-3p	6712	8487	7191	7759	7355	6437
26	miR-148b-3p	6712	10017	8739	7424	11253	8387
27	let-7g-5p	4934	4025	3533	4622	5133	4485
28	miR-185-5p	4779	5211	4688	3661	3811	3544
29	miR-126-5p	4491	3435	2436	5485	4525	3223
30	miR-30c-5p	4251	5300	4118	5804	6379	5772
31	miR-224-5p	4089	2722	2897	4815	3321	3185
32	miR-99a-5p	3762	2482	2499	2507	2164	1651
33	miR-148a-3p	3715	4714	4746	4367	4997	4280
34	miR-451a	3550	3203	4922	1886	1138	1023
35	miR-28-3p	3541	4393	3513	3793	4532	3277

36	let-7d-5p	3436	3923	3806	3862	4706	4694
37	miR-100-5p	3422	742	790	1935	551	414
38	miR-222-3p	3413	3962	5843	4154	3895	5945
39	miR-143-3p	3280	3358	3074	3763	3395	2930
40	miR-30a-5p	3128	3633	1826	4054	3654	1764
41	miR-186-5p	3067	3169	2641	2572	2183	1764
42	miR-122-5p	3010	761	490	2117	597	474
43	miR-140-3p	3002	3023	1905	2407	2048	1775
44	miR-192-5p	2909	2612	1607	1625	1286	1062
45	miR-101-3p	2908	2753	1742	2916	2092	1268
46	miR-320a-3p	2843	3175	2875	2164	2346	2705
47	miR-221-3p	2798	4857	4273	3029	4506	4582
48	miR-23a-3p	2213	2266	1480	1896	2283	1554
49	miR-24-3p	2073	2066	1950	1916	1971	1791
50	miR-150-5p	1970	1505	678	1769	940	421
51	miR-127-3p	1903	1885	5209	1907	1562	4888
52	miR-142-5p	1757	1405	1156	1674	1490	1262
53	miR-199a-5p	1668	2454	2288	2076	2316	2372
54	miR-484	1658	2075	2030	2074	1963	2208
55	miR-26b-5p	1612	1745	1494	1607	1641	1622
56	miR-125b-5p	1577	961	1208	1426	827	900
57	miR-151a-5p	1565	1877	1644	1857	2242	1820
58	miR-221-5p	1535	2007	2927	1137	1807	1395
59	miR-199a-3p	1460	1999	1984	1841	2453	2355
60	miR-1301-3p	1428	1708	1947	1310	1659	1845
61	let-7e-5p	1424	1917	1202	1836	2558	1644
62	miR-23b-3p	1412	2021	1279	1804	2413	1582
63	miR-27a-3p	1354	1516	1149	1940	1576	1215
64	miR-584-5p	1347	1809	1725	1597	1989	1929
65	miR-409-3p	1320	1027	3352	1755	1142	3052
66	miR-342-3p	1285	1064	755	1234	1127	563
67	miR-744-5p	1087	819	837	725	770	871
68	miR-103a-3p	1021	1135	1048	1234	1597	1551
69	miR-363-3p	929	877	520	679	492	531
70	miR-182-5p	909	624	953	925	572	786
71	miR-16-5p	892	646	645	1046	1294	787
72	miR-152-3p	891	644	717	886	880	718
73	miR-30b-5p	762	1002	1020	928	1007	910
74	miR-151b	741	664	571	717	731	593
75	miR-130b-5p	725	976	1165	814	1044	1387
76	miR-361-5p	723	739	637	805	1127	1130

77	miR-223-3p	723	1342	1207	812	1013	876
78	miR-320b	722	624	521	372	457	523
79	miR-25-3p	718	693	573	732	703	443
80	miR-106b-3p	702	577	488	364	251	288
81	miR-128-3p	700	1113	742	962	1158	1216
82	miR-654-3p	655	510	1197	791	510	1510
83	miR-877-5p	652	361	707	568	509	1121
84	miR-28-5p	622	543	347	397	365	243
85	miR-96-5p	543	198	643	157	128	276
86	miR-181b-5p	527	296	377	273	267	306
87	miR-16-2-3p	522	563	633	761	505	452
88	miR-29a-3p	520	219	290	292	198	124
89	miR-2110	506	476	281	349	389	463
90	miR-664a-5p	495	494	362	462	452	392
91	miR-501-3p	492	659	557	538	607	348
92	miR-409-5p	467	269	1298	220	270	843
93	miR-378a-3p	460	391	283	305	335	235
94	miR-15b-5p	458	620	415	389	663	579
95	miR-184	444	482	342	15893	191	744
96	miR-323b-3p	441	345	434	518	297	415
97	miR-425-5p	437	513	385	455	347	361
98	miR-769-5p	431	422	251	317	263	246
99	miR-340-3p	370	507	367	387	664	411
100	miR-335-3p	368	414	780	655	818	975
101	miR-500a-3p	353	307	214	250	236	203
102	miR-483-5p	350	396	125	366	367	182
103	let-7d-3p	348	333	200	391	305	365
104	miR-628-3p	341	592	551	383	570	547
105	miR-505-3p	332	561	282	294	339	301
106	miR-144-3p	328	189	216	209	132	245
107	miR-342-5p	319	141	229	217	193	145
108	miR-4433b-5p	319	592	578	507	725	891
109	miR-98-5p	290	202	186	231	352	375
110	miR-494-3p	285	246	627	447	353	909
111	miR-589-5p	284	304	431	271	266	321
112	miR-7-5p	282	243	178	481	163	116
113	miR-485-5p	268	110	421	175	121	405
114	miR-183-5p	262	33	147	117	81	110
115	miR-330-3p	256	263	369	352	324	190
116	miR-181a-2-3p	243	259	304	205	338	362
117	miR-335-5p	241	388	248	260	344	291

118	miR-139-5p	238	140	148	236	189	149
119	miR-652-3p	236	291	154	279	199	214
120	miR-370-3p	232	149	531	204	87	395
121	miR-1-3p	211	240	304	28876	181	610
122	miR-139-3p	209	382	287	247	337	274
123	miR-155-5p	209	144	121	73	171	96
124	miR-625-3p	207	232	83	133	255	148
125	miR-23b-5p	204	68	124	134	206	118
126	miR-95-3p	202	72	27	94	102	22
127	let-7c-5p	196	181	225	322	187	132
128	miR-320c	184	162	145	113	83	95
129	miR-20a-5p	179	108	156	248	238	134
130	miR-543	178	56	255	185	91	294
131	miR-144-5p	176	215	186	277	172	103
132	miR-1271-5p	176	211	220	191	239	205
133	miR-485-3p	167	56	295	202	111	301
134	miR-503-5p	167	90	70	130	102	93
135	miR-92b-3p	165	122	148	630	320	175
136	miR-340-5p	163	538	356	423	524	384
137	miR-432-5p	162	95	400	152	125	325
138	miR-30e-3p	161	287	188	128	294	251
139	miR-1307-3p	159	171	221	203	115	126
140	miR-505-5p	158	164	144	301	368	355
141	miR-421	149	123	89	137	214	146
142	miR-181a-3p	148	123	335	193	73	184
143	miR-361-3p	147	185	109	125	78	33
144	miR-320d	139	58	68	36	80	46
145	miR-17-5p	131	95	101	109	104	77
146	miR-548e-3p	131	185	118	71	88	130
147	miR-150-3p	131	189	28	20	81	15
148	miR-338-5p	130	109	60	58	177	149
149	miR-181c-3p	124	141	134	104	90	84
150	miR-629-5p	122	22	132	66	26	90
151	miR-323a-3p	117	79	325	154	139	332
152	miR-671-3p	116	218	210	195	183	195
153	miR-197-3p	116	149	86	152	83	102
154	miR-411-5p	112	68	210	173	126	383
155	miR-25-5p	108	82	82	62	83	27
156	miR-339-3p	107	86	71	40	62	35
157	miR-5010-5p	105	127	37	66	125	70
158	miR-93-5p	102	116	107	121	195	256

159	miR-374b-5p	97	160	138	94	133	138
160	miR-425-3p	89	106	86	184	126	115
161	miR-374a-5p	89	104	66	127	112	182
162	miR-1273h-3p	88	102	132	52	83	62
163	miR-3928-3p	88	69	36	34	65	66
164	miR-502-3p	88	43	57	8	21	18
165	miR-605-3p	86	72	52	65	34	74
166	miR-30a-3p	80	127	27	113	12	8
167	miR-532-5p	78	115	52	33	68	40
168	miR-4446-3p	77	69	44	51	115	18
169	miR-136-3p	76	103	115	130	50	139
170	miR-199b-5p	73	54	82	12	48	125
171	miR-194-5p	73	41	17	31	33	76
172	miR-4662a-5p	71	75	2	40	95	38
173	miR-93-3p	71	52	55	45	15	33
174	miR-15b-3p	71	96	138	42	19	145
175	miR-941	70	170	92	50	155	94
176	miR-26b-3p	68	70	88	80	78	79
177	miR-1908-5p	68	77	57	38	15	84
178	miR-654-5p	67	26	105	73	39	108
179	miR-379-5p	66	49	152	106	46	229
180	miR-134-5p	63	43	200	56	23	100
181	miR-374a-3p	61	94	55	81	78	92
182	miR-21-3p	56	72	29	76	23	26
183	miR-125b-2-3p	55	15	29	39	44	13
184	miR-493-5p	54	65	179	107	67	272
185	miR-339-5p	53	219	184	97	119	163
186	miR-758-3p	51	33	109	19	61	61
187	miR-345-5p	51	91	26	96	49	26
188	miR-411-3p	51	97	166	78	56	186
189	miR-6852-5p	51	82	140	118	55	303
190	miR-328-3p	50	77	144	79	145	76
191	miR-106b-5p	50	79	54	78	44	50
192	miR-29b-3p	47	47	47	77	13	46
193	miR-10399-3p	45	57	29	7	46	34
194	let-7a-3p	45	67	33	29	76	23
195	miR-4433b-3p	45	150	313	164	113	229
196	miR-204-5p	43	54	17	5	16	9
197	miR-146b-3p	43	69	31	55	18	66
198	miR-148a-5p	42	30	20	69	14	36
199	miR-495-3p	42	20	95	31	49	138

200	miR-577	42	9	29	15	7	13
201	miR-203a-3p	41	56	13	44	15	50
202	miR-142-3p	38	39	42	79	130	86
203	miR-548av-5p	36	73	102	86	79	7
204	miR-3177-3p	35	4	11	30	41	56
205	miR-574-5p	35	50	48	57	96	53
206	miR-200a-3p	35	22	16	14	19	16
207	miR-27b-5p	33	114	12	54	84	49
208	miR-107	33	30	49	58	55	25
209	miR-493-3p	31	36	181	85	104	169
210	miR-125a-3p	31	14	21	24	18	16
211	miR-1468-5p	31	27	10	24	24	14
212	miR-326	30	47	38	34	13	60
213	miR-382-5p	29	36	119	7	42	136
214	miR-486-3p	29	117	159	90	42	111
215	miR-766-3p	27	38	40	46	18	14
216	miR-7706	27	12	13	11	7	28
217	miR-450a-5p	26	27	3	10	20	53
218	miR-889-3p	26	26	33	36	7	92
219	miR-664b-5p	26	36	18	53	37	24
220	miR-92b-5p	24	45	10	12	22	12
221	miR-412-5p	22	6	35	58	11	86
222	miR-17-3p	21	16	40	11	19	38
223	miR-6721-5p	20	12	10	21	15	25
224	miR-3605-3p	19	16	15	22	8	26
225	miR-3615	17	16	92	67	91	59
226	miR-10527-5p	17	11	13	13	24	25
227	miR-4677-3p	17	80	63	63	26	31
228	miR-145-3p	16	79	69	119	130	152
229	miR-452-5p	15	54	36	50	25	26
230	miR-181d-5p	15	16	41	46	72	5
231	miR-19b-3p	15	26	30	29	52	43
232	miR-11400	14	103	178	12	106	83
233	miR-7976	14	12	93	19	14	5
234	miR-1343-3p	14	82	29	34	23	14
235	miR-1292-5p	13	16	40	35	17	8
236	miR-19a-3p	13	18	15	14	27	17
237	miR-200c-3p	12	14	35	31	40	23
238	miR-4732-5p	11	29	13	31	10	14
239	miR-329-3p	11	74	56	65	65	66
240	miR-6842-3p	6	56	49	56	21	25

Appendix 2

In order to compare the miR normalisation calculation used in this thesis (i.e. sample / control) against that used by Lovett *et al* (i.e. sample - control) [51], the miRs that presented with significant changes in Figure 6.9, 6.16 and 6.17 were recalculated and the results for both strategies are summarised in Appendix Figure 1. Although there were some changes in the significance levels between the two calculation methods, the trends noted in this thesis largely remained the same.

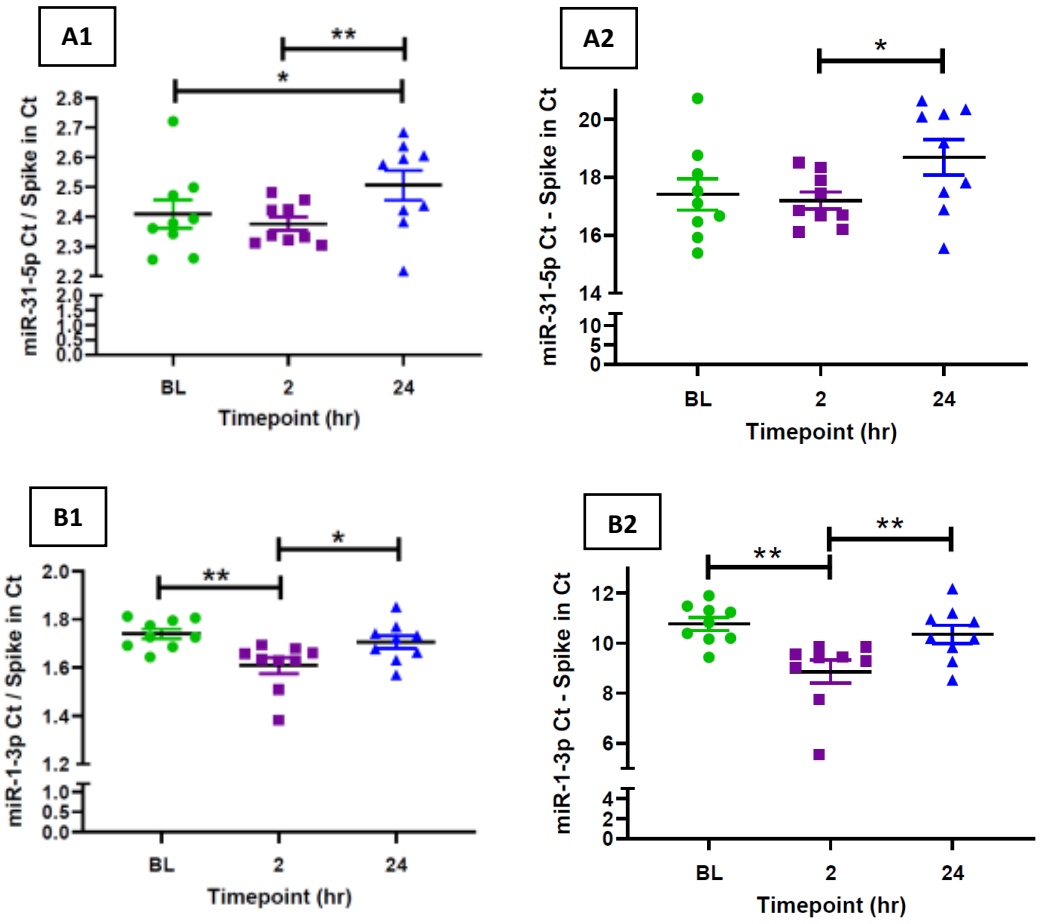

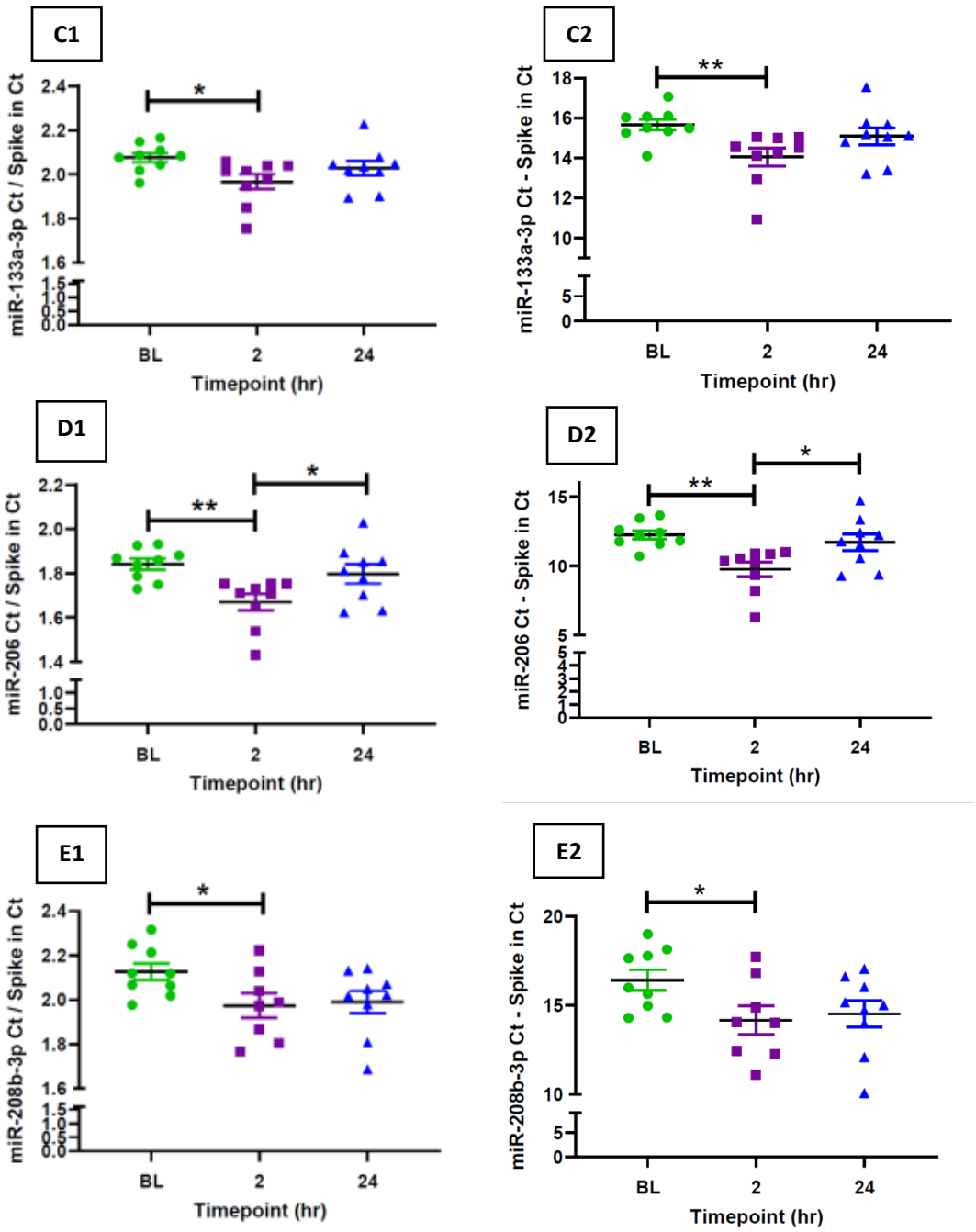

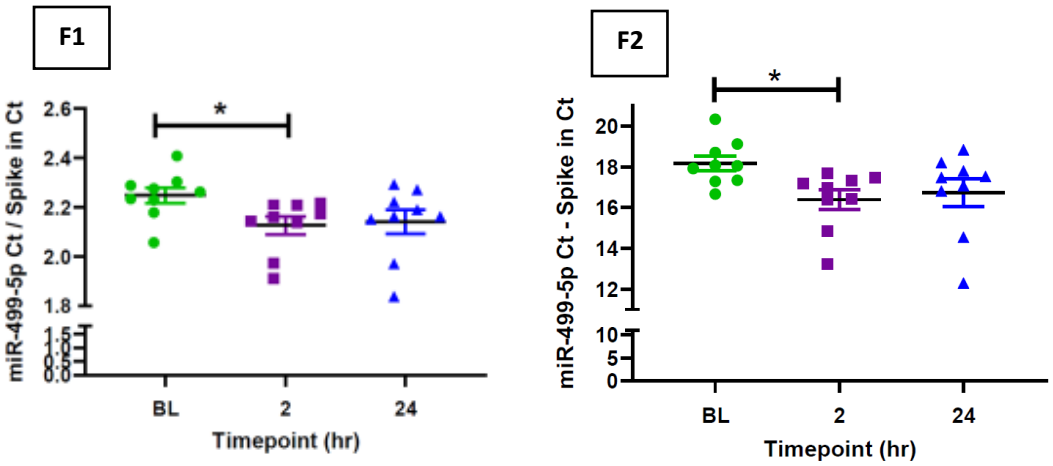

Appendix Figure 1. Abundance of small EV (A) and plasma (B - F) miRs that changed in this study, using two normalisation strategies with cel-miR-39 (column 1 – normalisation strategy used in the current study; column 2 – normalisation strategy used in the Lovett *et al* study [51]). (One-way ANOVA with LSD posthoc test. Mean ± SEM).